WL-TR-96-4064

SYNTHESIS AND STRUCTURE-PROPERTY CORRELATION OF PERFLUOROPOLYALKYLETHER BASE FLUIDS

K.J.L. PACIOREK

TECHNOLUBE PRODUCTS DIVISION
LUBRICATING SPECIALTIES CO.
3365 E. SLAUSON AVENUE
VERNON CA 90058

MAY 1996

FINAL REPORT FOR NOVEMBER 1989 TO MAY 1996

APPROVED FOR PUBLIC RELEASE; DISTRIBUTION IS UNLIMITED

MATERIALS DIRECTORATE
WRIGHT LABORATORY
AIR FORCE MATERIEL COMMAND
WRIGHT PATTERSON AFB OH 45433-7734

NOTICE

When government drawings, specifications, or other data are used for any purpose other than in connection with a definitely related government procurement operation, the United States Government thereby incurs no responsibility nor any obligation whatsoever; and the fact that the government may have formulated, furnished, or in any way supplied the said drawings, specifications, or other data, is not to be regarded by implication or otherwise as in any manner licensing the holder or any other person or corporation, or conveying any rights or permission to manufacture, use, or sell any patented invention that may in any way be related thereto.

This report is releasable to the National Technical Information Service (NTIS). At NTIS, it will be available to the general public, including foreign nations.

This technical report has been reviewed and is approved for publication.

William M. Warner

WILLIAM M. WARNER, Project Engineer
Nonstructural Materials Branch
Nonmetallic Materials Division

Wayne E. Ward

WAYNE E. WARD, Acting Chief
Nonstructural Materials Branch
Nonmetallic Materials Division

Charles E. Browning

CHARLES E. BROWNING, Chief
Nonmetallic Materials Division
Materials Directorate

If your address has changed, if you wish to be removed from our mailing list, or if the addressee is no longer employed by your organization, please notify WL/MLBT, Bldg 654, 2941 P Street, Suite 1, Wright-Patterson AFB OH 45433-7750 to help maintain a current mailing list.

Copies of this report should not be returned unless return is required by security considerations, contractual obligations, or notice on a specific document.

REPORT DOCUMENTATION PAGE

Form Approved
OMB No. 0704-0188

1. AGENCY USE ONLY *(Leave blank)*	2. REPORT DATE	3. REPORT TYPE AND DATES COVERED
	MAY 1996	FINAL 11/30/89 - 05/15/96

4. TITLE AND SUBTITLE

SYNTHESIS AND STRUCTURE-PROPERTY CORRELATION OF PERFLUOROPOLYALKYLETHER BASE FLUIDS

5. FUNDING NUMBERS

C F33615-89-C-5646
PE 62102
PR 2421
TA 01
WU 52

6. AUTHOR(S)

K. J. L. PACIOREK

7. PERFORMING ORGANIZATION NAME(S) AND ADDRESS(ES)

TECHNOLUBE PRODUCTS DIVISION
LUBRICATING SPECIALTIES CO.
3365 E. SLAUSON AVENUE
VERNON, CA 90058

8. PERFORMING ORGANIZATION REPORT NUMBER

SN-3522-F

9. SPONSORING/MONITORING AGENCY NAME(S) AND ADDRESS(ES)

MATERIALS DIRECTORATE
WRIGHT LABORATORY
AIR FORCE MATERIEL COMMAND
Wright-Patterson AFB, OH 45433-7734
POC: W.M. WARNER, WL/MLBT, WPAFB, OH; 785-9016

10. SPONSORING/MONITORING AGENCY REPORT NUMBER

WL-TR-96-4064

11. SUPPLEMENTARY NOTES

12a. DISTRIBUTION/AVAILABILITY STATEMENT

APPROVED FOR PUBLIC RELEASE; DISTRIBUTION IS UNLIMITED

12b. DISTRIBUTION CODE

13. ABSTRACT *(Maximum 200 words)*

Monomers for the preparation of the partially fluorinated model fluids were synthesized and limited investigations were carried out on their reactions. Direct fluorination processes were explored. A series of commercial and experimental perfluoropolyalkylether fluids was fully characterized and their thermal oxidative behavior in the presence of M-50 bearing steel alloy was determined. Computational treatments based on molecular mechanics, the input from the experimental data, and regression analysis led to the development of Quantitative Structure/Activity (Property) Relationships (QSAR). The developed expressions permit predictions, without synthesis of the candidate materials, of thermal oxidative stability, viscosity, viscosity/temperature and viscosity/molecular weight profiles.

14. SUBJECT TERMS

PERFLUOROPOLYALKYLETHERS
THERMAL OXIDATIVE STABILITY
METAL COMPATIBILITY
STRUCTURE-PROPERTY CORRELATIONS
COMPUTATIONAL PREDICTIONS
VISCOSITY

15. NUMBER OF PAGES
191

16. PRICE CODE

17. SECURITY CLASSIFICATION OF REPORT	18. SECURITY CLASSIFICATION OF THIS PAGE	19. SECURITY CLASSIFICATION OF ABSTRACT	20. LIMITATION OF ABSTRACT
UNCLASSIFIED	UNCLASSIFIED	UNCLASSIFIED	SAR

TABLE OF CONTENTS

LIST OF TABLES

LIST OF TABLES

LIST OF TABLES

LIST OF TABLES

LIST OF FIGURES

LIST OF FIGURES

LIST OF FIGURES

LIST OF FIGURES

LIST OF FIGURES

FOREWORD

This report was prepared by Technolube Products Division, Lubricating Specialties Co., Vernon, California, under Contract No. F33615-89-C-5646 "Synthesis and Structure-Property Correlations of Perfluoropolyalkylether Base Fluids" and covers work performed during the period 30 November 1989 through 15 May 1996. The investigations were carried out by K.J.L. Paciorek, Project Manager, with contributions by R.H. Kratzer, S.R. Masuda, W-H. Lin and J.H. Nakahara of Technolube, and J.G. Shih of Ultrasystems Defense. This contract was administered under the direction of the Wright Laboratory, Materials Directorate with Dr. William M. Warner (WL/MLBT) as the Project Engineer.

We wish to acknowledge the contribution of Wright Laboratory, Materials Directorate, Nonstructural Materials Branch personnel for providing the two series of experimental perfluoropolyalkylether fluids.

We also wish to acknowledge the contribution of Allied-Signal Inc., in the synthesis program under a subcontract.

1. EXECUTIVE SUMMARY

The goal of the subject contract was to develop structure/property (activity) relationships for perfluoropolyalkylether fluids to permit the identification of materials best suited for envisioned applications. The first portion of the program was performed at Ultrasystems Inc.; the majority of investigations were carried out at Technolube Products Division of Lubricating Specialties Co.

The goal of the synthesis effort was the preparation of partially fluorinated polyalkylether model fluids to be further fluorinated under subcontract with Allied-Signal Inc. The monomers, $HO_2CCF_2OCF_2CO_2H$, $ClOCCF_2OCF_2COCl$, $HOCH_2CF_2OCF_2CH_2OH$ and $(COF)_2$ were successfully prepared, although the yields were lower than anticipated. Only limited effort was expended on the synthesis of partially fluorinated model fluids due to problems associated with direct fluorination and the sudden availability of a series of perfluoropolyalkylether fluids.

The major thrust of the work was centered on characterization of the fluids supplied by the Air Force, including determining their viscosity/temperature and viscosity/molecular weight profiles, and thermal oxidative stability behavior in the presence of metal alloys. The aim was to provide experimental data necessary for structure/activity relationships studies.

Based on the experimental input using computational chemistry in conjunction with multivariate regression analyses quantitative structure/activity (property) expressions were developed which allow the prediction of viscosity/temperature and viscosity/molecular weight profiles as well as the thermal oxidative stability of perfluoropolyalkylether fluids. The significance of this achievement is the ability to select the optimum compositions for specific applications without the need to synthesize a series of candidates. The validity of the approach was proven by the correct prediction of properties of known perfluoropolyalkylethers using the developed parameters and expressions.

2. INTRODUCTION

Perfluoropolyalkylethers are the only class of materials which possess thermal oxidative stability and associated viscosity temperature characteristics, such as to permit, at least in theory, operation between -70 and 400°C. It is clear from the literature data [Ref. 1-7] that in the perfluoropolyalkylether series of fluids the linear arrangements exhibit better viscosity/temperature profiles; i.e., have a higher viscosity index (VI) than the corresponding branched chain analogues. The most important factor in improving the low temperature properties and increasing the VI is a high oxygen/carbon (O/C) ratio. Yet it is the same factor which appears to lead to lowered thermal oxidative stability in the presence of metals [Ref. 8]. Inasmuch as these materials are being considered as high temperature turbine engine oils for the future generation of aircraft, this aspect is of utmost concern.

The current study was undertaken to develop valid premises for the selection of the best compromise fluids for specific application. The goal was to prepare a series of well characterized "model" fluids and to develop structure/property relationships to permit identification of optimum arrangements without actual synthesis, based on the experimentally determined viscosity/temperature profiles and thermal oxidative behavior in the presence of metals. The goal of the synthesis portion of the program was to concentrate on the preparation of partially

fluorinated intermediates. These were to be transformed by direct fluorination, (to be carried out by Allied-Signal, Inc. under a subcontract), into a series of model fluids. The perceived advantage of this approach, as compared to direct fluorination of multicomponent hydrocarbon precursors (pioneered by Exfluor Research Corp.) was the formation of a single component fluid with well defined end groups, as well as avoidance of rearrangements, bond scissions and related problems inherent to fluorination of hydrocarbons. Having fluorinated entities in a given molecule moderates the initial reaction and prevents the formation of by-products.

As work proceeded the low yields obtained of the required intermediates and the difficulties encountered in the preliminary attempts to form the actual partially fluorinated precursors of the model fluids, together with the disappointing results of the direct fluorination efforts on test materials by Allied-Signal, led to the abandonment of this approach. The deciding factor in taking this action was the availability of a series of experimental fluids from Exfluor Research Corp. which appeared to offer, based on ^{19}F NMR and GC/MS studies a viable alternative to the representative perfluoropolyalkylether systems. Furthermore work proceeding at that time at Exfluor Research Corp., under the Air Force sponsorship, indicated clearly that "purer" experimental fluids with a larger variety of chain arrangements were forthcoming. Accordingly, the latter fluids were utilized in the investigations which provided the

experimental data for the development of quantitative structure/activity (property) relationships (QSAR) for predicting the viscosities and the thermal oxidative stabilities of perfluoropolyalkylether fluids. The developed expressions were based on molecular mechanics/molecular dynamics computations and multivariate linear regression analysis.

3. RESULTS AND DISCUSSION

The overall program was composed of a number of tasks which provide a logical breakdown for the orderly presentation of the data. Thus this portion of the report has been divided into: Synthesis and Related Aspects, Characterization and Study of the First Series of Experimental Perfluoropolyalkylether Fluids, Characterization and Thermal Oxidative Stability Testing of Chlorofluoropolyalkylether Fluids, Characterization and Study of the Second Series of Experimental Perfluoropolyalkylether Fluids, Development of Quantitative Structure/Viscosity Relationships, Thermal Oxidative Stability Investigations and Development of Quantitative Structure/Stability Relationships.

3.1 SYNTHESIS AND RELATED ASPECTS

The major synthesis effort under this contract was directed at the preparation of the monomers $O(CF_2CO_2H)_2$, $O(CF_2COCl)_2$, $O(CF_2CH_2OH)_2$ and $(COF)_2$. These monomers together with derivatives such as $O(CF_2COF)_2$, $O(CF_2I)_2$ and $O(CF_2CH_2Br)_2$, in conjunction with the commercially available hexafluoropropene oxide, potentially provide the starting materials for a series of different fluorinated and partially fluorinated perfluoropoly-alkylethers or their precursors.

A small portion of the synthesis work was expended on the evaluation of the direct fluorination capability at Allied-

Signal. Originally the subcontract with Allied-Signal, Inc. was to provide the direct fluorination support and computational expertise.

3.1.1 Synthesis of Monomers

The key starting material for the model fluid synthesis was $HO_2CCF_2OCF_2CO_2H$. One of the approaches pursued was originally described by the group at Dow Corning [Ref. 9] and is described in Scheme I.

The major problem we have encountered with the process, given in Scheme I, was the low yield of the isolated first intermediate, $Cl_2C{=}CClCCl{=}CClOC_2H_5$, which ranged from 23 to 32%. The tedious fractionation required to obtain the pure product complicated matters further. The next two steps proceeded essentially in quantitative yields. The 2,2,5,5-tetrafluoro-3,4-dichlorofuran was obtained in a 52% yield. Its oxidation to the acid $HO_2CCF_2OCF_2CO_2H$ was initially attempted in acetone, but yields were poor and isolation difficult. Using alkaline permanganate gave the desired product in a 61% yield. Although the starting material for the Scheme I was inexpensive, the overall yield for the reactions up to the furan was very low, approximately 11%.

SCHEME I

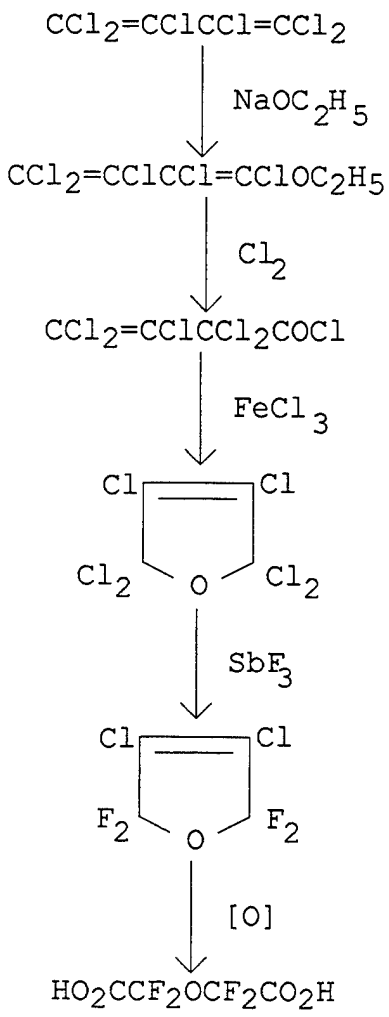

As mentioned earlier attempts to optimize the first step were largely unsuccessful. Treatment of dichloromaleic anhydride with SF_4 afforded another route to 2,2,5,5-tetrafluoro-3,4-dichlorofuran [Ref. 10, 11]. The advantage here was the one step process. The drawback was the cost of the starting material and of SF_4.

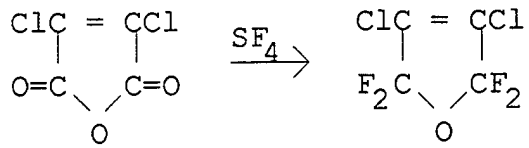

Unfortunately the desired furan was invariably admixed with the lactone $O{=}\overset{\overset{\Large O}{\frown}}{C}\text{-}CCl{=}CClCF_2$, at best in equal proportions. Combined yields of the two products amounted to approximately 70%. Another treatment with SF_4 was necessary to attain reasonable yields approximately 45-50%, of the furan. This compares to the 11-20% attained using the multi-step reaction. Some process optimization was attempted in both of the instances however, the main thrust was to determine the feasibility of the formation of the desired model fluids.

The synthesis of the alcohol $HOCH_2CF_2OCF_2CH_2OH$, took place smoothly, in a 81% yield from the diethyl ester, following the reported procedure [Ref. 13]. It is of interest that using the methyl ester incomplete reaction was achieved. The diethyl ester was obtained in a 75% yield from the free acid and in 94% yield from mixture of the corresponding diacyl chloride and anhydride. Attempts to prepare pure diacyl chloride, $O(CF_2COCl)_2$, invariably resulted in mixture of the diacyl chloride and anhydride.

Oxalyl fluoride, $(COF)_2$, was obtained in a 52% yield by treatment of oxalyl chloride with sodium fluoride following the procedure of Tullock and Coffman [Ref. 14]. Interaction of the diol $HOCH_2CF_2OCF_2CH_2OH$ with $SOBr_2$ failed to give

$BrCH_2CF_2OCF_2CH_2Br$. The latter was one of the co-reactants required for the synthesis of certain classes of model fluids.

3.1.2 Synthesis of Model Fluid Precursors

The route to the intermediate hydroxy-terminated polyesters was outlined in the original proposal [Ref. 15], i.e.

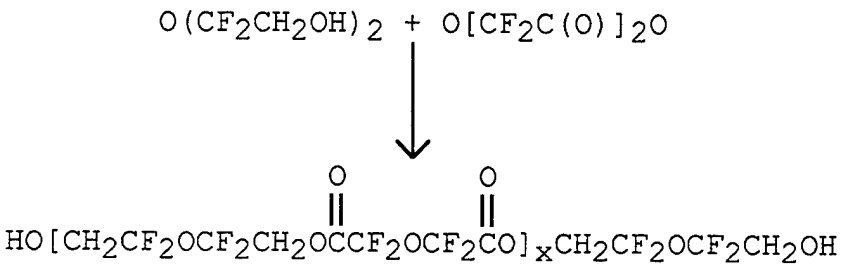

The value of x is dependent on the stoichiometry of the two reagents. Initial reaction was carried out in refluxing tetrahydrofuran using a mixture of the anhydride and the corresponding acyl chloride with the diol $O(CF_2CH_2OH)_2$ (in the mole ratio of 1:1.5) in the presence of pyridine. Only unreacted diol and the acid $O(CF_2CO_2H)_2$ were observed after workup. A reaction performed in the absence of solvent in a sealed tube at 80°C gave the expected oligomers.

A parallel approach to acid terminated polyesters i.e.

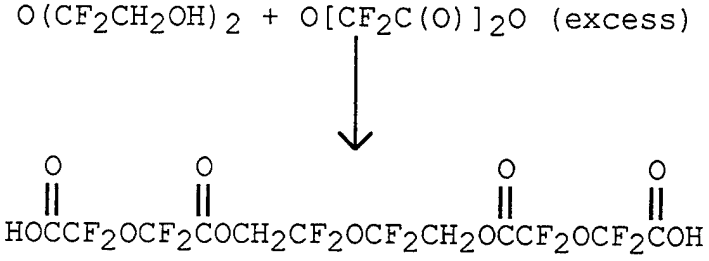

using a reaction of a mixture of anhydride and acyl chloride with the diol in a ratio of 7.5 to 1 at 85°C in the absence of solvent gave what appeared to be the expected product. However, in view of the lack of progress in the direct fluorinations carried by Allied-Signal, Inc., purification of neither of the above systems was carried out.

Based on work performed earlier at Ultrasystems [Ref 16], the reaction of hexafluoropropene oxide with oxalyl fluoride should proceed readily to give, under selected conditions, $FC(O)CF(CF_3)OCF_2CF_2OCF(CF_3)COF$:

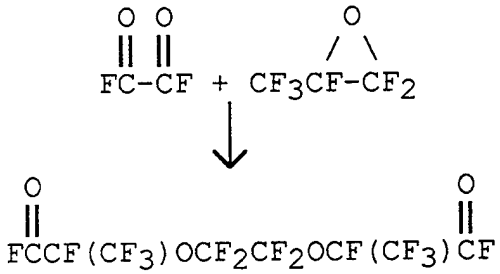

The product distribution is strongly dependent upon the reaction conditions. Thus, at low temperatures it was assumed that the cesium/oxalyl fluoride complex should be the primary nucleophilic species which would then attack the secondary carbon atom of the oxide [Ref. 17]. Higher temperatures favor the oligmerization of hexafluoropropene oxide. These investigations, as evident from Table 1, show clearly that the use of low temperature does lead to promising yields of the desired product. Optimization of the process was not pursued in view of lack of progress in the direct fluorination and the sudden availability

TABLE 1

ATTEMPTED SYNTHESIS OF $F(O)CCF(CF_3)[OCF_2CF(CF_3)]_xOCF_2CF_2O[CF(CF_3)CF_2O]_yCF(CF_3)COF$

Run No	$(COF)_2$ mmol	CsF mmol	TG mL	Conditions Temp °C	Conditions Time hr	HFPO mmol	Conditions Temp °C	Conditions Time hr	Products (GC area %)[a] $(HFPO)_2$	$(HFPO)_3$	$(HFPO)_4$	Desired[b] Product	Recovered HFPO, mmol
1	9.45	9.45	2.9	-23 0	2 2	18.9	-23	18	22.4	31.5	6.5	22.6	7.9
2	21.3	2.63	5.3	-12	2	84.3	-12	18	1.6	59.1	9.9	24.1	22.3
5	39.9	7.83	6.0	0	2	183	0 -78-RT	7 16	25.6	8.4	8.4	7.6[c]	18.3

a) Analyzed as methyl esters.

b) Desired product x + y = 0, i.e., $F(O)CCF(CF_3)OCF_2CF_2OCF(CF_3)COF$.

c) Major product (42.2%, analyzed by GC as methyl ester): $MeCO_2CF(CF_3)[OCF_2CF(CF_3)]_xOCF_2CF_2O[CF(CF_3)CF_2O]_yCF(CF_3)CO_2Me$; 29.5% (GC) x + y = 1; 9.2% x + y = 2; 3.5% x + y = 3.

Runs 3 and 4 were unsuccessful in leading to any appreciable copolymerization products.

of the desired experimental fluids from Exfluor Research Corporation.

3.1.3 Direct Fluorination Results

Two materials, tetraglyme and diglycolic acid, were subjected to direct fluorination by Allied-Signal, Inc. to determine the applicability of the process for the synthesis of the envisioned model fluids.

The 8-hour treatment of tetraglyme resulted in 10.7 g of product which after purification was still contaminated by hydrogen- and carbonyl-containing impurities. A corresponding sample prepared by Exfluor Research Corp. and obtained from NASA Lewis was free from these impurities.

The attempts to prepare $O(CF_2COF)_2$ from diglycolic acid were totally unsuccessful. The 0.95 g sample received, based on the analysis performed, did not contain the desired acid fluoride nor the corresponding lactone or anhydride. The presence of hydrogenated compounds was clearly shown. Based on the failure of the fluorination process, the low yield tedious synthesis of the precursors and most importantly the sudden availability of experimental fluids of different arrangements, the synthesis efforts were abandoned in favor of the utilization of the experimental fluids in the development of the structure/property relationships.

3.2 CHARACTERIZATION AND STUDY OF THE FIRST SERIES OF EXPERIMENTAL PERFLUOROPOLYALKYLETHER FLUIDS

Based on the results presented in Section 3.1 the feasibility of preparing model fluids at a reasonable cost in a reasonable time period became doubtful. At the same time the experimental fluids, prepared by Exfluor Research Corp. from hydrocarbon precursors, became available and consequently it was decided by the Project Engineer to determine whether these materials could be utilized in the development of meaningful structure/property relationships. These fluid compositions were mixtures of telomers having also different end-groups. Furthermore, the hydrocarbon precursors for the experimental fluids, in the majority of instances, were not well characterized. In addition during the fluorination process a certain degree of rearrangement was to be expected. Thus, characterization of the fluids was of great importance.

3.2.1 Fluid Characterization

Four fluids: MLO 88-48, MLO 88-51, MLO 88-129, and MLO 88-132, prepared by direct fluorination by Exfluor Research Corp., were received from the Air Force. The originally assigned structures, together with the structures proposed, based on ^{19}F NMR and GC/MS data, are given in Table 2. Also included in Table 2 are molecular weights (determined by osmometry and by ^{19}F NMR end-group ratios), viscosity data (received from WL/MLBT), and summary of GC results (the retention times denoting the limits of the elution envelope). As noted earlier, each of the fluids

TABLE 2

ANALYTICAL DATA AND STRUCTURE CORRELATIONS FOR SELECTED PERFLUOROALKYLETHER COMPOUNDS[a]

Sample ID MLO	Chemical Structure[b] Originally Assigned	Chemical Structure Assigned[c]	MW Measured[d] (^{19}F NMR)[e]	Viscosity cSt[f]			GC r.t., min.[g]	
				-18°C	40°C	100°C	Start	End
88-48	$CF_3O[CF_2CF_2CF_2CF_2O]_nCF_3$	$C_3F_7O[CF_2CF_2CF_2CF_2O]_nC_3F_7$ $C_4F_9O[CF_2CF_2CF_2CF_2O]_nC_3F_7$ $C_2F_5O[CF_2CF_2CF_2CF_2O]_nC_3F_7$	3100 (4328)	2581	57.8	8.4	17.5	28.0
88-51	$CF_3O(CF_2CF_2O)_nCF_3$	$CF_3O[CF_2CF_2O]_nCF_3$ $C_2F_5O[CF_2CF_2O]_nCF_3$	2800 (3015)	NF[h]	15.8	3.85	14.2	24.5
88-129	$CF_3O(CF_2OCF_2CF_2O)_nCF_3$	$CF_3O[CF_2OCF_2CF_2O]_nCF_3$ $CF_3O[CF_2OCF_2CF_2O]_nCF_2OC_2F_5$ plus others	3250 (2542)	ND	13.4	4.04	14.1	28.7
88-132	$CF_3O[(CF_2CF_2O)_4CF_2O]_nCF_3$	$CF_3O[(CF_2CF_2O)_3CF_2O]_nCF_3$ plus others	3250 (2635)	ND	16.4	4.24	15.0	28.0

a) These samples were received from AFML (WRDC/MLBT).

b) This was the structure given.

c) These structures were assigned based on ^{19}F NMR and GC/MS analysis.

d) This molecular weight was measured by osmometry.

e) This molecular weight was calculated from ^{19}F NMR based on CF_3- end group and an internal segment.

f) These data were provided by WRDC/MLBT.

g) These values pertain to GC elution envelope of the given fluid.

h) Material turned white and failed to flow.

comprises a series of homologues, as illustrated by the actual GC traces given in Figures 1-4.

In the case of MLO 88-48, the specific end-groups assigned originally to the fluid appear to be absent, based on ^{19}F NMR data. The GC trace (Figure 1) shows a repeating pattern of two low intensity peaks and one high intensity peak. It has been established from GC/MS that there are three types of homologues present: 1) $C_3F_7O(CF_2CF_2CF_2CF_2O)_nC_3F_7$ (major component); 2) $C_4F_9O(CF_2CF_2CF_2CF_2O)_nC_3F_7$; 3) $C_2F_5O(CF_2CF_2CF_2CF_2O)_nC_3F_7$. In Figure 1 the peak at 19.3 minutes was found to be due to a material terminated by C_3F_7 at both ends. At 19.7 minutes the termination is C_4F_9; at 20.3 minutes C_2F_5 and C_3F_7. The listing of the revelant ions is presented in Table 3. The assignments for the specific components, which were differentiated by the end-groups, are based on the presence or absence of characteristic ions, for C_4F_9, m/e 435; for C_3F_7, m/e 385; and for C_2F_5, m/e 335.

The 3100 number average molecular weight determined by osmometry is significantly lower than the 4300 value obtained from the ^{19}F NMR. Small quantities of low molecular weight impurities could be responsible.

The experimental fluid, MLO 88-51, exhibited in its GC trace (Figure 2) the presence of two distinct compositions. Based on ^{19}F NMR spectroscopy in conjunction with the GC/MS data, the major peak is $CF_3O(CF_2CF_2O)_nCF_3$ and the minor peak is

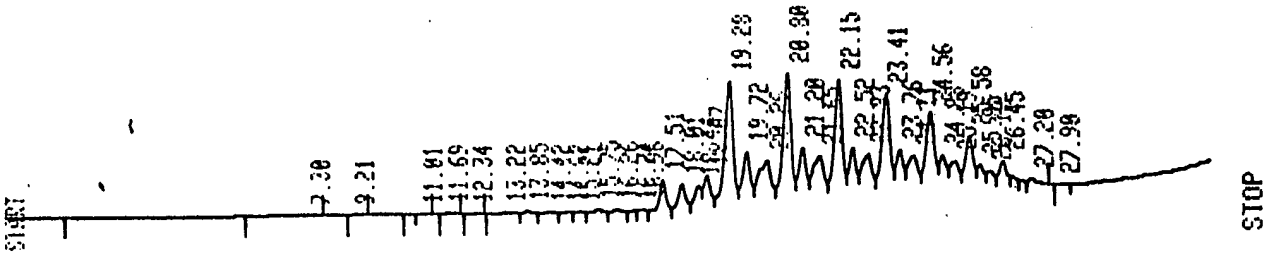

Figure 1. GC trace of MLO 88-48; $C_3F_7O[(CF_2)_4O]_nC_3F_7$, $C_4F_9O[(CF_2)_4O]_nC_3F_7$, $C_2F_5O[(CF_2)_4O]_nC_3F_7$.

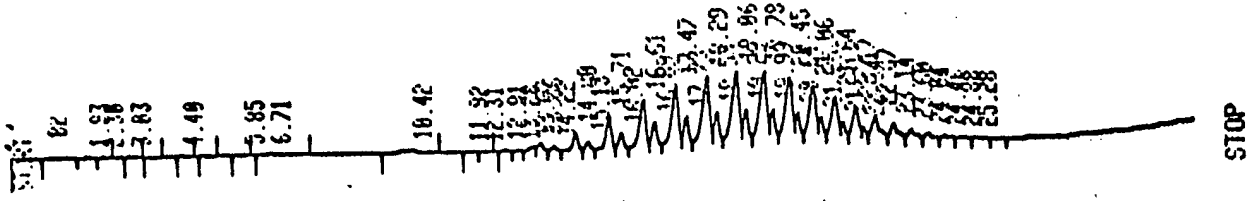

Figure 2. GC trace of MLO 88-51; $CF_3O[CF_2CF_2O]_nCF_3$, $C_2F_5O[CF_2CF_2O]_nCF_3$.

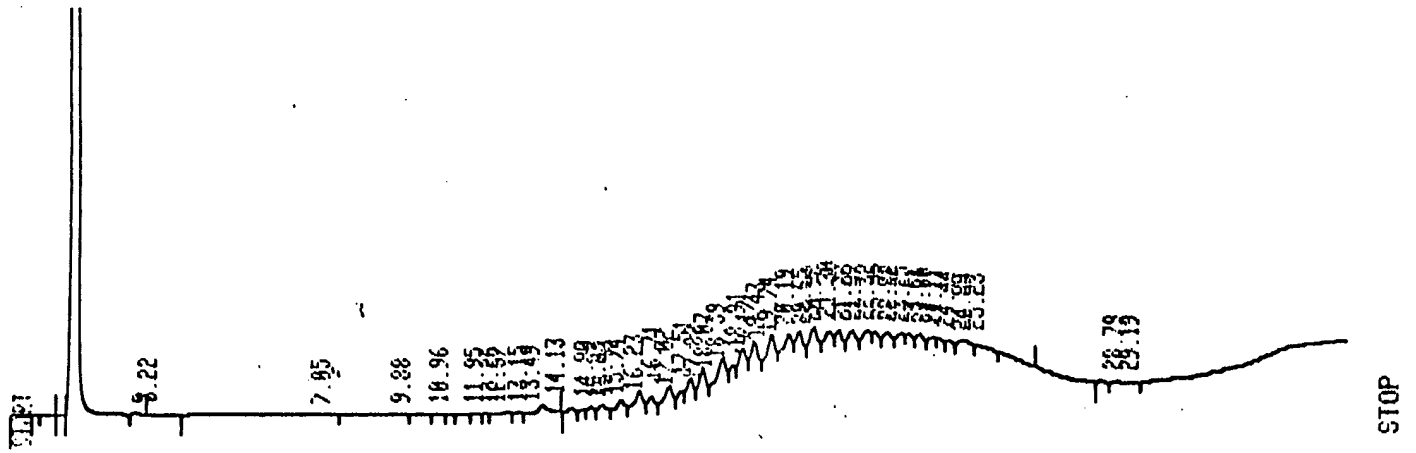

Figure 3. GC trace of MLO 88-129; $CF_3O[CF_2OCF_2CF_2O]_nCF_3$, $CF_3O[CF_2OCF_2CF_2O]_nCF_2OC_2F_5$ and other structures.

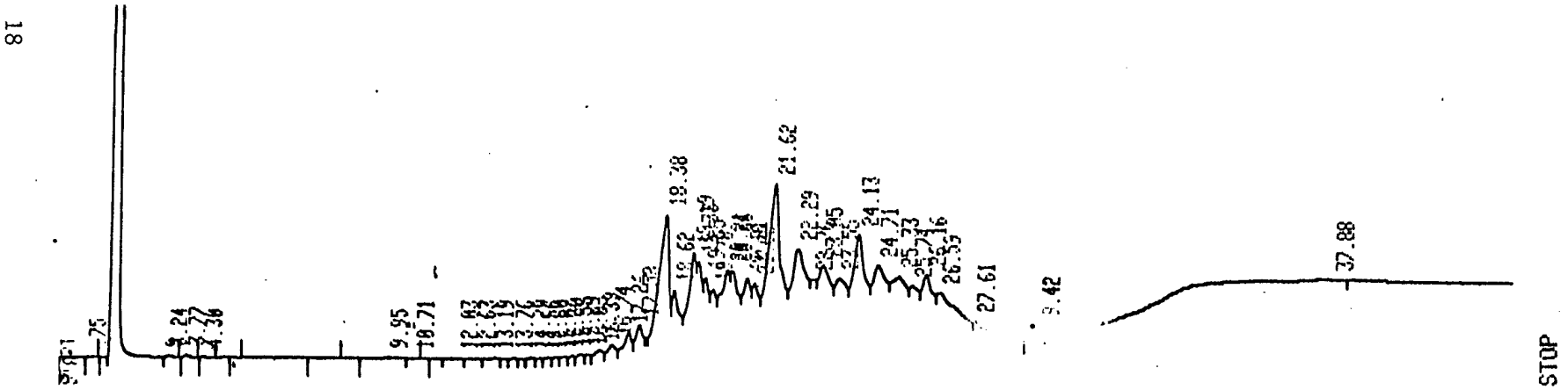

Figure 4. GC trace of MLO 88-132; $CF_3O[(CF_2CF_2O)_3CF_2O]_nCF_3$ and other structures.

TABLE 3

LISTING OF PROMINENT IONS SUPPORTING THE STRUCTURE ASSIGNMENT FOR MLO 88-48

Major Component: $C_3F_7O[CF_2CF_2CF_2CF_2O]_nC_3F_7$

Minor Components: $C_4F_9O[CF_2CF_2CF_2CF_2O]_nC_3F_7$
$C_2F_5O[CF_2CF_2CF_2CF_2O]_nC_3F_7$

m/e	ion
150	$CF_2CF_2CF_2$
169	C_3F_7
197	$CF_2CF_2CF_2COF$
219	C_4F_9
235	$C_3F_7OCF_2$
335	$C_2F_5OCF_2CF_2CF_2CF_2$
385	$C_3F_7OCF_2CF_2CF_2CF_2$
435	$C_4F_9OCF_2CF_2CF_2CF_2$

$C_2F_5O(CF_2CF_2O)_nCF_3$. The prominent MS peak assignments for the two compounds are given in Table 4.

The molecular weights as determined by osmometry and ^{19}F NMR are within experimental error. The molecular weight data, low temperature properties, and structural arrangements of MLO 88-48 and MLO 88-51 cannot be readily correlated. Ignoring the higher molecular weight of MLO 88-48 (due to the discrepancy in the two values), but based solely on the O to CF_2 ratio, MLO 88-48 would be expected to exhibit a much higher viscosity at -18°C than MLO 88-51. This would also be in line with the reported viscosities at 40 and 100°C. On the other hand the well ordered structure of $-(CF_2CF_2O)_n-$ most likely promotes crystallization reflected by a drastic increase in viscosity at low temperature.

The GC data obtained for MLO 88-129, as evident from Figure 3, were poor. The ^{19}F NMR spectroscopy indicated the presence of CF_3 and C_2F_5 end-groups with the former predominating approximately in a 2:1 ratio. Thus, the major components seem to be $CF_3O(CF_2OCF_2CF_2O)_nCF_3$ and $CF_3O(CF_2OCF_2CF_2O)_nC_2F_5$. The MS data support fully the ^{19}F NMR assignments. The molecular weights, Table 2, determined by the two different methods, do not correspond closely. The only explanation for the higher value obtained by osmometry is chain branching.

MLO 88-132 could not be satisfactorily analyzed by GC/MS. The GC trace, Figure 4, points to many different arrangements; these could not be resolved. The ^{19}F NMR data does not agree with the basic structure originally postulated. The

TABLE 4

LISTING OF PROMINENT IONS SUPPORTING THE STRUCTURE ASSIGNMENT FOR MLO 88-51

Major Component: $CF_3O[CF_2CF_2O]_nCF_3$

Minor Component: $C_2F_5O[CF_2CF_2O]_nCF_3$

m/e	ion
75	O-C-COF
135	CF_3OCF_2
185	$CF_3CF_2OCF_2$, $CF_3OCF_2CF_2$
213	$CF_2CF_2OCF_2COF$, $CF_2OCF_2CF_2COF$
235	$CF_3CF_2OCF_2CF_2$
301	$CF_3OCF_2CF_2OCF_2CF_2$
329	$CF_2CF_2OCF_2CF_2OCF_2COF$
351	$C_2F_5OCF_2CF_2OCF_2CF_2$
417	$CF_3O[CF_2CF_2O]_2CF_2CF_2$
445	$[CF_2CF_2O]_3CF_2COF$
467	$C_2F_5[OCF_2CF_2]_3$
561	$[CF_2CF_2O]_4CF_2COF$
677	$[CF_2CF_2O]_5CF_2COF$

arrangement $CF_3O[(CF_2CF_2O)_3CF_2O]_nCF_3$ is supported both by ^{19}F NMR and mass spectral data. Also there is a discrepancy in the molecular weights determined by ^{19}F NMR and osmometry. The lower value by NMR indicates branching. Based on the $O:CF_2$ ratio, the viscosities of MLO 88-129 should be lower than that of MLO 88-132, the experimental data verifies this assumption.

3.2.2 Stability Evaluations

To determine the effect of structural arrangement on the thermal oxidative stability, the perfluoropolyalkylether fluids MLO 88-48, -51, -129 and -132 described in Section 3.2.1, were subjected to thermal oxidative evaluations in the presence of M-50 steel bearing alloy. The results of these tests are summarized in Tables 5 and 6. As requested by the Project Engineer 15°C temperature increases starting with 260°C were employed to determine the stability as a function of temperature. Based on the results obtained, it can be seen that MLO 88-48, $R_fO[CF_2CF_2CF_2CF_2O]_nR_f$, undergoes steady degradation up to 330°C in direct agreement with Arrhenius rule of rate doubling for every 10°C. This would imply not the breakdown of the major component, but rather decomposition of an impurity.

The results for MLO 88-51, $R_fO[CF_2CF_2O]_nR_f$, indicate that between 300 and 315°C drastic increase in the degradation rate takes place. This break point for MLO 88-129, $R_fO[CF_2OCF_2CF_2O]_nR_f$, is between 275 and 290°C, whereas for MLO 88-132, $R_fO[(CF_2CF_2O)_4CF_2O]_nR_f$, the value lies between 300 and

TABLE 5

COMPARISON OF THERMAL OXIDATIVE BEHAVIOR OF VARIOUS PERFLUOROALKYLETHER FLUIDS[a]

Test No	Fluid Type	g	Temp °C	Volatiles mg/g	Coupon Weight Change, mg/cm^2	Reference
1	Krytox (MLO 71-6)	3.02	260	0.13	+0.1	2-90-101
2	Fomblin Z (Z25-P28)	3.17	260	57.4	-0.2	2-90-102
3	Demnum S20 (MLO 86-51)	3.74	260	1.0	+0.2	2-90-107
4	Brayco 814Z (MLO 78-80)	3.32	260	4.8	+0.2	2-90-108
5	$R_fO[(CF_2)_4O]_nR_f$ (MLO 88-48) $R_f = C_2F_5$, C_3F_7, C_4F_9	3.21	260	0.06	0.0	2-90-115
9	ditto	3.20	275	0.50	-0.1	5-90-8
13	ditto	3.16	290	1.55	+0.06	5-90-14
17	ditto	3.18	315	6.95	+0.3	5-90-60
24	ditto	3.19	330	21.7	+0.4	5-90-105
6	$R_fO(CF_2CF_2O)_nR_f$ (MLO 88-51) $R_f = CF_3$, C_2F_5	3.22	260	0.50	0.0	2-90-116
10	ditto	3.22	275	0.52	0.0	5-90-9
14	ditto	3.22	290	0.53	+0.06	5-90-15
19	ditto	3.20	300	1.47	+0.3	5-90-96
18	ditto	3.20	315	63.7	0.0	5-90-61
21	ditto	3.20	315	157.6	-4.2	5-90-100
7	$R_fO[CF_2OCF_2CF_2O]_nR_f$ (MLO 88-129) $R_f = CF_3$, $CF_2OC_2F_5$	3.26	260	0.52	+0.1	2-90-134
11	ditto	3.24	275	2.1	+0.1	5-90-10
15	ditto	3.22	290	19.3	+0.4	5-90-24
8	$R_fO[(CF_2CF_2O)_4CF_2O]_nR_f$ (MLO 88-132) $R_f = CF_3$	3.28	260	0.67	-0.1	2-90-135
12	ditto	3.23	275	1.7	+0.1	5-90-11
16	ditto	3.19	290	4.67	+0.5	5-90-25
20	ditto	3.22	300	9.63	+0.8	5-90-97
22	ditto	2.84	315	446.5	+0.4	5-90-101

(a) All the tests were performed in pure oxygen at the denoted temperature in the presence of an M-50 coupon over a 24 h period using the modified, scaled-down, sealed version of the AFML Micro-O-C-Test arrangement

TABLE 6

COMPARISON OF THERMAL OXIDATIVE BEHAVIOR OF VARIOUS PFPAE FLUIDS IN THE PRESENCE OF M-50, O_2 FOR 24 H.

Fluid	MLO	Volatiles, mg/g						
		260°C	275°C	290°C	300°C	315°C	330°C	345°C
$R_fO[CF_2CF_2CF_2CF_2O]_nR_f$	88-48	0.06	0.50	1.6		7.0	21.7 28.3	
$R_fO[CF_2CF_2O]_nR_f$	88-51	0.50	0.52	0.53	1.5	63.7 157.6		
$R_fO[CF_2OCF_2CF_2O]_nR_f$	88-129	0.52	2.1	19.3				
$R_fO[(CF_2CF_2O)_4CF_2O]_nR_f$	88-132	0.67	1.7	4.7	9.6	446.5		
Fomblin Z25-P28 $R_fO[CF_2O]_n[CF_2CF_2O]_mR_f$	-	57.4						
Brayco 814Z $R_fO[CF_2O]_n[CF_2CF_2O]_mR_f$	78-80	4.8	62.2					
Krytox 143AC $R_fO[CF(CF_3)CF_2O]_nR_f$	71-6	0.13		4.0[a] (288°C)	38.2[a] (72 h)	44.0 47.5[a] (316°C)		
Krytox 143AC (pretreated)						0.2[a] (316°C)		15.4[a] (343°C)
Aflunox 2509 $R_fO[CF(CF_3)CF_2O]_nR_f$						0.5[c] (316°C)		
Demnum S20 $R_fO(CF_2CF_2CF_2O)_nR_f$	86-51 88-177	1.0 0.7[d] (68 h)			1.4		13.3	

(a) Data from AFML-TR-77-150.
(b) Test conducted for 72 h.
(c) Data from NASA CR-180872.
(d) Test conducted for 68 h.

315°C. In view of the high degree of decomposition at 315°C, about 50%, actual degradation "onset" would appear to be closer to 300°C than 315°C. These data are presented graphically in Figure 5. The comparison given for commercial fluids at the top of Table 5 shows clearly the instability of the Fomblin Z family of fluids. The latter were the only materials tested having $-OCF_2OCF_2O-$ segments believed to be responsible for the observed poor Fomblin Z stability [Ref. 8].

3.3 CHARACTERIZATION AND THERMAL OXIDATIVE STABILITY TESTING OF MLO 90-9 CHLOROFLUOROPOLYALKYLETHER FLUID

3.3.1 Characterization

MLO 90-9 was one of chlorofluoropolyalkylether fluids selected for thermal oxidative stability testing in order to determine if chlorinated species could be detected among the degradation products. The structure originally assigned to this fluid was $ClCF_2CF(CF_2Cl)O[CF_2CF(CF_2Cl)O]_nX$, where X = CF_2Cl, CF_2CF_2Cl, $CF_2CF_2CF_2Cl$, and CF_3. From ^{19}F NMR spectroscopy the end group $ClCF_2CF(CF_2Cl)-$ appears to be absent; however, there is evidence for the presence of $-CF_2CF_2Cl$, $-CF_2CF_2CF_2Cl$, and $-CF_3$ end groups in the ratio of 2:1:1.5. The gas chromatogram (Figure 6) of the fluid shows a repeating pattern of two main peaks followed by group of much smaller peaks. Based on ^{19}F NMR and GC/MS data, the larger of the two peaks was identified as $ClCF_2CF_2O[CF(CF_2Cl)CF_2O]_nCF_3$ and the smaller as $ClCF_2CF_2O[CF(CF_2Cl)CF_2O]_nCF_2CF_2CF_2Cl$.

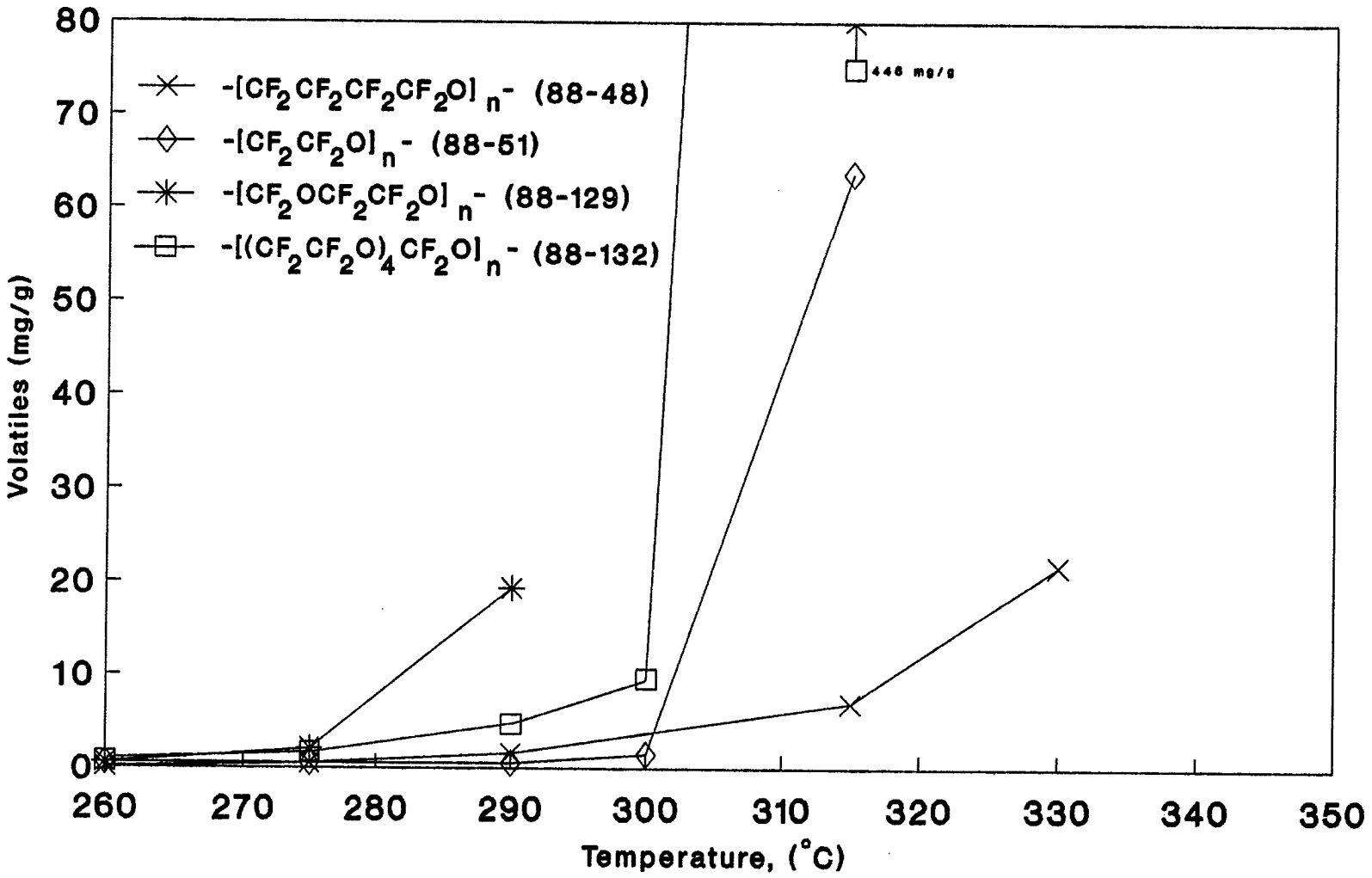

Figure 5. Comparison of thermal oxidative degradation data for MLO 88 series of experimental fluids.

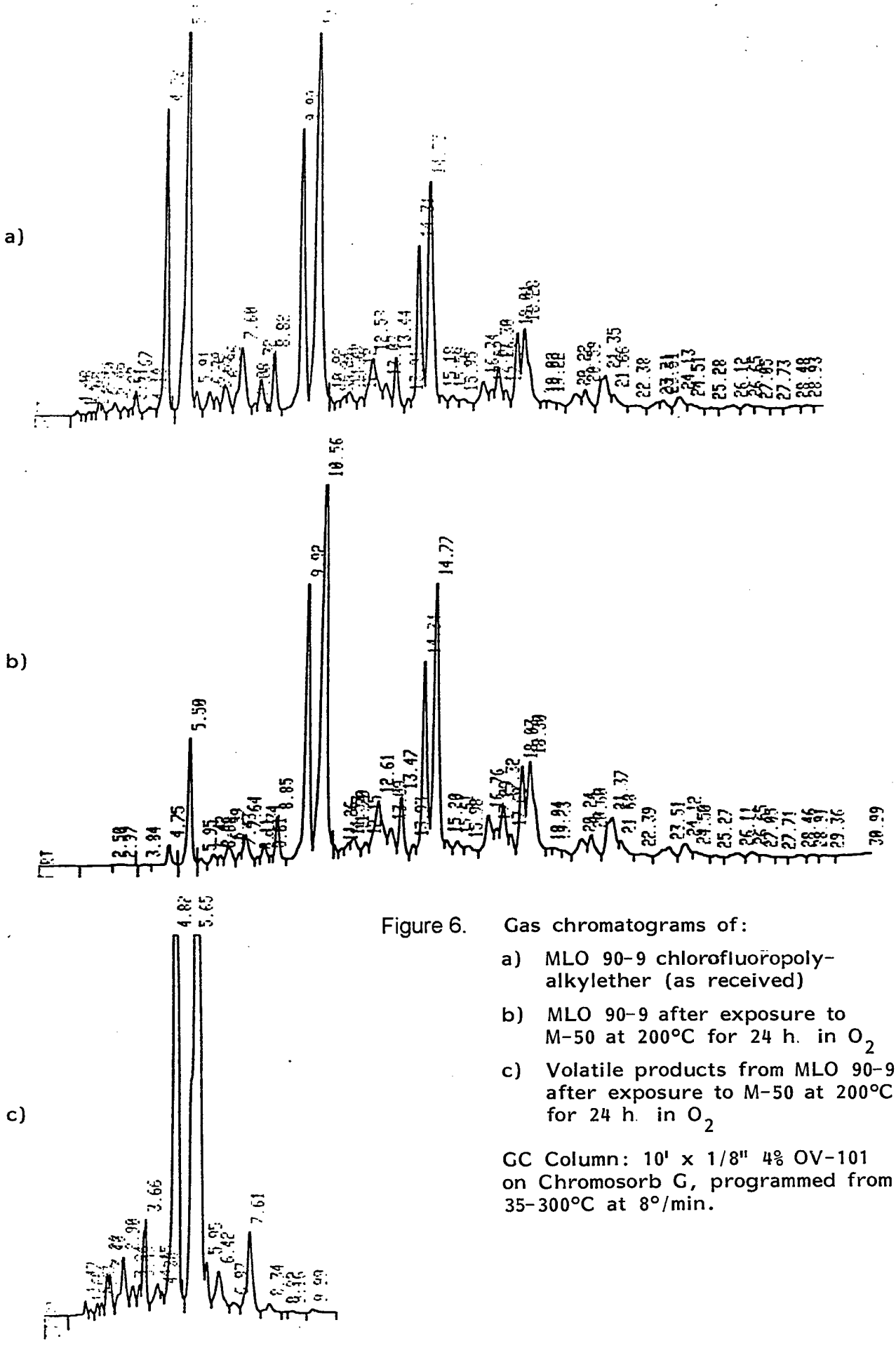

Figure 6. Gas chromatograms of:

a) MLO 90-9 chlorofluoropolyalkylether (as received)

b) MLO 90-9 after exposure to M-50 at 200°C for 24 h. in O_2

c) Volatile products from MLO 90-9 after exposure to M-50 at 200°C for 24 h. in O_2

GC Column: 10' x 1/8" 4% OV-101 on Chromosorb G, programmed from 35-300°C at 8°/min.

For the other characterized chlorofluoropolyalkylether fluid, MLO 88-134, the postulated structure was $ClCF_2CF_2O[CF_2CF(CF_2Cl)O]_nCF_3$. ^{19}F NMR analysis shows the end groups to be $-CF_2CF_2Cl$, $-CF_2CF_2CF_2Cl$, and $-CF_3$ in a ratio of 1.5:1.8:1. The gas chromatogram of the fluid is given in Figure 7. Based on GC/MS analysis, the main peak of the series consists of a mixture of $ClCF_2CF_2O[CF_2CF(CF_2Cl)O]_nCF_2CF_2CF_2Cl$ and $ClCF_2CF_2O[CF_2CF(CF_2Cl)O]_{n+1}CF_3$; the smaller peak appears to be $ClCF_2CF_2O[CF_2CF(CF_2Cl)O]_nCF_2CF(CF_3)OCF_2CF_2CF_2Cl$.

3.3.2 Stability Evaluations

The fluid, MLO 90-9, was subjected to thermal oxidative stability testing at 200°C. As shown by the data listed in Table 7 at 200°C there was minimal or no degradation. Based on the GC analysis, the volatile products consisted mainly of the fluid's most volatile components, which apparently can be distilled out under vacuum at room temperature (compare Figures 6c and 6a). Consequently, the gas chromatogram of the fluid after exposure (Figure 6b) shows that most of the initially eluting components (up to ~6 minutes) have been removed. The fluid was retested at a higher temperatures 230°C and 260°C; the amount of volatiles collected increased slightly. The gas chromatogram of the vapor phase of the volatiles from the 230°C exposure (Figure 8a) shows some early eluting peaks (<2 minutes) not observed in the original fluid. Based on GC/MS analysis, two of the peaks have been identified as $ClCF_2CF=CF_2$ and $ClCF_2CF_2OCF_2CF=CF_2$. The

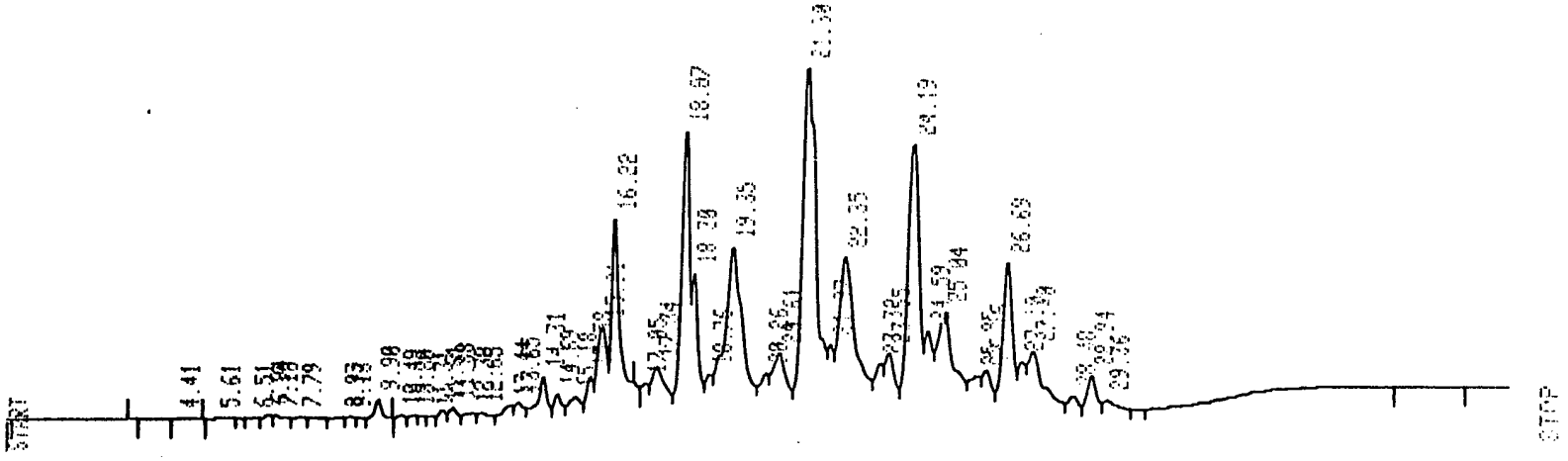

Figure 7. Gas chromatogram of MLO 88-134 chloroperfluoropolyalkylether (as received).

GC column: 10' x 1/8" 4% OV-101 on Chromosorb G programmed from 35-300°C at 8°/min.

TABLE 7

THERMAL OXIDATIVE BEHAVIOR OF MLO 90-9
CHLOROFLUOROPOLYALKYLETHER FLUID[a]

Test No	Wt., g	Temp °C	Volatiles mg/g	Coupon Weight Change, mg/cm^2	ID No.
23	3.22	200	13.1[b]	+0.06	5-90-102
25	3.22	230	75.1[b]	+0.01	5-90-106
26	3.23	260	183.3[b]	+0.02	5-90-117

(a) All the tests were performed in pure oxygen at the denoted temperature in the presence of an M-50 coupon over a 24 hr period using the modified, scaled-down, sealed version of the AFML Micro-O-C-Test arrangement.

(b) Consisted mainly of the most volatile components of the original fluid.

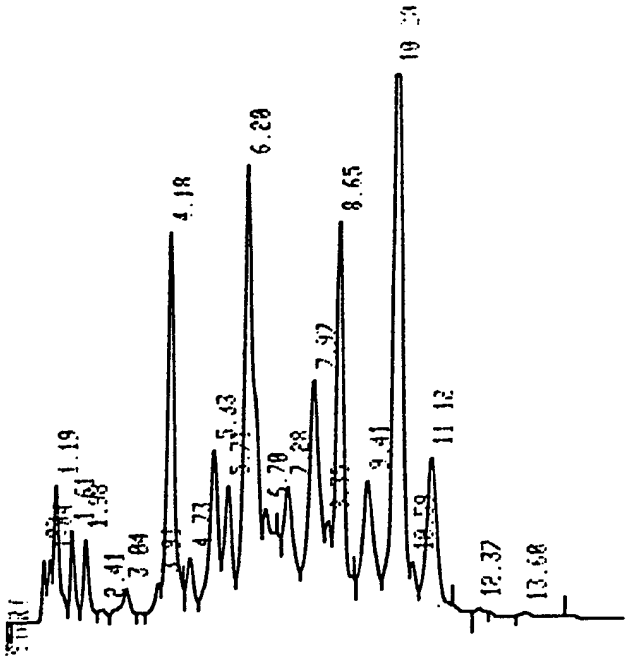

a) Vapor phase, programmed from 35(2 mm hold)-300°C at 8°/min.

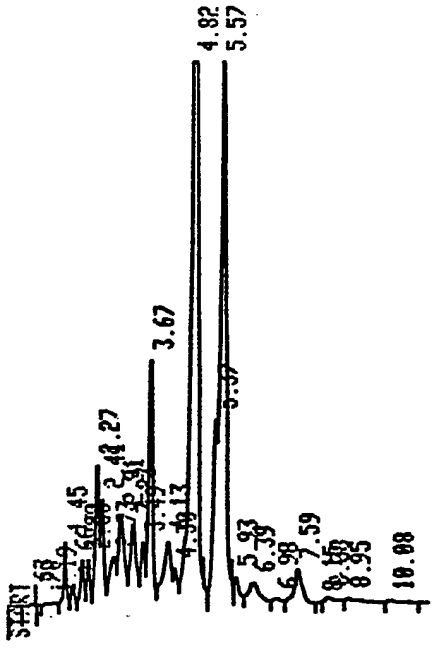

b) Liquid phase, programmed from 35-300°C at 8°/min.

Figure 8. Gas chromatograms of the vapor (a) and liquid (b) phases of the volatile products from MLO 90-9 after exposure to M-50 at 230°C for 24 h in O_2. GC column: 10' x 1/8" 4% OV-101 on Chromosorb G.

latter are definitely products of degradation; however, these compounds were produced only in trace quantities. The gas chromatogram of the liquid phase of the volatiles produced at 230°C (Figure 8) is very similar to that of the volatiles formed at 200°C (see Figure 6a). As mentioned earlier, these peaks are the volatile components of the original fluid. The GC trace of the fluid following the heat exposure at 230°C (Figure 9) shows depletion of the most volatile components.

3.4 CHARACTERIZATION AND STUDY OF THE SECOND SERIES OF EXPERIMENTAL PERFLUOROPOLYALKYLETHER FLUIDS AND COMMERCIAL FLUIDS

This series of fluids, listed in Table 8, was prepared using optimized direct fluorination procedures and more extensive post treatments than was the case for the materials discussed in Section 3.2. Inasmuch as these perfluoropolyalkylethers were to be employed in derivation of structure/property relationships the characterization and establishment of structures, on which to build the unavoidable assumptions, were mandatory. The commercial fluids listed in Table 9 provided both additional structural arrangements as well as different molecular weight fractions which permitted the development of molecular weight-viscosity curves. The latter were of great importance since none of the fluids are unimolecular and it was assumed that the use of an average molecular weight for a given spectrum of homologues does not invalidate computational treatments, and that the structural arrangements are the primary factors in imparting

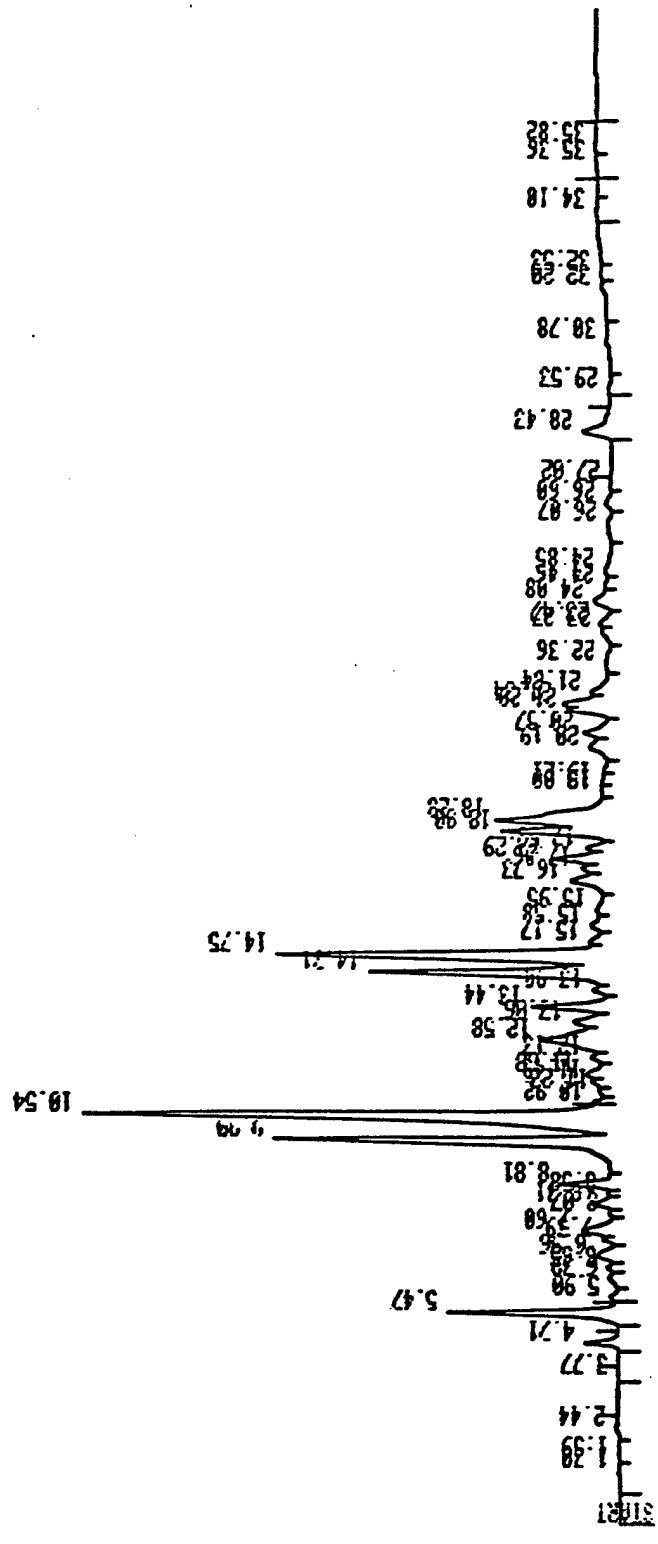

Figure 9. Gas chromatogram of MLO 90-9 after exposure to M-50 at 230°C for 24 h in O_2.

GC column: 10' x 1/8" 4% OV-101 on Chromosorb G programmed from 35-300°C at 8°/min.

TABLE 8

PROPERTIES OF PERFLUOROPOLYALKYLETHERS

Fluid	MLO No.	Molecular Weight[a]			Viscosity[b] cSt/°C			VI[c]	C/O
		Tech.	Exfl.	Osm.	-18	40	100		
Fluorinated Pluronic L-31	91-87	2850	3000	2800	599	47.8	7.18	109	~2.3
Fluorinated Polyglycol P15-200	91-88	4900	5400	4250	480	54.1	8.67	137	~2.3
$-(CF_2CF_2CF_2CF_2OCF_2O)_n-$	91-105	2700	2500	2500	-	20.8	5.04	183	2.5
$-(CF_2CF_2CF_2CF_2CF_2OCF_2O)_n-$	91-106	2800	2600	2500	602	27.7	5.80	159	3.0
$-(CF_2CF_2CF_2CF_2O)_n-$	91-126	3100	3000	2600	2370	52.0	7.73	114	4.0
Perfluoropoly(propylene oxide)	91-127	3250	3650	3100	7120	76.9	9.73	105	3.0
$-[CF_2CF_2OCF_2CF(CF_2CF_3)OCF_2O]_n-$	91-131	2750	2900	2900	-	22.6	5.00	155	2.3
$-[CF_2CF(CF_3)OCF_2CF(CF_3)OCF_2O]_n-$	91-132	2700	3300	3050	-	28.4	6.00	165	2.3
$-[(CF_2CF_2O)_4CF_2O]_n-$	91-157	1800	2100	2850	-	15.4	3.95	161	1.8
$-[CF_2CF(CF_2OCF_2CF_2OCF_2CF_2OCF_3)O]n-$	91-158	5650	4700	3950	4370	67.1	8.71	102	2.0
$-(CF_2CF_2O)_n-$ (cross-linked)	91-159	1500	1300	3250	1190	31.1	5.53	115	2.0
$-(CF_2CF_2OCF_2O)_n-$	91-160	2800	2300	2650	-	10.5	3.32	215	1.5
$-(CF_2CF_2O)_n-$ (linear)	91-161	2450	2450	3000	d	16.7[e]	3.99[e]	537	2.0
$-[(CF_2CF_2O)_3CF(CF_3)O]_n-$	91-162	1700	1750	2950	922	24.7	4.79	115	2.0

a) Number average molecular weights as calculated by Technolube and Exfluor from NMR data and as measured by vapor pressure osmometry by Technolube.
b) Viscosity determined by WL/MLBT except where noted.
c) Viscosity Index calculated by Technolube.
d) After 24 and 72 h crystals formed in fluid, viscosity 4618 and 4714 cSt respectively
e) These viscosity values were determined by Technolube.

TABLE 9

PROPERTIES OF COMMERCIAL PERFLUOROPOLYALKYLETHERS

Fluid	MLO No.	Molecular Weight NMR	Molecular Weight OSM.	Viscosity[a] cSt/°C -18	Viscosity[a] cSt/°C 40	Viscosity[a] cSt/°C 100	VI
Krytox 143AZ	66-92	-	1800	-	15.2	3.05	21
Krytox 143AA	66-91	-	2400	-	36.9	5.74	93
Krytox 143AB	42420[b]	4200	3200	-	66.9	8.86	106
Krytox 143AB	66-93	-	3450	-	78.5	10.3	114
Krytox 143AC	53538[b]	6300	5250	-	220	22.6	125
Krytox 143AC	71-6	6800	5400	33830	257	27.3	140
Krytox 143AD	66-95	-	6650	-	420	40.9	148
Aflunox 606	88-295	-	2350	-	28.6	4.84	84
Aflunox 1406	88-296	-	2900	-	53.2	7.64	107
Aflunox 2507	88-298	4300	3800	8550	95.2	12.0	117
Perfluoropoly(propylene oxide)	91-127	3250	3100	7120	76.9	9.73	105
Fluorinated Krytox 143AC	91-21	7250	6000	-	329	33.3	143
Demnum S-20	-	-	2500	-	23.8	5.48	179
Demnum S-65	-	-	4700	-	63.8	12.6	201
Demnum S-100	-	-	5700	-	86.1	16.4	206
Demnum S-200	-	-	7900	-	176	31.7	225

a) All viscosities listed were determined by Technolube except for the -18°C values which were determined by WL/MLBT.
b) Manufacturer batch number.

properties (i.e., viscosity, thermal oxidative stability) whereas the nature of the end-groups is of negligible influence.

3.4.1 Characterization

All the experimental fluids were subjected to detailed ^{19}F NMR analysis. The main objectives were to ascertain that the arrangements postulated were correct, to identify end-groups and their relative ratios, to determine molecular weights, and to identify the nature and proportion of impurities. The actual spectra are compiled in the Experimental Section. All the materials consisted of a series of analogues having different end-groups. This is clearly evident from the gas chromatograms presented in Figures 10-19 confirming the ^{19}F NMR data. The specific end-groups present in representative perfluoropolyalkylether analogues were identified by GC/MS in the first series of the experimental fluids. The data were discussed in Section 3.2 and will be not reiterated here. The commercial fluids likewise consist of a homologous series of differently end-capped telomers. This is illustrated by the chromatograms for Krytox family of materials given in Figures 20 and 21 (wherein the elution envelopes are associated with the average molecular weights). Corresponding chromatograms were obtained for representative Aflunox fluids as shown by Figures 22 and 23. The small adjacent peaks in Krytox fluids were in the past believed to be due to the presence of the hydrogen-terminated chains. Since Aflunox is hydrogen-free, as determined by ^{1}H NMR,

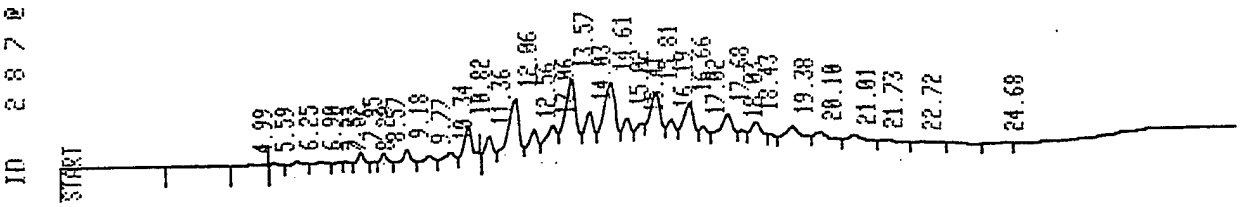

Figure 10. GC trace of MLO 91-105; $-(CF_2CF_2CF_2CF_2OCF_2O)_n-$

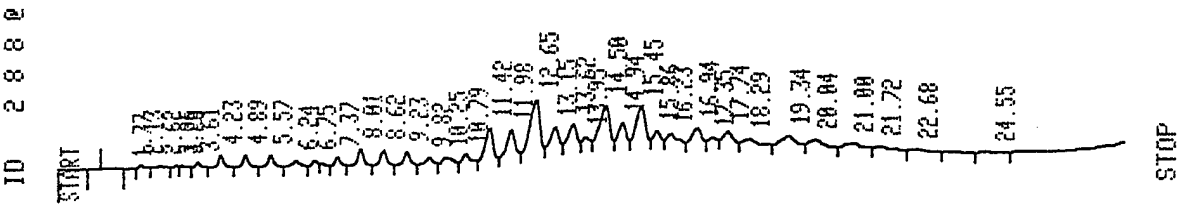

Figure 11. GC trace of MLO 91-106; $-(CF_2CF_2CF_2CF_2CF_2OCF_2O)_n-$

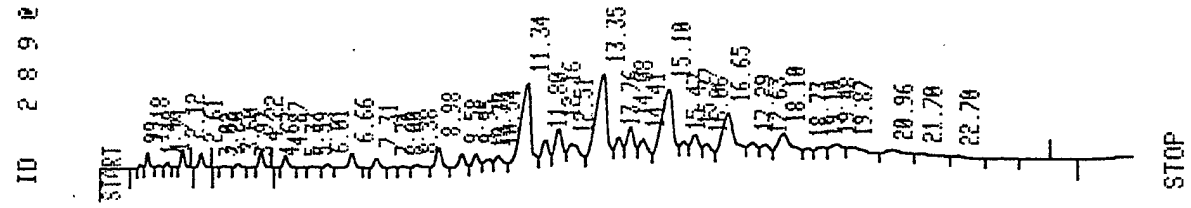

Figure 12. GC trace of MLO 91-126; $-(CF_2CF_2CF_2CF_2O)_n-$

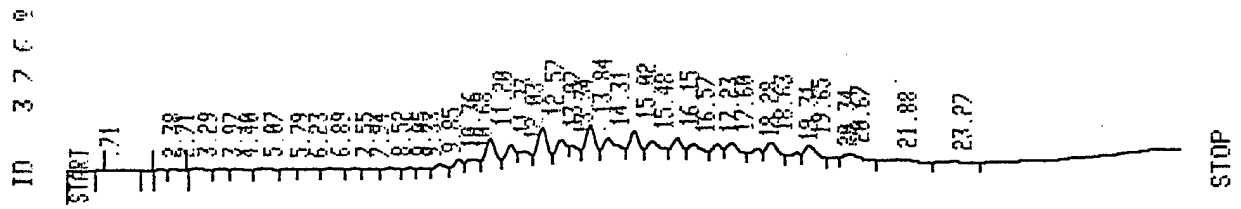

Figure 13. GC trace of MLO 91-127; $-[CF(CF_3)CF_2O]_n-$

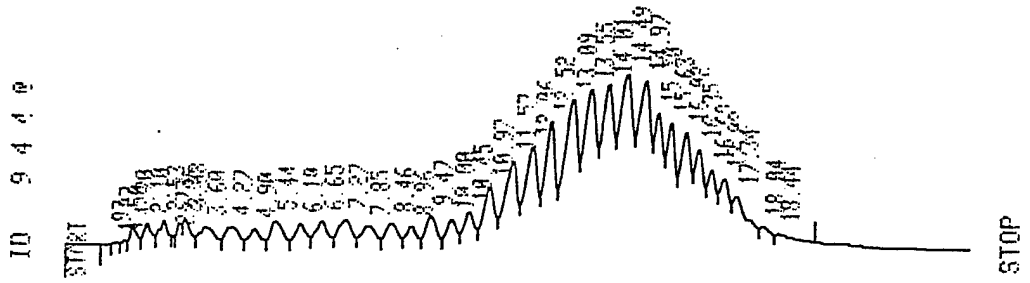

Figure 14. GC Trace of MLO 91-131; $-[CF_2CF_2OCF_2CF(CF_2CF_3)OCF_2O]_n-$

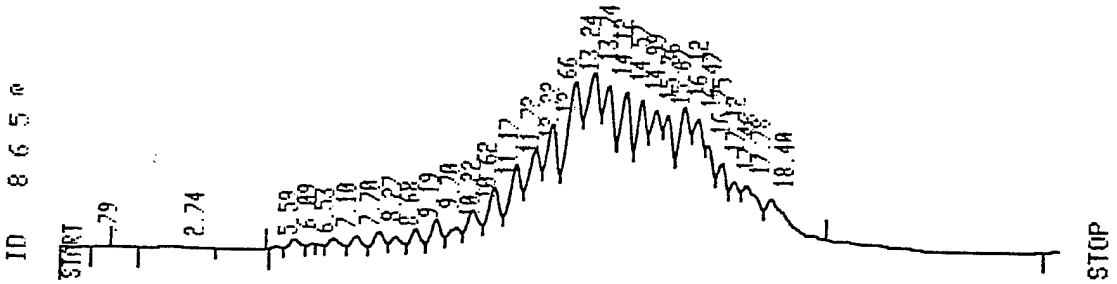

Figure 15. GC trace of MLO 91-132; $-[CF_2CF(CF_3)OCF_2CF(CF_3)OCF_2O]_n-$

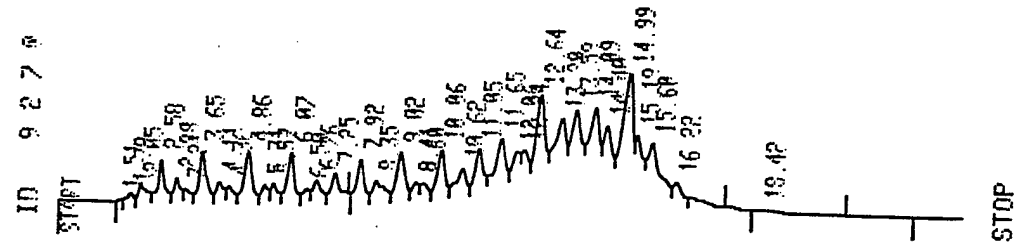

Figure 16. GC Trace of MLO 91-157; $-[(CF_2CF_2O)_4CF_2O]_n-$

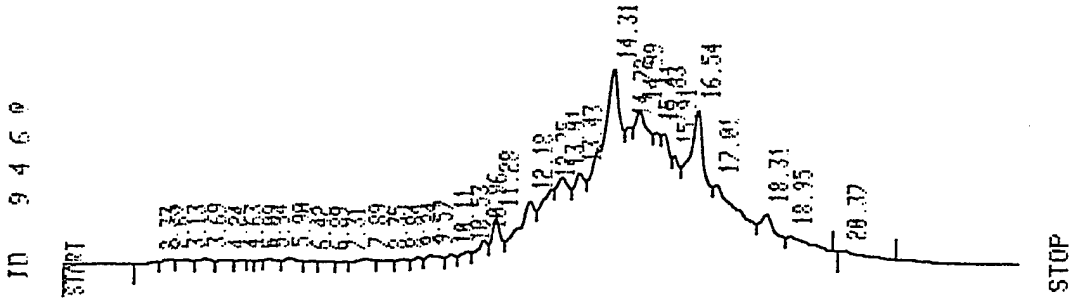

Figure 17. GC Trace of MLO 91-158; $-[CF_2CF(CF_2OCF_2CF_2OCF_2CF_2OCF_3)O]_n-$

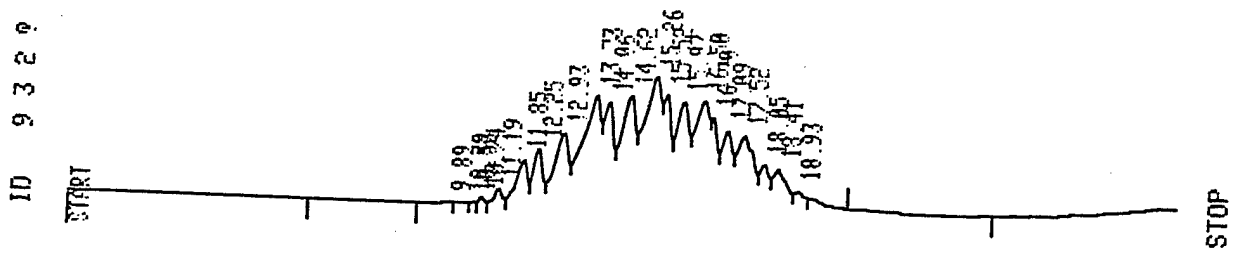

Figure 18. GC Trace of MLO 91-160; $-(CF_2CF_2OCF_2O)_n-$

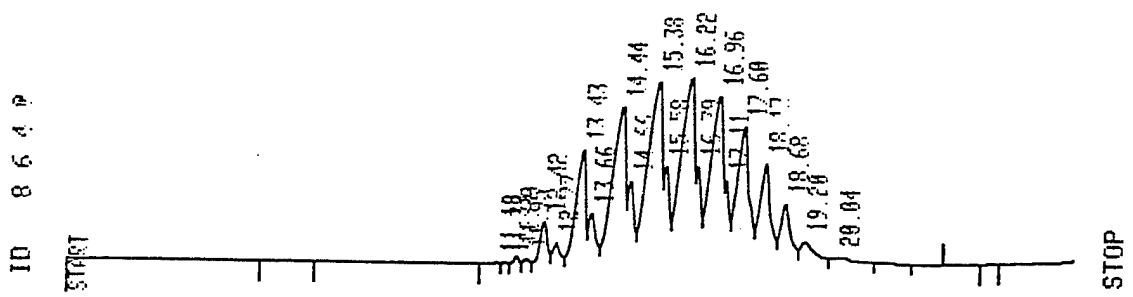

Figure 19. GC trace of MLO 91-161; $-(CF_2CF_2O)_n-$

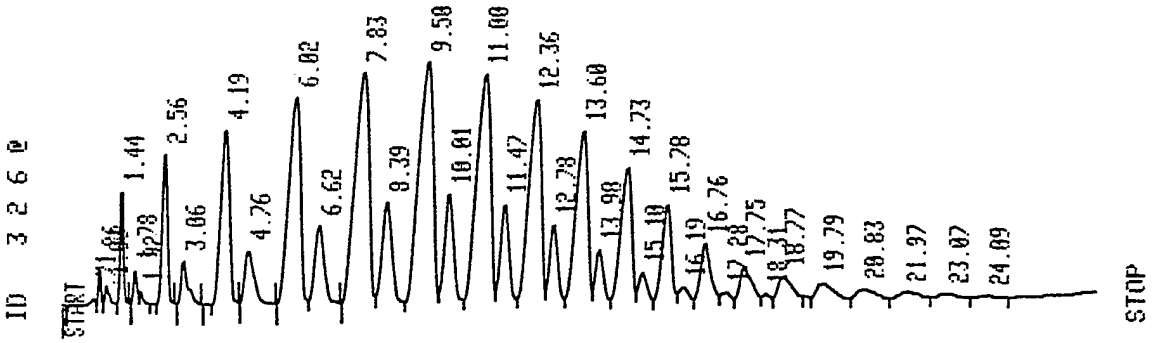

Figure 20. **GC trace of Krytox 143AZ (ELO 66-92).**

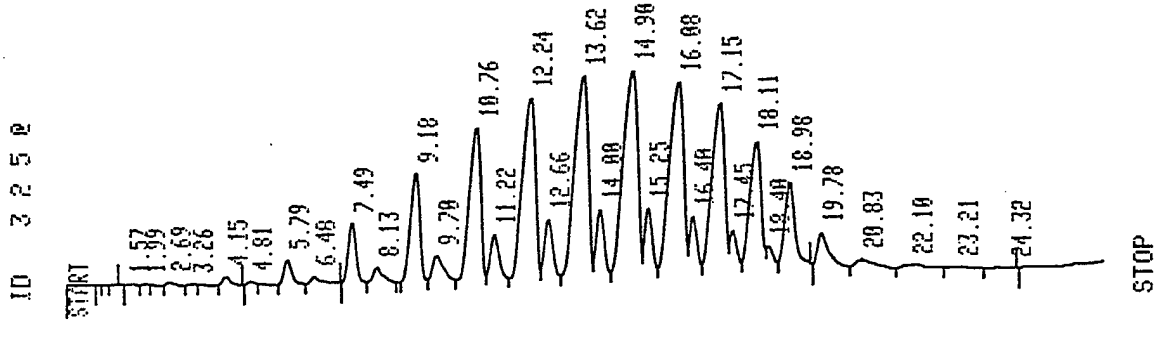

Figure 21. **GC trace of Krytox 143AA (ELO 66-91).**

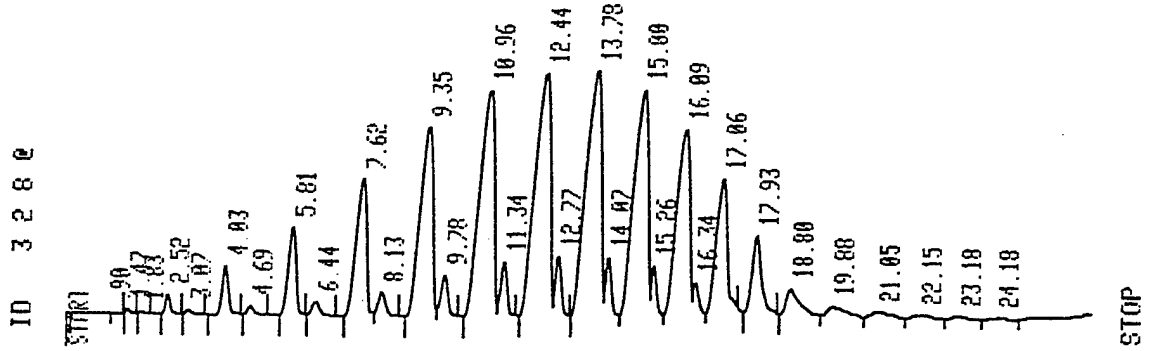

Figure 22. GC trace of Aflunox 606 (MLO 88-295).

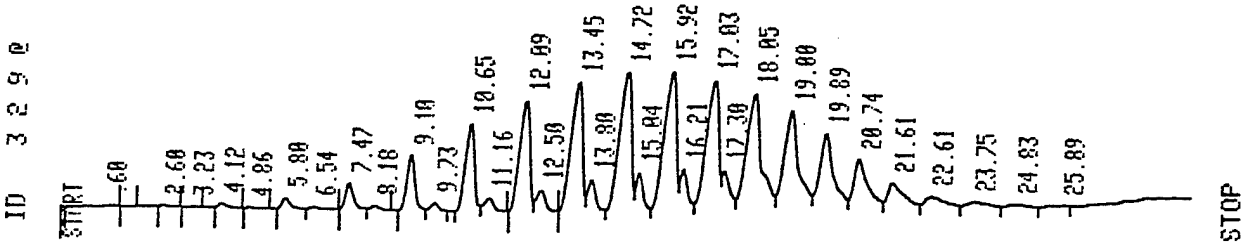

Figure 23. GC trace of Aflunox 1406 (MLO 88-296).

it is apparent that the observed pattern is due to different perfluoroalkyl end-groups. This aspect is clearly illustrated for Demnum S-20 in Figure 24 where each of the peaks in the repeating pattern was identified.

As mentioned earlier, all the experimental fluids —Krytox 143AC, fluorinated Krytox 143AC, Demnum S-20, Demnum S-100 and Aflunox— were analyzed by NMR spectroscopy. These data are given in the Experimental Section. It should be emphasized that ^{1}H NMR spectra of Demnum, Aflunox and the fluorinated Krytox did not show the presence of hydrogen. Hydrogen-containing end-group, $-OCF(CF_3)H$, was clearly evident in the ^{1}H NMR multi-scan spectrum of Krytox 143AC.

Viscosity of any perfluoropolyalkylether is dependent both on its composition, i.e., structure, and its molecular weight. This number average molecular weight dependence is illustrated for the Krytox 143 series by the curve given in Figure 25. Regardless of the poly(perfluoropropene oxide) origin the molecular weight/viscosity profile is relatively consistent. Even the material obtained by direct fluorination of its hydrocarbon precursor was accommodated by the curve shown in Figure 26. Some discrepancy would be expected here since the structure, due to the synthesis path, is not as regular as that of the materials obtained by telomerization of hexafluoropropene oxide. As will be discussed later, it is the regularity which leads to a closely wound helix arrangement, which translates into the high viscosity characteristics.

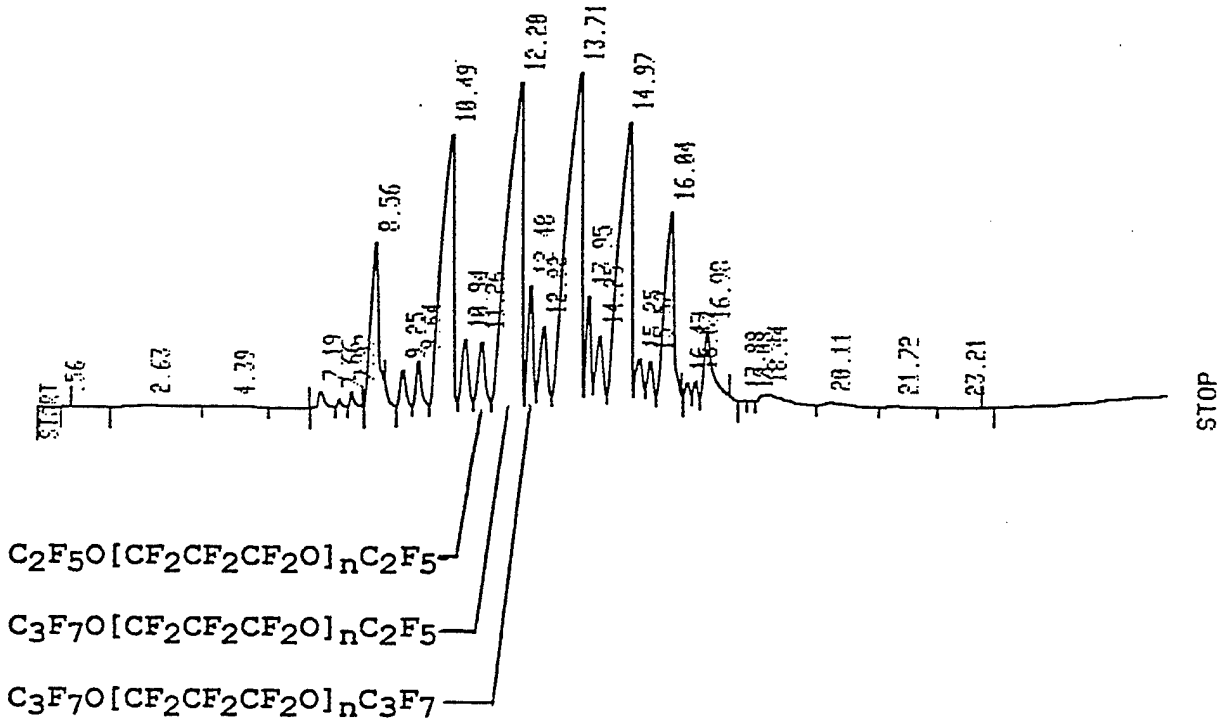

Figure 24. Gas chromatogram of fraction 1 from distillation of Demnum S-20 (MLO 88-177).

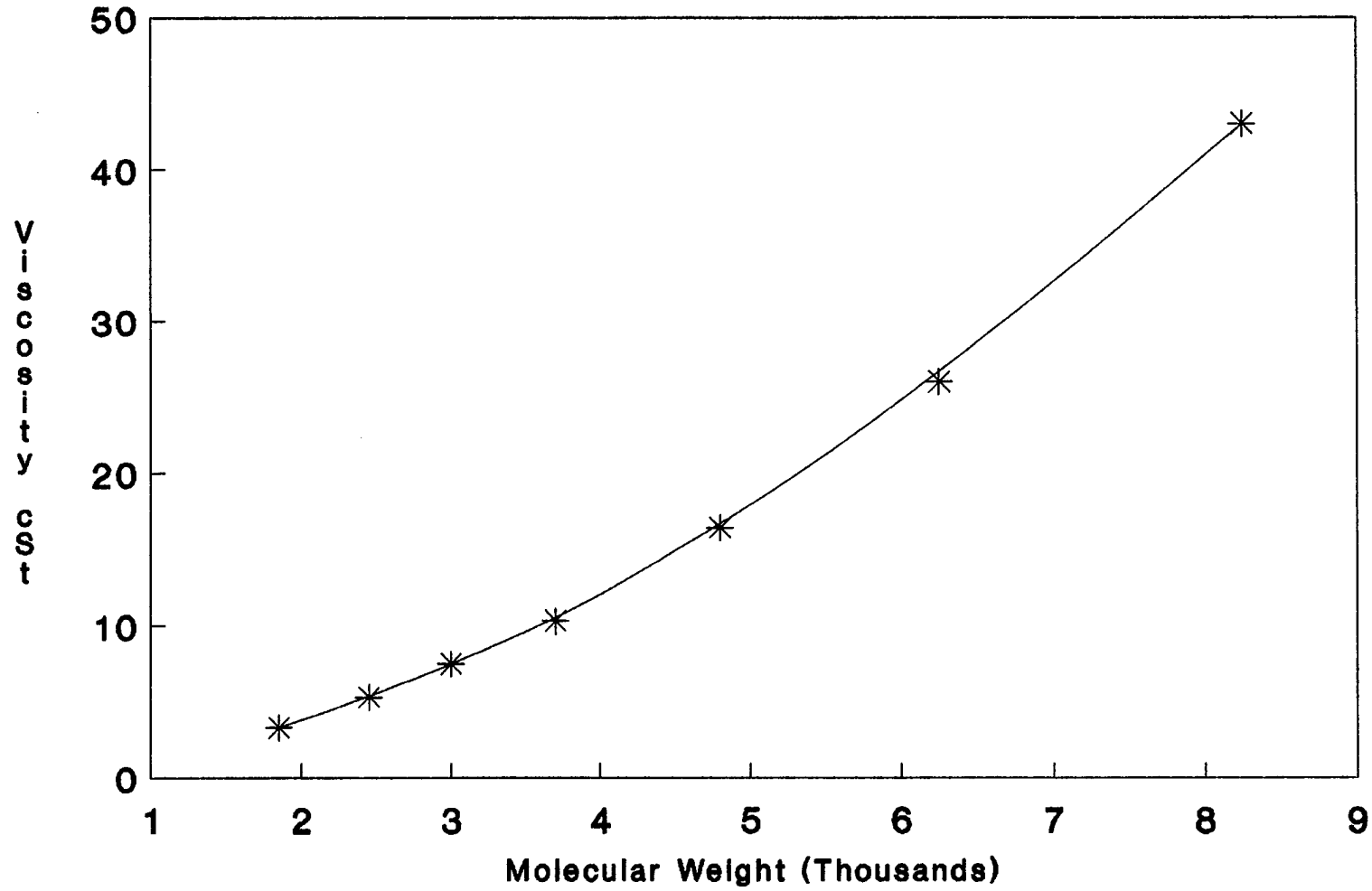

Figure 25. Plot of 100°C viscosity versus molecular weight for Krytox 143 fluids

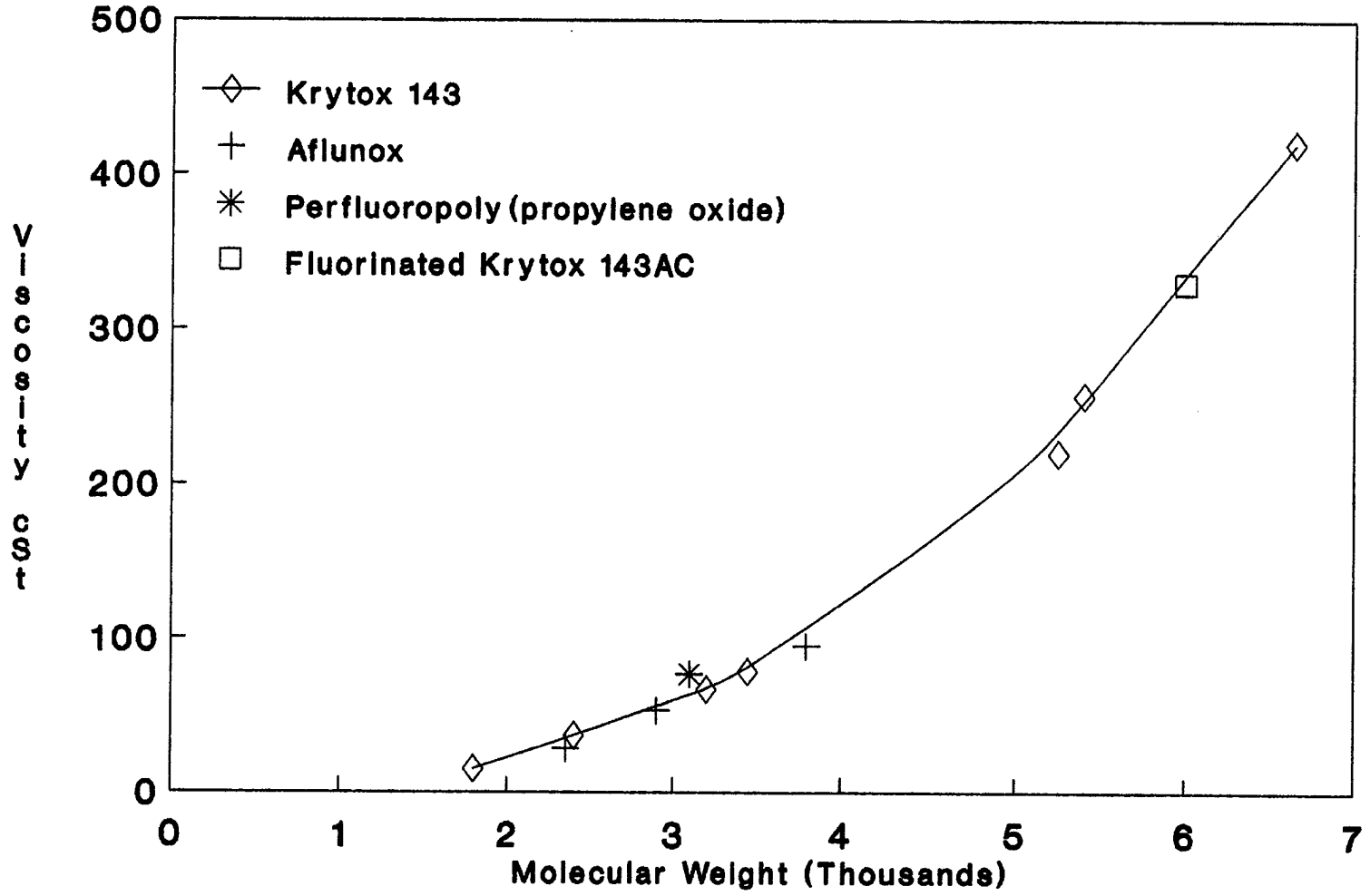

Figure 26. Plot of 40°C viscosity versus molecular weight for $C_3F_7O[CF(CF_3)CF_2O]_nC_2F_5$ fluids from different sources.

To develop any viscosity/structure relationships requires the materials under consideration to be of identical molecular weights or molecular weight ranges. The obtaining of data for the poly(perfluoropropene oxide) family of fluids could be readily accomplished since a number of different molecular weight range fractions were available (see Table 9). In the case of Demnum and the experimental fluids, fractional distillation into more narrow molecular weight components was necessary to obtain the data points required for the viscosity/molecular weight plots. The distillation details are compiled in the Experimental Section (Table 60). The viscosity/molecular weight relationships for the fluids, employed in the development of the viscosity/structure relationships are given in Figures 27 and 28 for the 40°C and 100°C viscosities, respectively.

3.5 DEVELOPMENT OF QUANTITATIVE STRUCTURE/ACTIVITY (VISCOSITY) RELATIONSHIPS

None of the relatively high molecular weight perfluoropolyalkylethers that exhibit desirable viscosities and volatilities are unimolecular. All consist of telomer mixtures due to the nature of syntheses. An ability to correlate the structural arrangements and molecular weights, or rather molecular weight ranges, with viscosity characteristics would permit the identification of optimum perfluoropolyalkylethers for specific applications. Predictions of fluoroelastomer/chloro-fluorocarbon swell [Ref. 18] and polysilahydrocarbon structure/viscosity [Ref. 19] were successfully accomplished

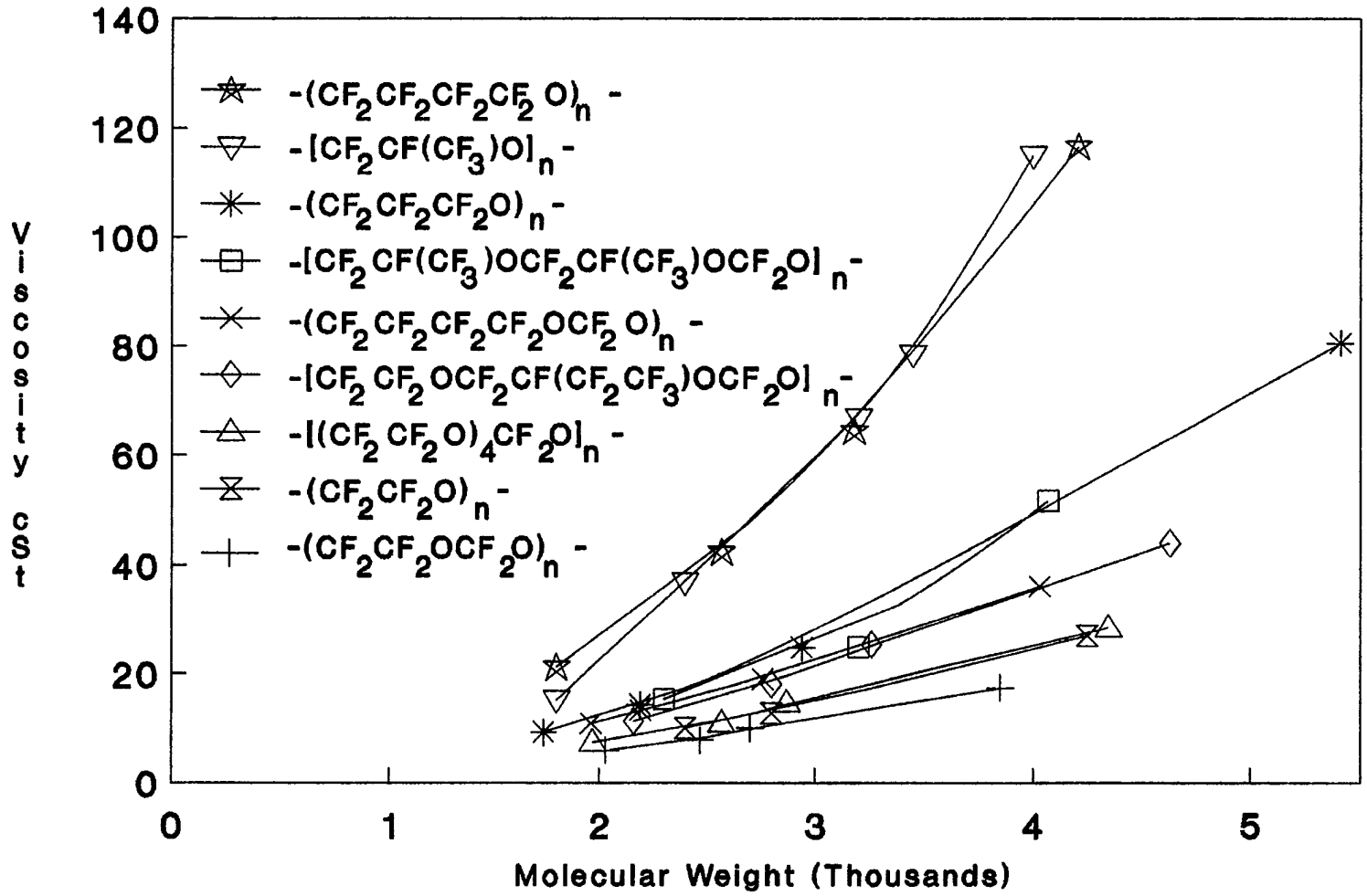

Figure 27. Viscosity/molecular weight profiles for perfluoropolyalkylethers at 40°C.

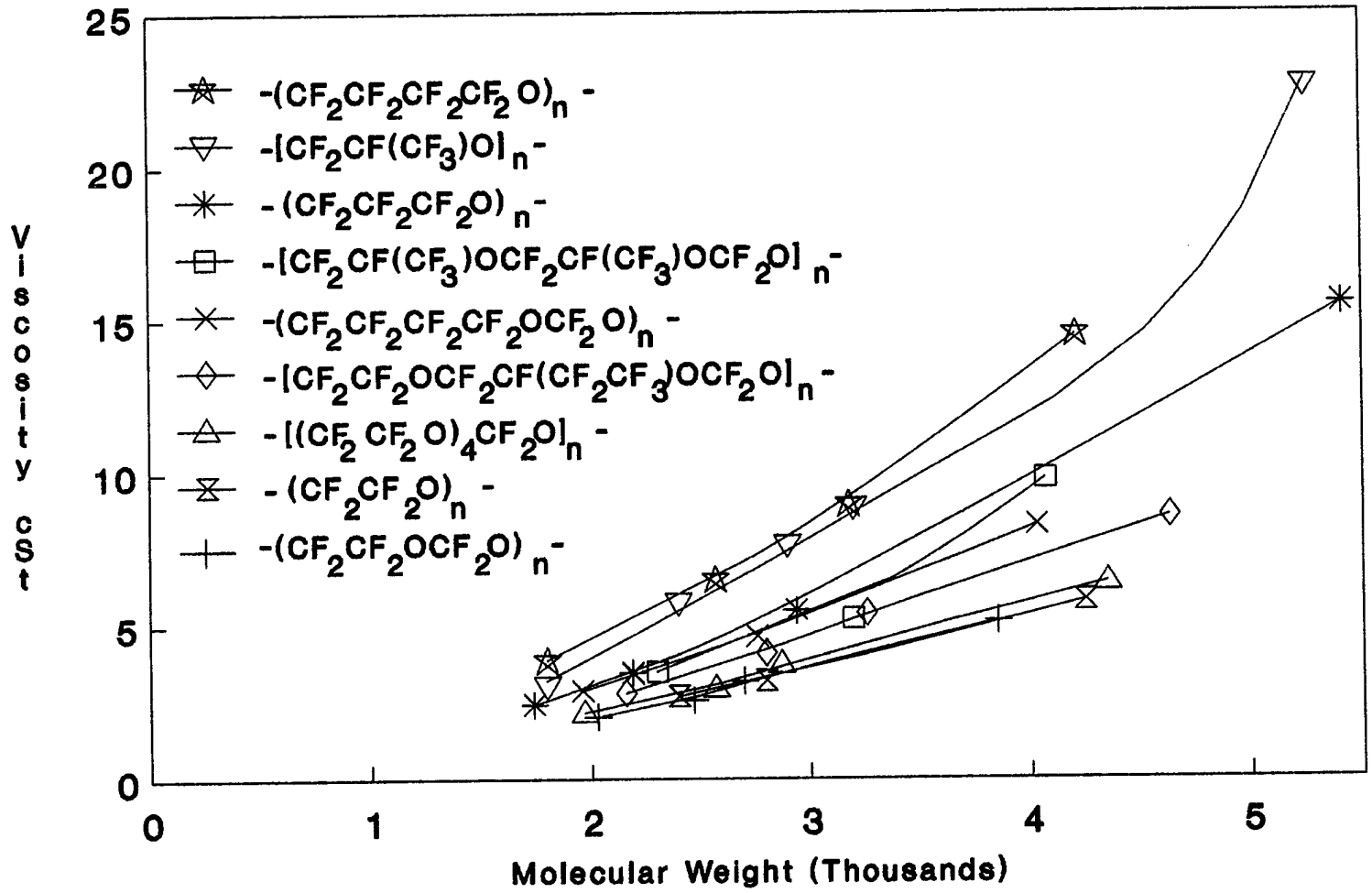

Figure 28. Viscosity/molecular weight profiles for perfluoropolyalkylethers at 100°C.

using a quantitative structure-activity relationships (QSAR). These studies provided the basis for the present undertaking.

For comparison of inherent viscosities and the determination of viscosity/structure relationships, as mentioned, materials of identical molecular weights or molecular weight ranges are required. The data used, compiled in Table 10, was obtained from plots given earlier in Figures 27 and 28. To develop QSAR expressions, the descriptors listed in Table 11 were employed in multivariate linear regression analysis. Using three descriptors with n = 9 (data points) gave r (Pearson correlation coefficient) of 0.963 and s (standard error estimate) of 4.27. The data point scatter is illustrated in Figure 29. With six descriptors r was raised to 0.985, s was 4.33; the actual plot is presented in Figure 30. In view of these results and the difficulty in encoding more complex structures, an approach involving energy parameters was investigated next.

The flexibility of a molecule, i.e., the ease to bend, is one of the major factors affecting the flow i.e., viscosity. In perfluoropolyalkylethers the carbon to oxygen ratio to a degree is related to this property. However, the latter relationship breaks down completely in the case of branched materials, as evident from the comparison of the relative viscosities of the isomers $-(CF_2CF_2CF_2O)_n-$ and $-(CF(CF_3)CF_2O)_n-$. In the case of longer CF_2 chains the C/O ratio provides an inadequate correlation as exemplified by the large difference in relative viscosities of $-(CF_2CF_2CF_2O)_n-$ and $-(CF_2CF_2CF_2CF_2O)_n-$.

TABLE 10

PERFLUOROPOLYALKYLETHER LISTING AND VISCOSITY DATA

Structure	MW 2500 Viscosity, cSt		MW 4000 Viscosity, cSt	
	40°C	100°C	40°C	100°C
$-(CF_2CF_2OCF_2O)_n-$	8.61	2.78	18.5	5.5
$-(CF_2CF_2O)_n-$	10.7	2.88	23.5	5.0
$-[(CF_2CF_2O)_4CF_2O]_n-$	10.8	3.03	25.0	5.5
$-[CF_2CF_2OCF_2CF(CF_2CF_3)OCF_2O]_n-$	15.0	3.55	35.0	7.0
$-(CF_2CF_2CF_2CF_2OCF_2O)_n-$	16.5	4.05	35.7	8.15
$-[CF_2CF(CF_3)OCF_2CF(CF_3)OCF_2O]_n-$	17.1	3.80	37.0	7.0
$-(CF_2CF_2CF_2O)_n-$	18.9	4.30	49.0	9.0
$-[CF_2CF(CF_3)O]_n-$	40.8	6.05	115.0	12.0
$-(CF_2CF_2CF_2CF_2O)_n-$	41.8	6.36	106.0	13.0

TABLE 11

STRUCTURAL DESCRIPTORS CONSIDERED

Carbon to oxygen ratio
Total number of carbons
Total number of oxygens
Total number of tertiary carbons
Number of segments in repeating group
Number of carbons in segment 1
Number of oxygens in segment 1
Carbon to oxygen ratio in segment 1
Number of carbons adjacent in segment 1
Number of tertiary carbons in segment 1
Number of carbons in branch of segment 1
Number of oxygens in branch of segment 1
Carbon to oxygen ratio in branch of segment 1
Number of carbons in segment 2
Number of oxygens in segment 2
Carbon to oxygen ratio in segment 2
Number of carbons adjacent in segment 2
Number of tertiary carbons in segment 2
Number of carbons in branch of segment 2
Number of oxygens in branch of segment 2
Carbon to oxygen ratio in branch of segment 2

Group and segment defined for e.g. $[(CF_2CF_2O)_4CF_2O]$ are as follows: Group = $[(CF_2CF_2O)_4CF_2O]$, Segment = $(CF_2CF_2O)_4$, CF_2O. The same values are assigned for type 2 as type 1 segments when only one type of segment is present.

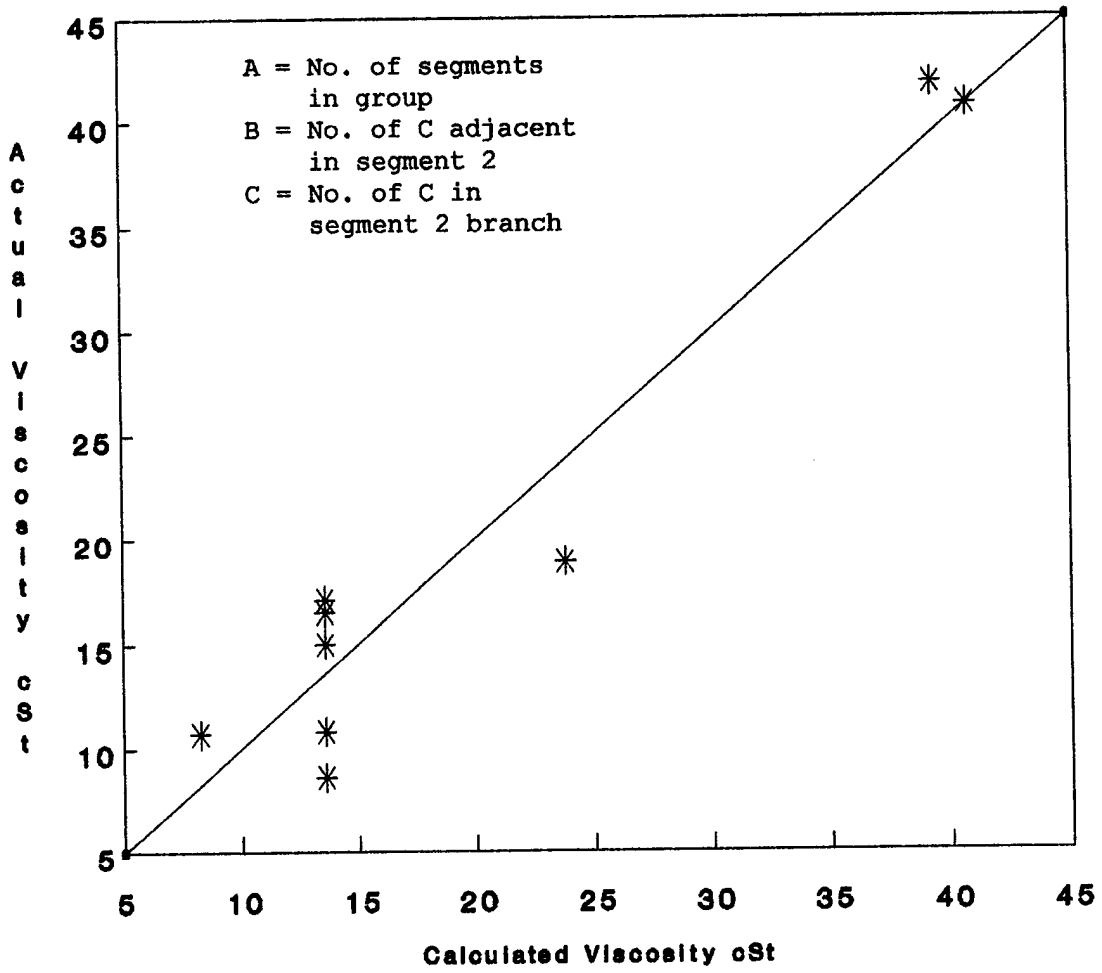

40°C Viscosity = 20.90(A) + 15.55(B) + 32.55(C) - 43.75

Figure 29. Calculated versus actual viscosity at 40°C as a function of three descriptors.

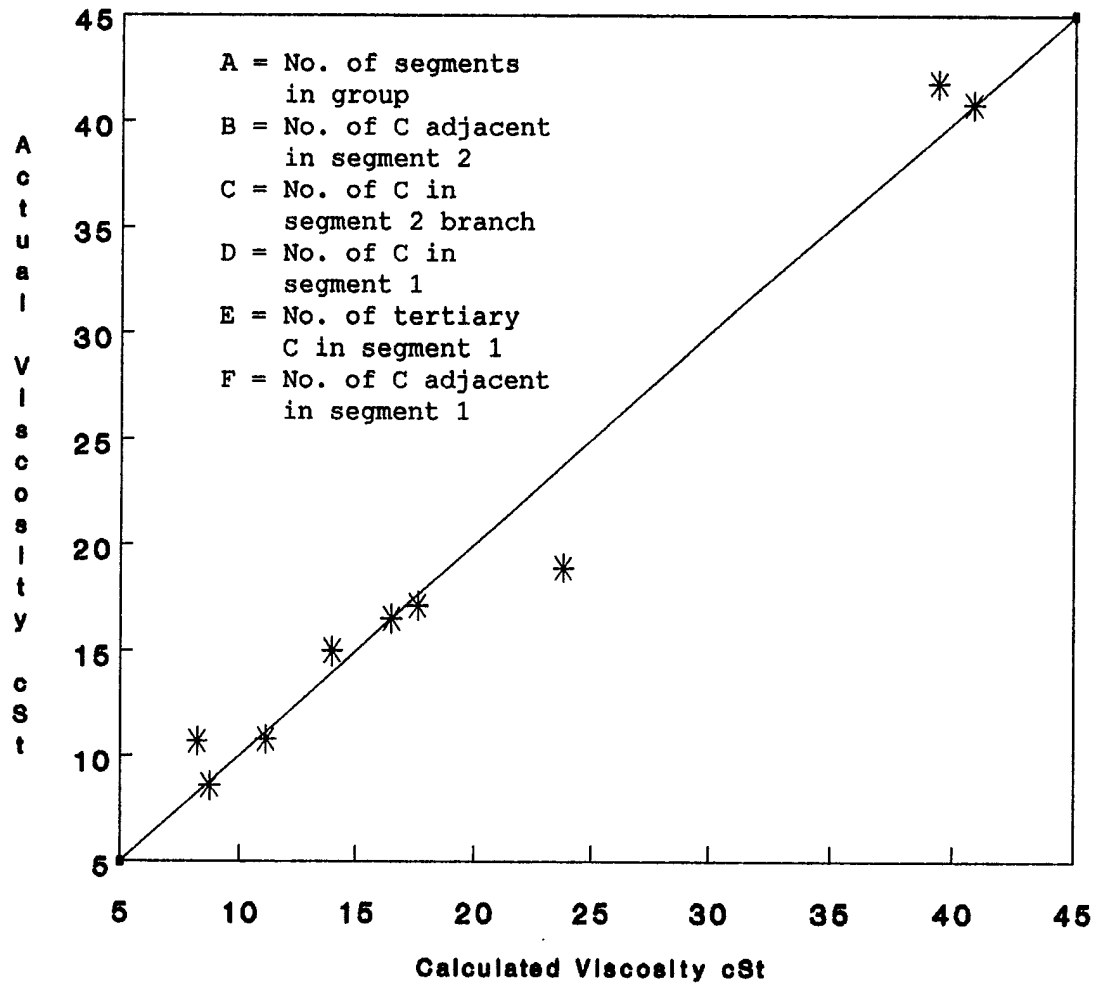

$$40°C\ \text{Viscosity} = 12.22(A) + 11.69(B) + 28.53(C) + 0.39(D) + 3.63(E) + 3.47(F) - 35.07$$

Figure 30. Calculated versus actual viscosity at 40°C as a function of six descriptors.

Molecular conformations of the perfluoropolyalkylethers presented in Figures 31-34 illustrate these aspects. Of special interest are the closely packed helical structures exhibited by the branched arrangements namely:

$CF_3O[CF_2CF_2OCF_2CF(CF_2CF_3)OCF_2O]_6CF_3$,

$CF_3O[CF_2CF(CF_3)OCF_2CF(CF_3)OCF_2O]_6CF_3$ and $CF_3O[CF_2CF(CF_3)O]_{14}CF_3$. Another oligomer of the last material was reported by Pacansky et al [Ref. 20]. The coiling effect is absent in the short chain analogues [Ref. 21]; this aspect illustrates the inherent danger in developing theories regarding the behavior of polymers based on low molecular weight model compounds.

It is obvious that bonding energies, in particular bending energies, are major factors contributing to viscosity characteristics of a given material. To calculate the energy parameters, a number of assumptions and simplifications had to be made. Thus, it was assumed that the behavior of a unimolecular fluid parallels that of a telomer mixture of the same number average molecular weight. Furthermore, that the end-groups as such do not affect viscosity. Using these constraints the bending energies were calculated for the 2500 and 4000 molecular weight systems. The molecular weights of actual arrangements were selected as close as possible to these limits. These data are listed in Table 12.

Using C/O ratios and bending energies the expressions given below were developed for viscosities of the 2500 and 4000 molecular weight series at 40 and 100°C.

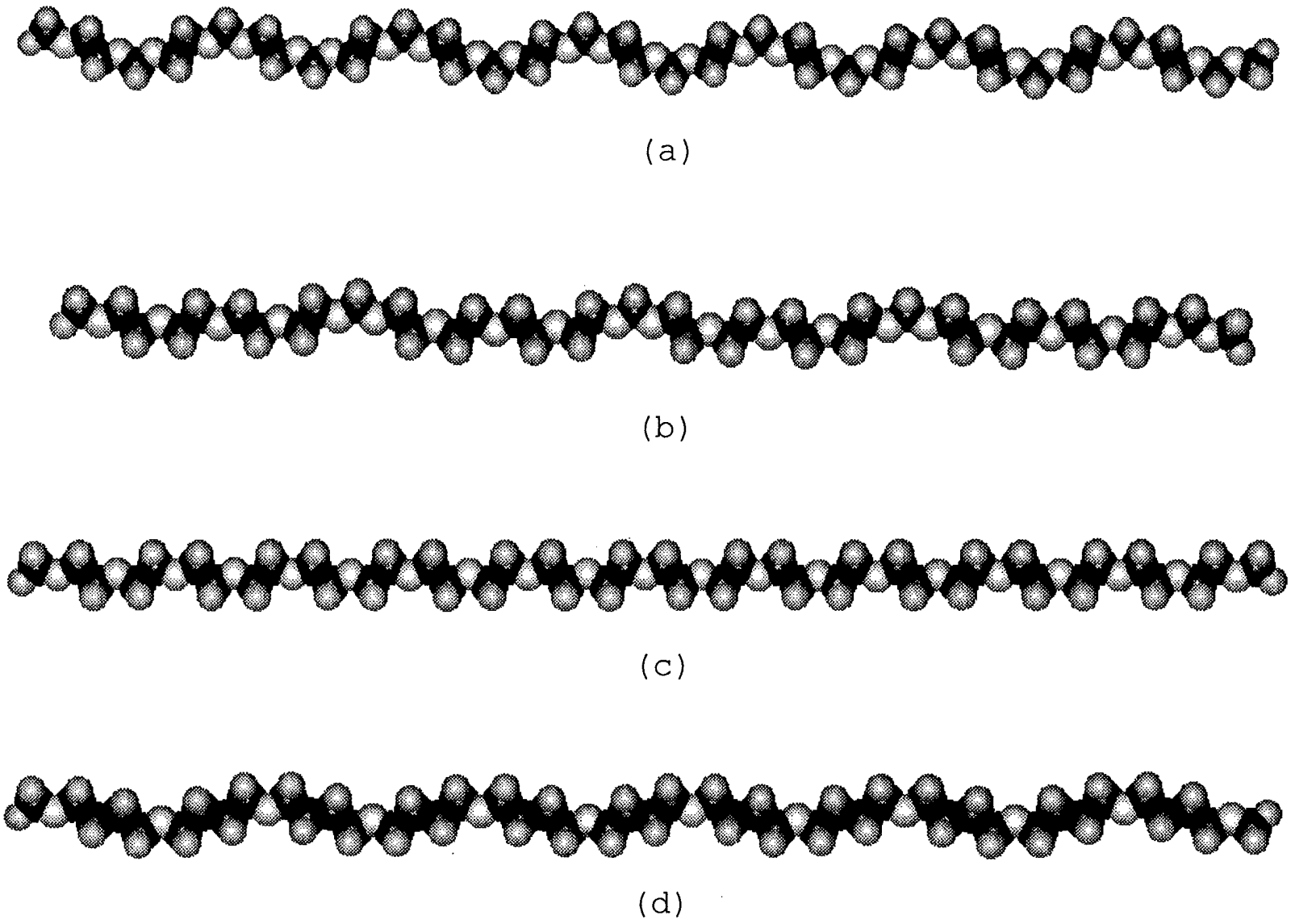

Figure 31. The conformations obtained with molecular mechanics for perfluoropolyalkylethers: (a) $CF_3O(CF_2CF_2OCF_2O)_{13}CF_3$, (b) $CF_3O[(CF_2CF_2O)_4CF_2O]_4CF_3$, (c) $CF_3O(CF_2CF_2O)_{20}CF_3$, (d) $CF_3O(CF_2CF_2CF_2CF_2O)_{11}CF_3$.

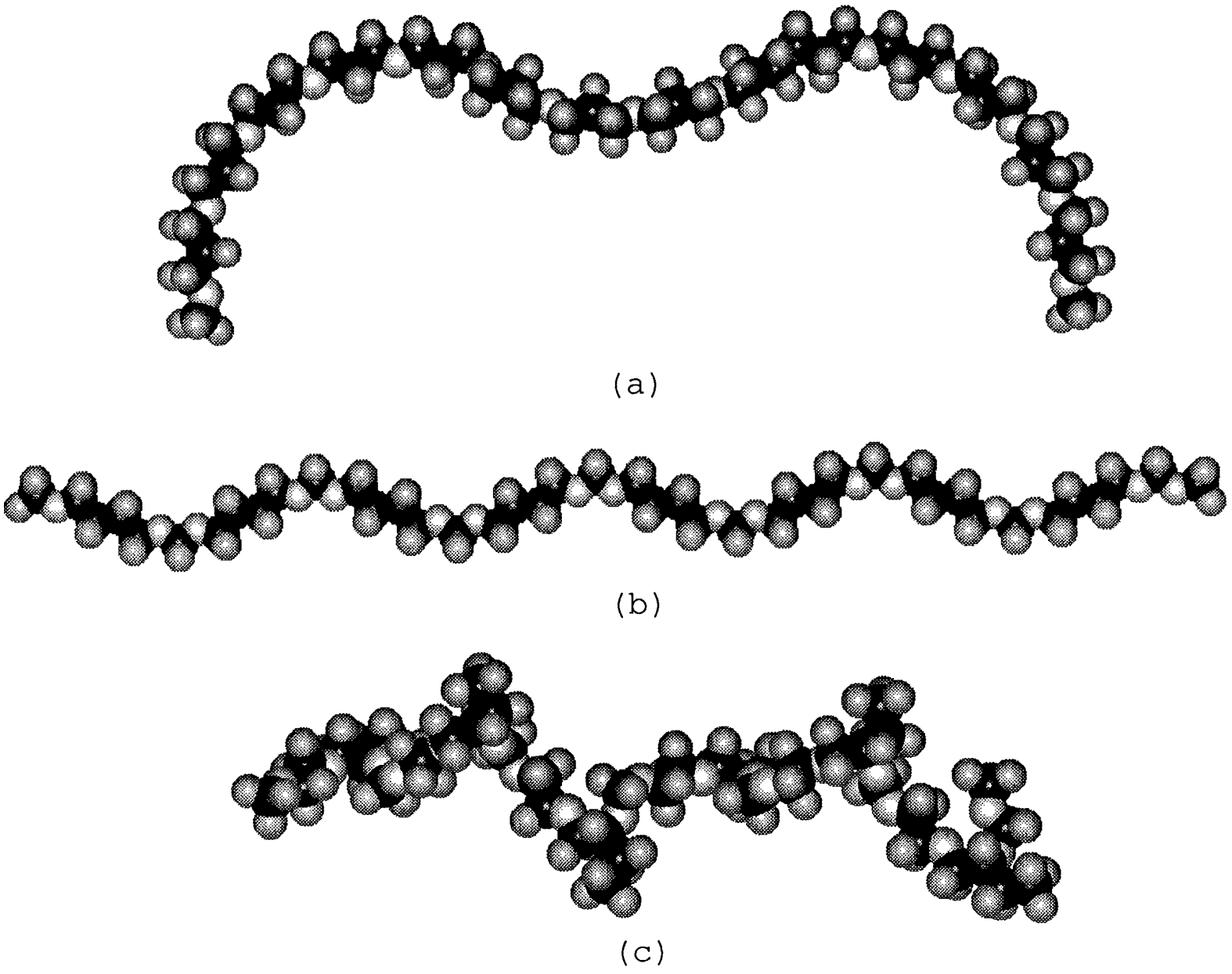

Figure 32. The conformations obtained with molecular mechanics for perfluoropolyalkylethers: (a) $CF_3O(CF_2CF_2CF_2O)_{14}CF_3$, (b) $CF_3O(CF_2CF_2CF_2CF_2OCF_2O)_8CF_3$, (c) $CF_3O[CF_2CF_2OCF_2CF(CF_2CF_3)OCF_2O]_6CF_3$

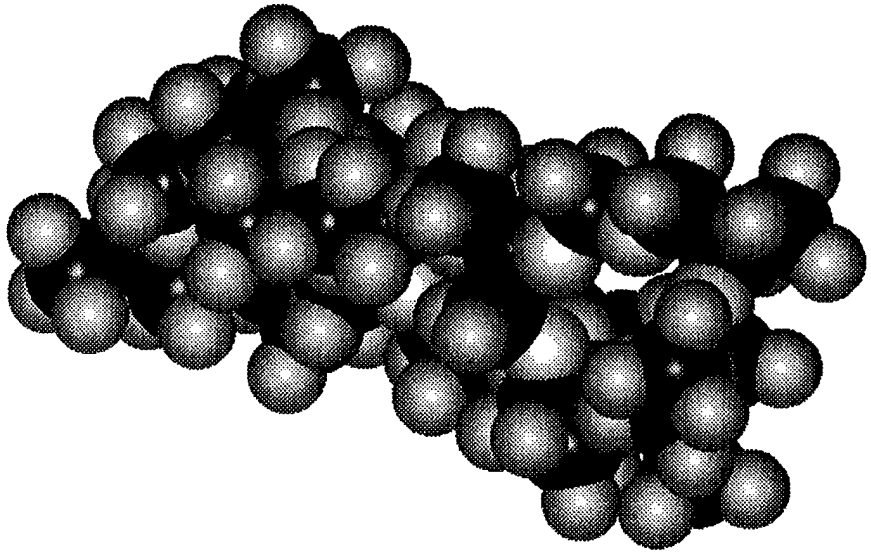

(a)

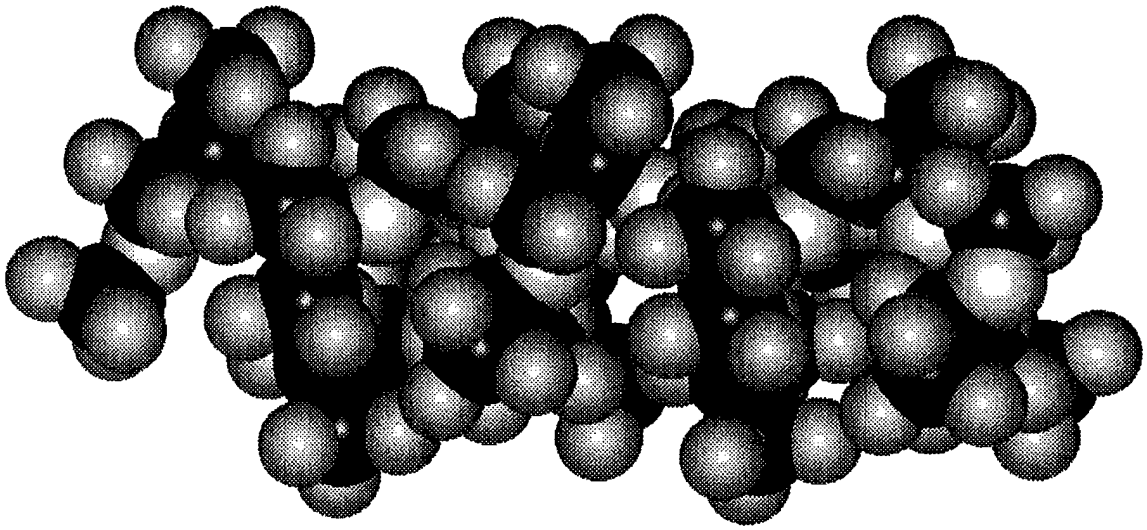

(b)

Figure 33. The conformations obtained with molecular mechanics for perfluoropolyalkylethers: (a) $CF_3O[CF_2CF(CF_3)OCF_2CF(CF_3)OCF_2O]_6CF_3$, (b) $CF_3O[CF_2CF(CF_3)O]_{14}CF_3$.

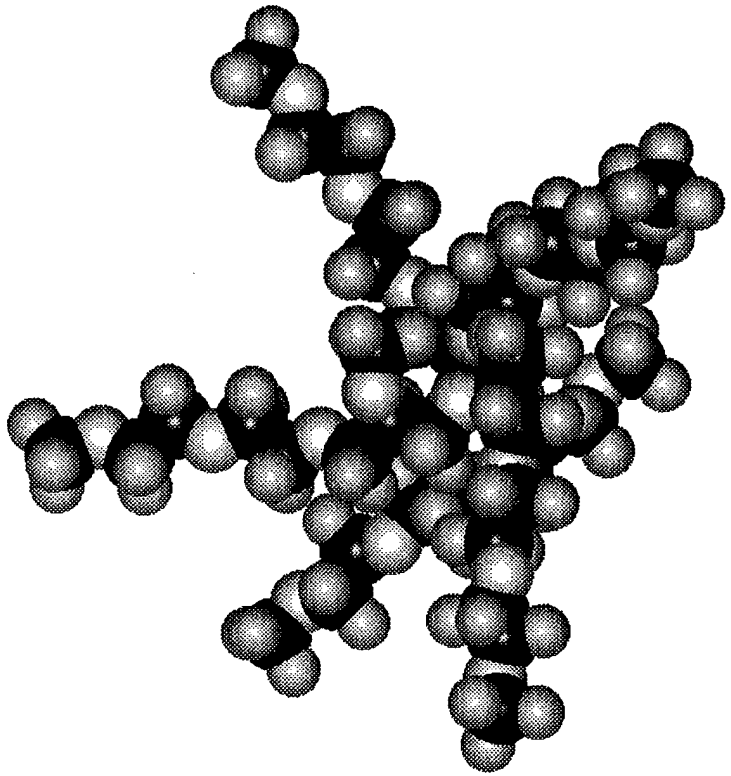

Figure 34. The conformation obtained with molecular mechanics for perfluoropolyalkylether: $CF_3O[CF_2CF(CF_2OCF_2CF_2OCF_2CF_2OCF_3)O]_5CF_3$.

TABLE 12

PERFLUOROPOLYALKYLETHER BENDING ENERGY DATA

Structure	MW ~2500			MW ~4000		
	n	MW	BEND (kcal mol^{-1})	n	MW	BEND (kcal mol^{-1})
$CF_3O(CF_2CF_2OCF_2O)_nCF_3$	13	2520	13.4	21	3977	21.1
$CF_3O(CF_2CF_2O)_nCF_3$	20	2474	11.3	33	3983	18.1
$CF_3O[(CF_2CF_2O)_4CF_2O]_nCF_3$	4	2274	11.9	7	3865	20.5
$CF_3O[CF_2CF_2OCF_2CF(CF_2CF_3)OCF_2O]_nCF_3$	6	2542	17.0	10	4135	28.3
$CF_3O(CF_2CF_2CF_2CF_2OCF_2O)_nCF_3$	8	2410	15.6	14	4103	26.9
$CF_3O[CF_2CF(CF_3)OCF_2CF(CF_3)OCF_2O]_nCF_3$	6	2542	18.9	10	4135	30.3
$CF_3O(CF_2CF_2CF_2O)_nCF_3$	14	2478	13.6	23	3973	22.4
$CF_3O[CF_2CF(CF_3)O]_nCF_3$	14	2478	25.9	23	3973	48.3
$CF_3O(CF_2CF_2CF_2CF_2O)_nCF_3$	11	2530	15.7	18	4043	25.1

$$\log 40°C \text{ Viscosity } (MW,2500) = 0.244(C/O) + 0.022(BEND) + 0.279$$

$$r = 0.992,\ s = 0.04,\ n = 9$$

$$\log 100°C \text{ Viscosity } (MW,2500) = 0.137(C/O) + 0.011(BEND) + 0.084$$

$$r = 0.990,\ s = 0.02,\ n = 9$$

$$\log 40°C \text{ Viscosity } (MW,4000) = 0.278(C/O) + 0.013(BEND) + 0.572$$

$$r = 0.991,\ s = 0.04,\ n = 9$$

$$\log 100°C \text{ Viscosity } (MW,4000) = 0.158(C/O) + 0.006(BEND) + 0.340$$

$$r = 0.979,\ s = 0.04,\ n = 9$$

The corresponding graphical presentations are depicted in Figures 35-38. As evident from the high r values using just the two parameters, gives an unexpectedly good correlation in particular considering the assumptions made in developing these expressions. The actual graphs also show relatively low scatter.

To test the validity of the above relationships, analogous expressions were developed using eight of the materials. The viscosity of the excluded perfluoropolyalkylether was then calculated from these equations. This was done for each member of the series. The comparisons between the actual (obtained from the experimental plots given in Figures 27 and 28) and calculated viscosities are compiled in Table 13. The agreements, with the exception of $-(CF_2CF(CF_3)O)_n-$, are reasonably close. It is believed, based on the conformation presented in Figure 33, that this perfluoropolyalkylether due to its tightly coiled structure, deviates strongly from the other

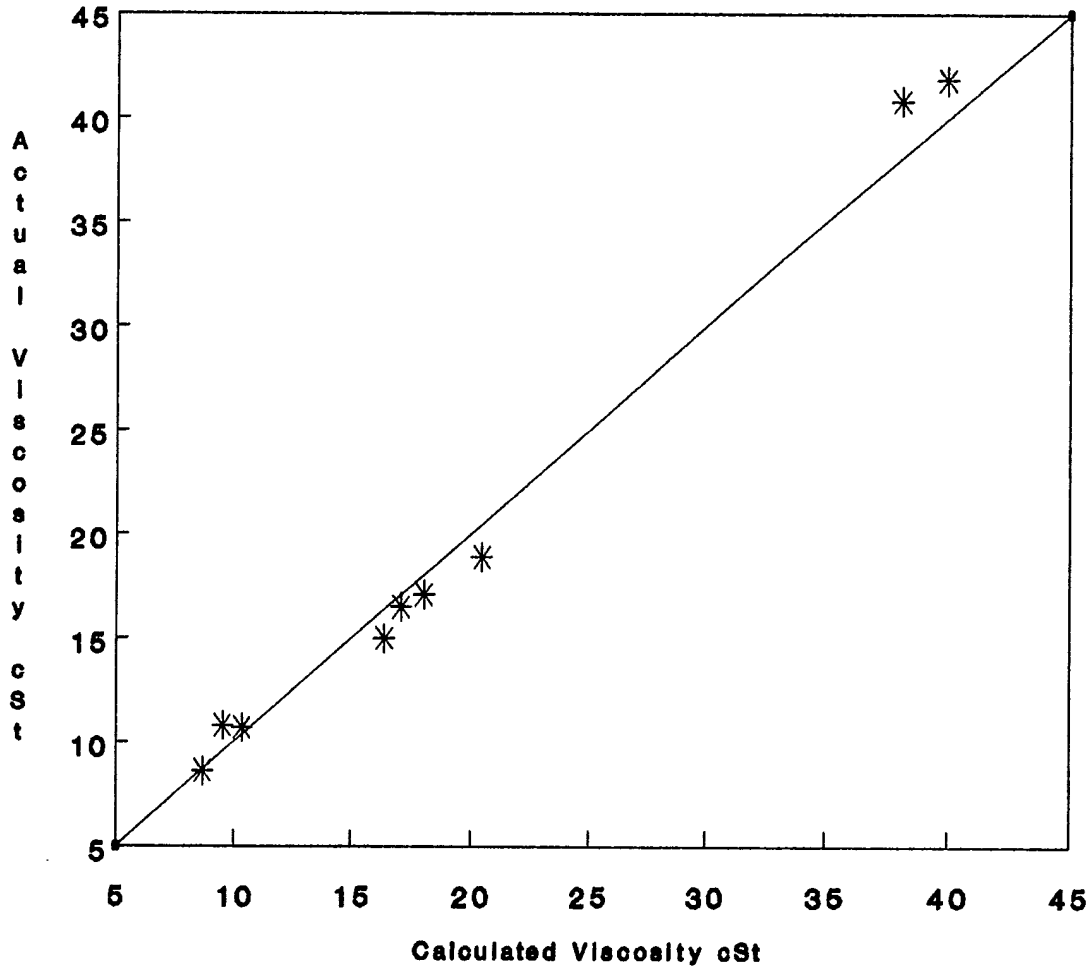

Log 40°C Viscosity 2500 MW = 0.244(C/O) + 0.022(BEND) + 0.279

Figure 35. Calculated versus actual viscosity at 40°C of ~2500 MW perfluoropolyalkylethers as a function of the carbon to oxygen ratio and the bending energy.

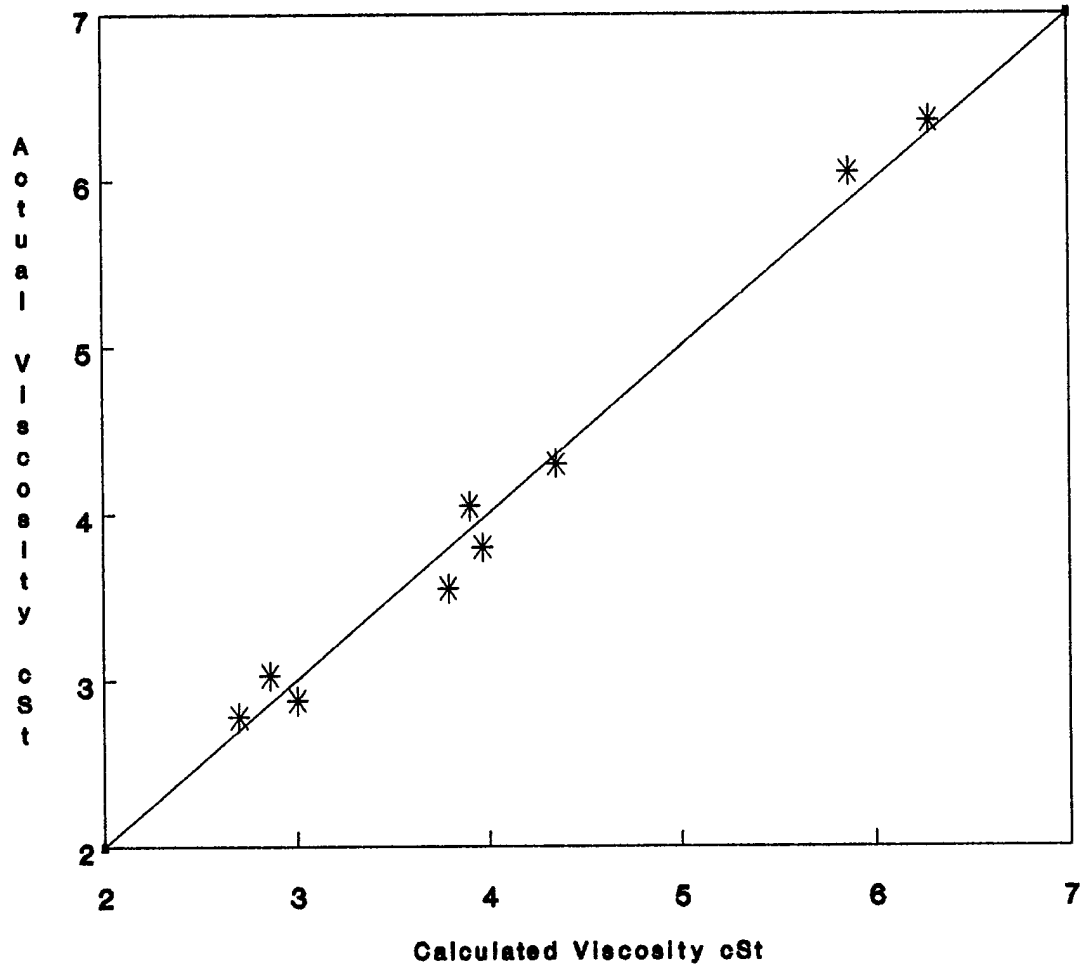

Log 100°C Viscosity 2500 MW = 0.137(C/O) + 0.011(BEND) + 0.084

Figure 36. Calculated versus actual viscosity at 100°C of ~2500 MW perfluoropolyalkylethers as a function of the carbon to oxygen ratio and the bending energy.

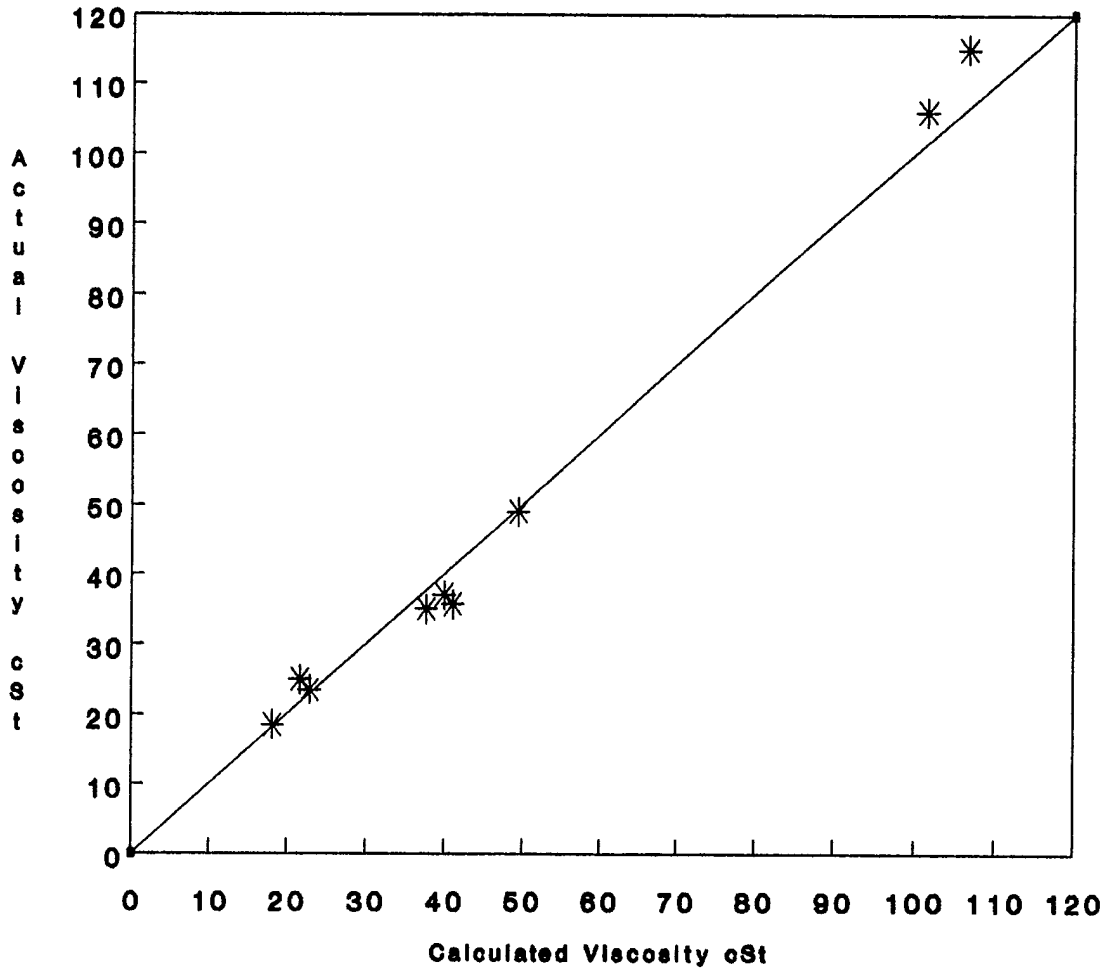

Log 40°C Viscosity 4000 MW = 0.278(C/O) + 0.013(BEND) + 0.572

Figure 37. Calculated versus actual viscosity at 40°C of ~4000 MW perfluoropolyalkylethers as a function of the carbon to oxygen ratio and the bending energy.

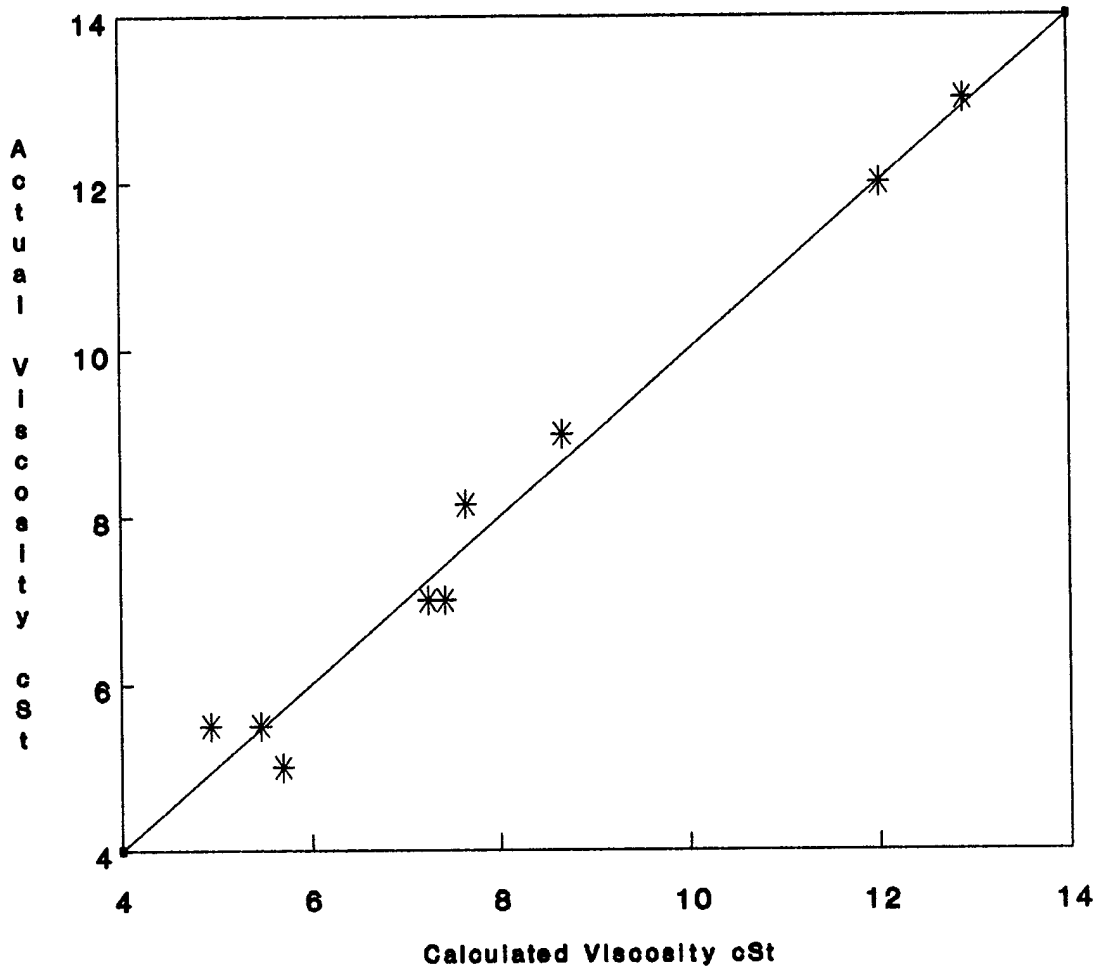

Log 100°C Viscosity 4000 MW = 0.158(C/O) + 0.006(BEND) + 0.340

Figure 38. Calculated versus actual viscosity at 100°C of ~4000 MW perfluoropolyalkylethers as a function of the carbon to oxygen ratio and the bending energy.

TABLE 13

VISCOSITIES CALCULATED FROM EQUATIONS DERIVED FROM DATA EXCLUDING THE FLUID OF INTEREST

Structure	MW 2500 Viscosity, cSt				MW 4000 Viscosity, cSt			
	40°C		100°C		40°C		100°C	
	actual	calc	actual	calc	actual	calc	actual	calc
$-(CF_2CF_2OCF_2O)_n-$	8.61	8.75	2.78	2.66	18.5	18.1	5.5	4.7
$-(CF_2CF_2O)_n-$	10.7	10.3	2.88	3.05	23.5	22.8	5.0	5.9
$-[(CF_2CF_2O)_4CF_2O]_n-$	10.8	9.15	3.03	2.80	25.0	20.8	5.5	5.4
$-[CF_2CF_2OCF_2CF(CF_2CF_3)OCF_2O]_n-$	15.0	16.6	3.55	3.83	35.0	38.0	7.0	7.3
$-(CF_2CF_2CF_2CF_2OCF_2O)_n-$	16.5	17.2	4.05	3.89	35.5	41.8	8.0	7.6
$-[CF_2CF(CF_3)OCF_2CF(CF_3)OCF_2O]_n-$	17.1	18.3	3.80	4.02	37.0	40.5	7.0	7.5
$-(CF_2CF_2CF_2O)_n-$	18.9	21.0	4.30	4.37	49.0	49.6	9.0	8.6
$-[CF_2CF(CF_3)O]_n-$	40.8	31.4	6.05	5.39	115.0	73.6	12.0	12.3
$-(CF_2CF_2CF_2CF_2O)_n-$	41.8	35.8	6.36	6.10	106.0	90.7	13.0	12.6

arrangements. Consequently, an equation derived without an input from a related conformation would not be expected to provide valid results. Allowing for this inconsistency the relationships thus developed, using as the only parameters carbon to oxygen ratios and the bending energies, provide surprisingly reliable expressions for predicting viscosity/temperature and viscosity/molecular weight profiles. This capability is of great value in assessing the behavior of potential lubricants without a need to synthesize the actual materials. These techniques permit also accurate predictions for an increase in viscosity with increase in molecular weight for known compositions. It is apparent from the molecular conformations and related considerations that any predictions derived by extrapolation from low molecular weight arrangements, i.e. model compounds are unreliable if not meaningless.

3.6 THERMAL OXIDATIVE STABILITY INVESTIGATIONS OF FULLY CHARACTERIZED PERFLUOROPOLYALKYLETHER FLUIDS

This program, as mentioned in preceding sections, involved four commercial fluids, Krytox 143AC, Aflunox, Demnum S-20 and Demnum S-100, as well as a series of perfluoropolyalkylether experimental fluids. None of these materials are unimolecular; all consist of telomer mixtures due to the nature of the synthesis. The end groups tend to vary. These aspects were discussed earlier in this report. It is believed that insofar as stability is concerned the nature of the end groups whether CF_3O, C_2F_5O, C_3F_7O, etc., is of a minor

importance compared to the effect of the type of repeating segments. On the other hand, impurities do affect the stability. This is obvious in comparing the thermal oxidative behavior of the first series of experimental fluids, listed in Table 6, with the data for the MLO 91 series discussed below and listed in Table 14. It must be stressed that perfluoropolyalkylethers exhibit very high thermal oxidative stabilities in the absence of metals i.e., when exposed to high temperatures in oxygen in glass. However, metals promote greatly the fluid degradation [Ref. 8] and lower significantly the degradation onset. In view of the envisioned application, namely a contact of the fluid at elevated temperatures with components manufactured from M-50 alloy or a related bearing material, all the evaluations were carried out in the presence of this metal. To facilitate the discussion the tabulation of experimental details for each test is given in the Experimental Section.

From the data presented in Figure 39 it is apparent that the commercial fluids, Krytox and Demnum, contain impurities which lower the degradation onset compared to materials given stabilization treatment. The Aflunox series, although believed to be prepared by the same or related process to Krytox, exhibit much better stability. It has been established that in Krytox fluids the impurities responsible for the decreased stability consist of hydrogen-terminated chains $-OCF(CF_3)H$ [Ref. 8]. The nature of the impurities in Demnum is unknown, although in view of the synthesis process [Ref. 5] residual hydrogen is again

TABLE 14

FLUIDS STUDIED

ID	Fluid	Origin	Molec weight NMR	Molec weight Osm.	Degradation[a] Temp°C
71-6	$-[CF_2CF(CF_3)O]_n-$	Krytox 143AC[b]	6800	5400	<288
91-21	$-[CF_2CF(CF_3)O]_n-$	F-Krytox 143AC[c]	7250	6000	325
88-177	$-(CF_2CF_2CF_2O)_n-$	Demnum S-20[d]	2750	2500	<300
88-177T	$-(CF_2CF_2CF_2O)_n-$	T-Demnum S-20[e]			315
91-157	$-[(CF_2CF_2O)_4CF_2O]_n-$	-[f]	1800	2850	280
91-160	$-(CF_2CF_2OCF_2O)_n-$	-[f]	2800	2650	285
91-132	$-[CF_2CF(CF_3)OCF_2CF(CF_3)OCF_2O]_n-$	-[f]	2700	3050	300
91-161	$-(CF_2CF_2O)_n-$	-[f]	2450	3000	310
91-158	$-[CF_2CF(CF_2OCF_2CF_2OCF_2CF_2OCF_3)O]n-$	-[f]	5650	3950	310
91-105	$-(CF_2CF_2CF_2CF_2OCF_2O)_n-$	-[f]	2700	2500	310
91-106	$-(CF_2CF_2CF_2CF_2CF_2OCF_2O)_n-$	-[f]	2800	2500	310
91-126	$-(CF_2CF_2CF_2CF_2O)_n-$	-[f]	3100	2600	315

a) This is the degradation onset temperature at which volatile condensables amounted to 0.5 ± 0.25 mg/g.
b) Product of DuPont.
c) Krytox 143AC which was subjected to fluorination at elevated temperatures.
d) Product of Daikin Industries.
e) Demnum S-20 which was exposed to oxygen at 315 and 330°C in the presence of M-50 alloy for consecutive 24 h periods.
f) All of these fluids were prepared by direct fluorination of their hydrocarbon precursors.

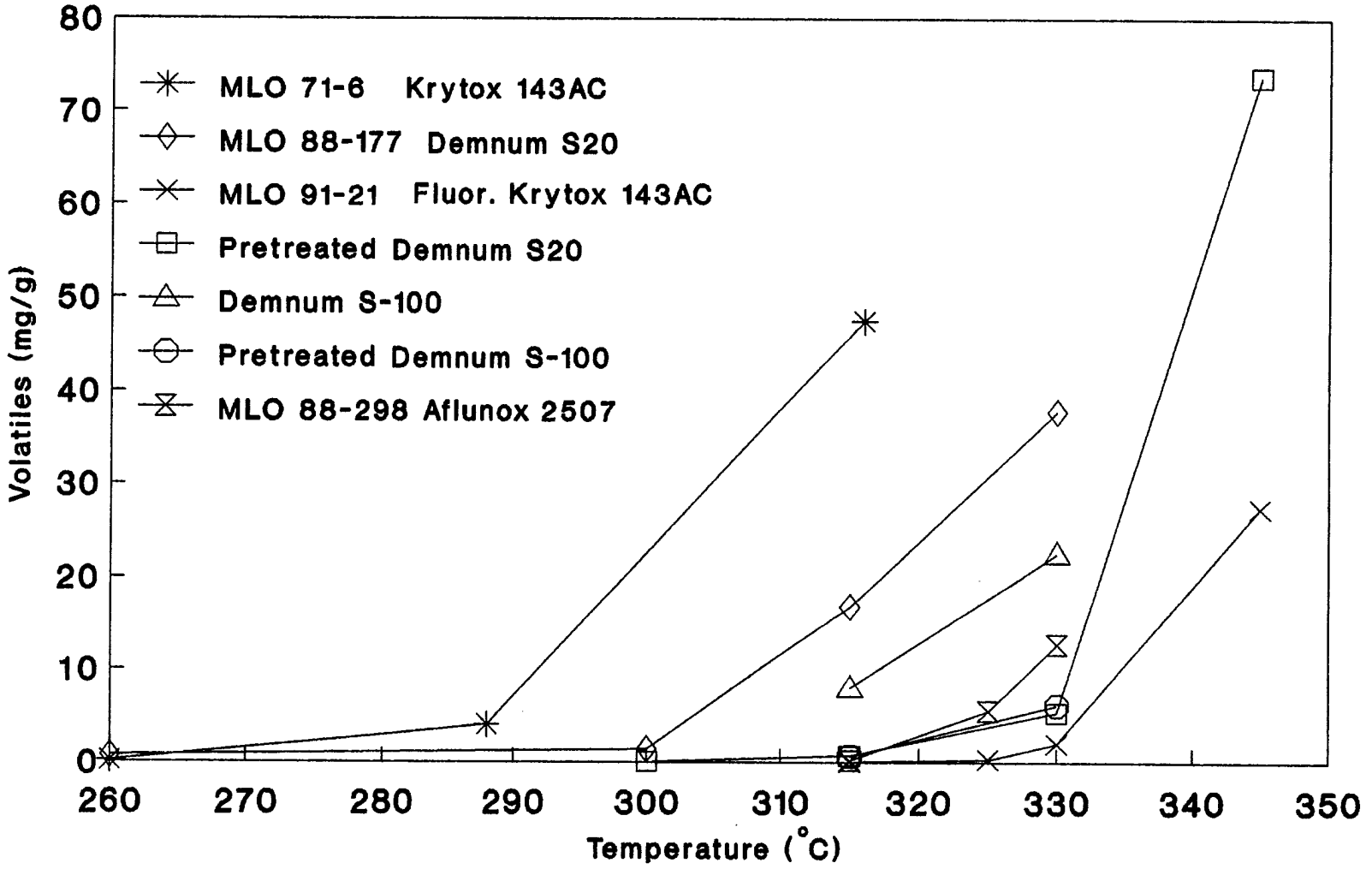

Figure 39. Plots of thermal oxidative degradation data in the presence of M-50 for MLO 71-6, MLO 88-177, MLO 91-21, pretreated MLO 88-177, Demnum S-100, pretreated Demnum S-100 and MLO 88-298.

suspected. In both instances pretreatment at 316-330°C in oxygen, in the presence of M-50 alloy, degrades the low stability chains into volatile products which are then removed. Fluorination provides another way to remove residual hydrogen and was successfully employed in the case of the Krytox 143AC fluid by Exfluor Research Corp.

It would appear from the degradation profiles shown in Figure 39 that the inherent thermal oxidative stability of a branched poly(hexafluoropropene oxide) is higher than that of its linear analogue. Specifically, at 315°C the mg/g value for $-[CF(CF_3)CF_2O]_n-$ was found to be 0.03 versus 0.70 for $-(CF_2CF_2CF_2O)_n-$.

As noted earlier all the other fluids studied were obtained by direct fluorination of their hydrocarbon precursors. No difference was observed in the degradation onset of hydrogen free $-[CF(CF_3)CF_2O]_n-$ prepared by hexafluoropropene oxide telomerization, and of the compound obtained by direct fluorination of poly(propylene oxide) (Figure 40). This confirms that stability is inherent in a given structure and proves the validity of the experimental approach. It is the weakest link or unit which determines the stability of the given material. This is illustrated by the comparison of the degradation onset of 310°C, determined for $-(CF_2CF_2O)_n-$, and for $-[CF_2CF(CF_2OCF_2CF_2OCF_2CF_2OCF_3)O]_n-$, as shown in Figures 40 and 41. In the second material the sequence of tetrafluoroethylene oxide groups in the branch provides the instability site.

The fluorinated Pluronic L-31 was shown to undergo drastic decomposition between 315 and 330°C (see Figure 42). These results when compared to those obtained for $(-CF_2CF_2O-)_n$, for which at 315°C the extent of degradation was 18 mg/g (see Figure 40), tend to indicate that adjacent $-CF_2CF_2O-$ units are absent in this material. The molecular weight of 2800 [see Table 8], the 1:8 ratio of CF_2CF_2O to $CF_2CF(CF_3)O$ segments based on ^{19}F NMR and the method of preparation, (wherein a block of $CF(CF_3)CF_2O$ segments is terminated by reaction with ethylene oxide), imply structure $CF_3OCF_2CF_2O[CF(CF_3)CF_2O]_{16}CF_2CF_2OCF_3$. The material most likely consists of a telomer mixture; however, the general structure must be predominantly $CF_3OCF_2CF_2O[CF(CF_3)CF_2O]_xCF_2CF_2OCF_3$.

With respect to the fluorinated polyglycol, P15-200, the plot in Figure 42 is in a full agreement with the ^{19}F NMR which gives the ratio of $CF(CF_3)CF_2O$ to CF_2CF_2O segments of 1:1.8 and shows clearly the presence of adjacent CF_2CF_2O units. The latter is further supported by the molecular weight of 4250. Yet, the material degrades less rapidly at 315°C, by a factor of 8, than $CF_3O(CF_2CF_2O)_nCF_3$, by a factor of 8, based on volatiles formed. Due to its structure, namely the presence of three terminal $CF_2CF_2OCF_3$ groups per molecule, one would expect this material to undergo degradation at a faster rate than $CF_3O(CF_2CF_2O)_nCF_3$.

Introduction of a difluoroformyl group into the octafluorobutene oxide system, $-(CF_2CF_2CF_2CF_2O)_n-$, to give the $-(CF_2CF_2CF_2CF_2OCF_2O)_n-$ structure, lowers the degradation onset by

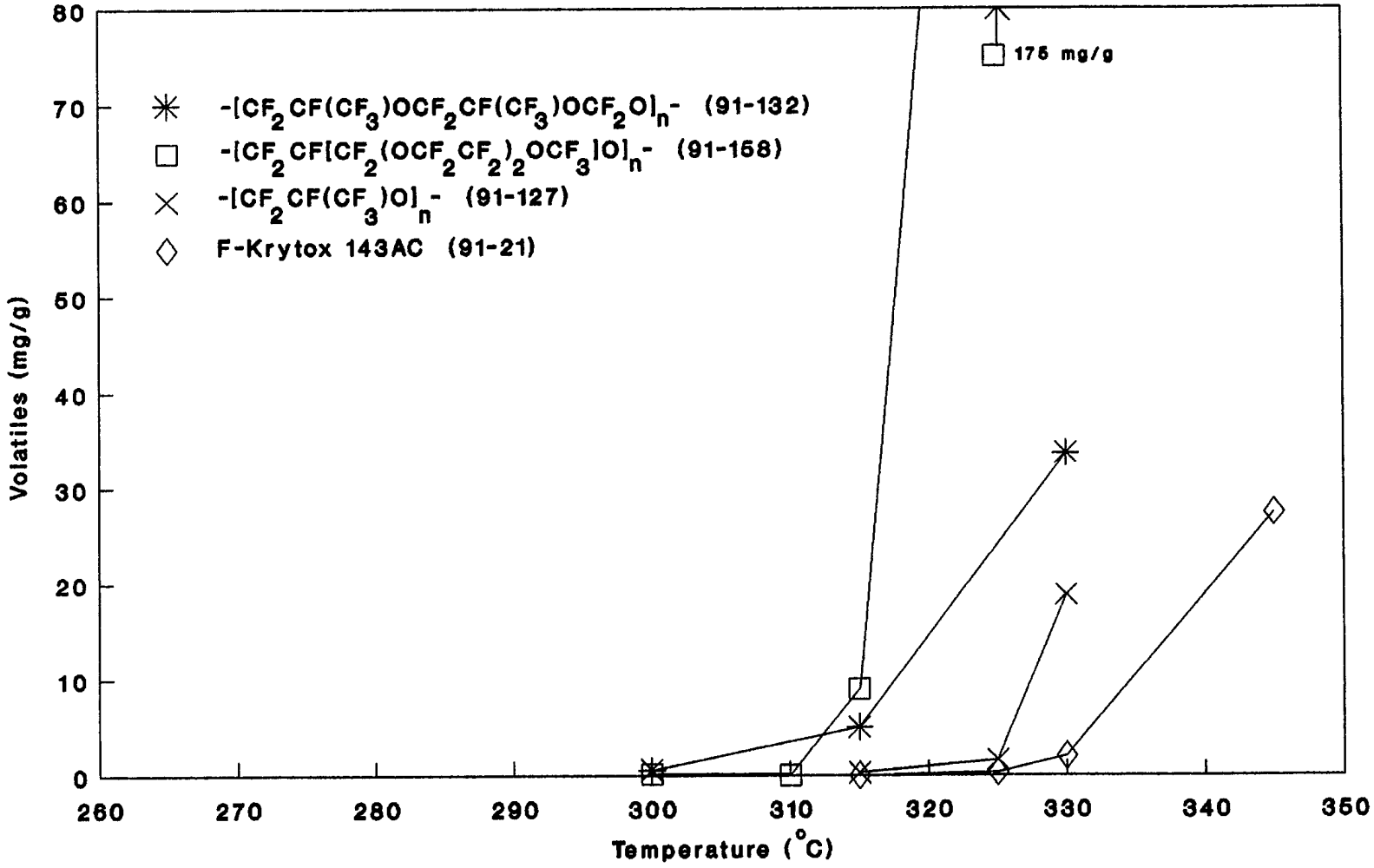

Figure 40. Effect of the presence of difluoroformyl groups and tetrafluoroethylene oxide branching on the thermal oxidative stability of poly(hexafluoropropene oxide).

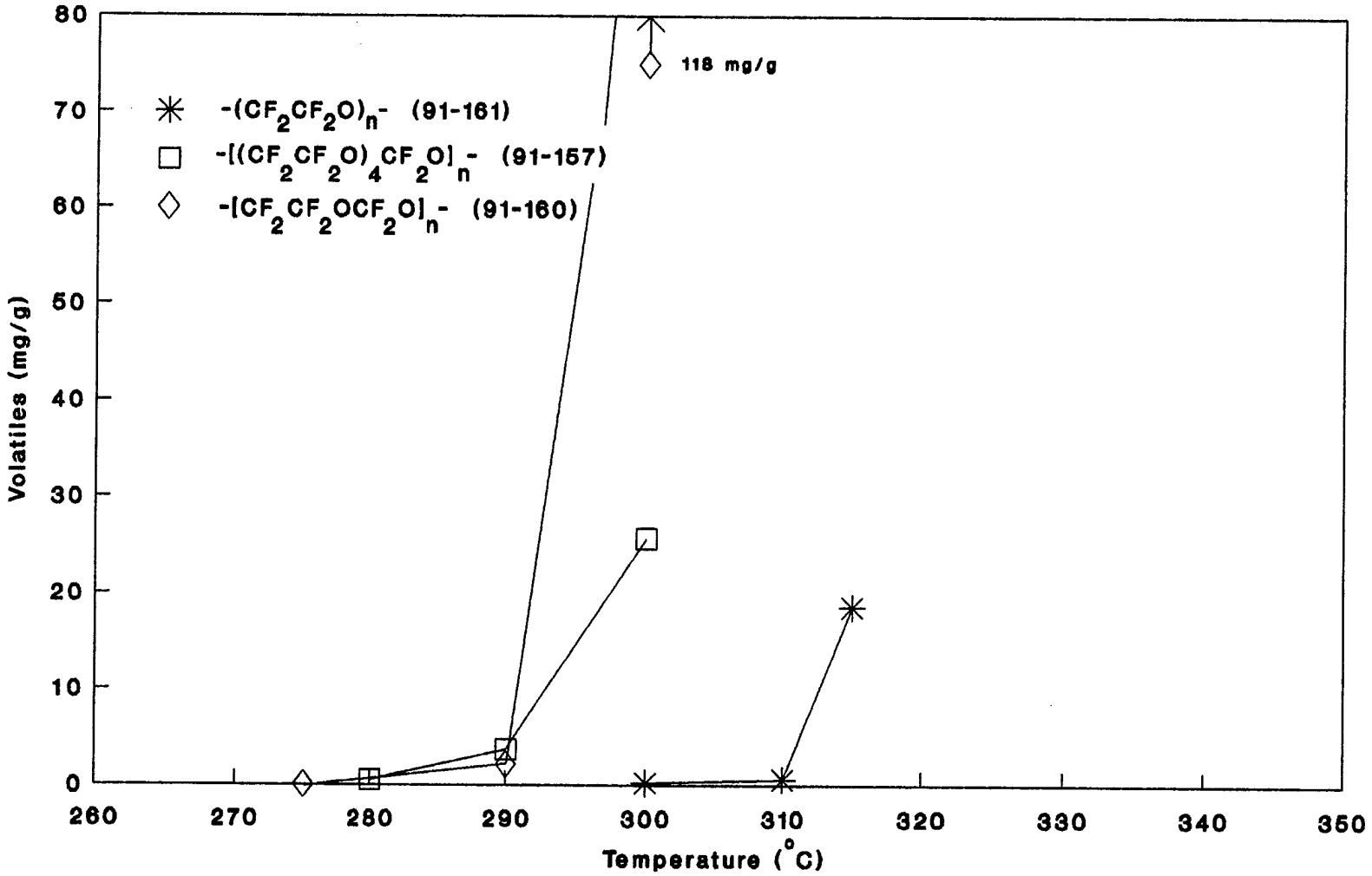

Figure 41. Effect of the presence and relative proportions of difluoroformyl groups on the thermal oxidative stability of poly(tetrafluoroethylene oxide) fluids.

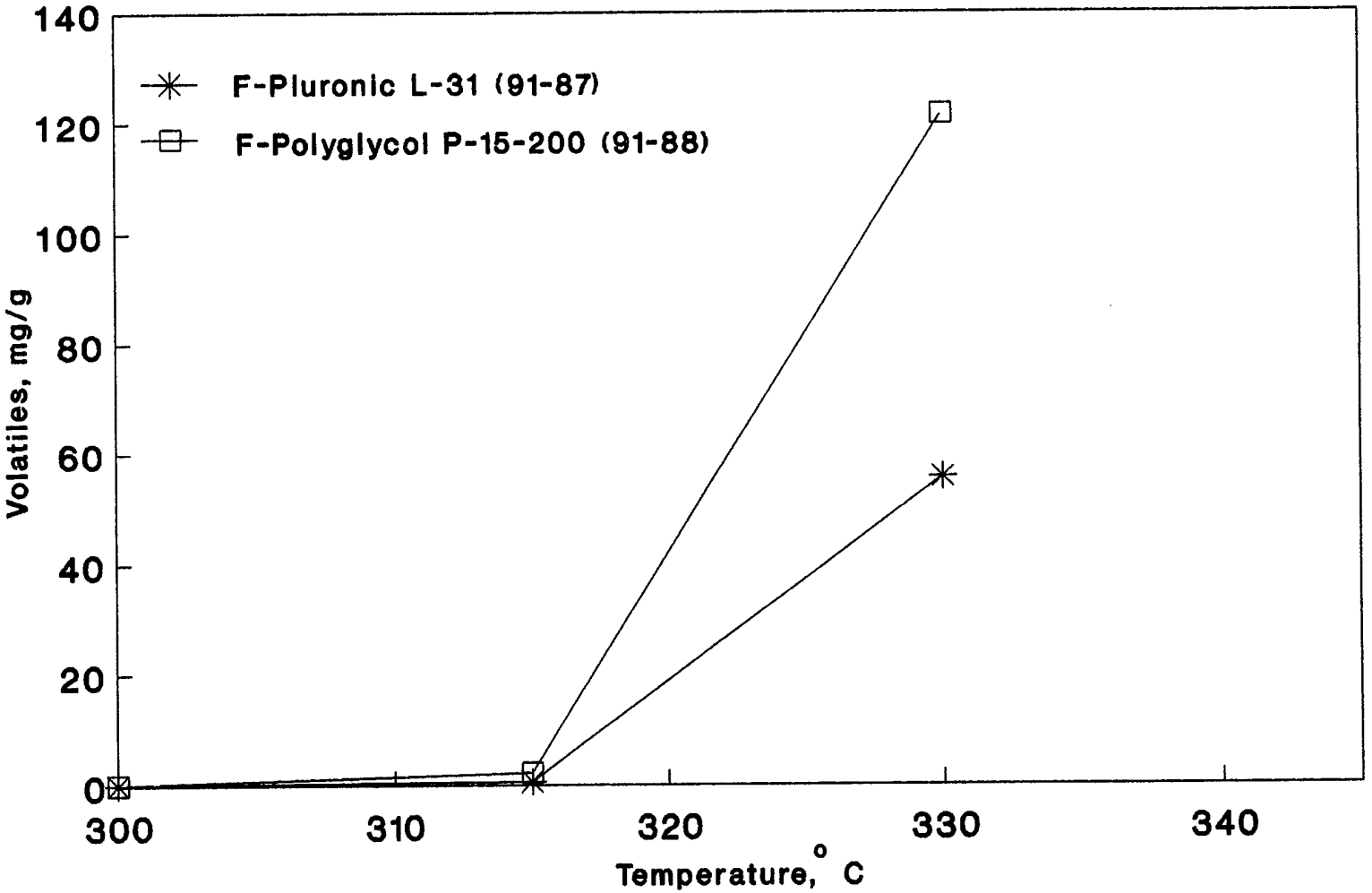

Figure 42. Plots of thermal oxidative degradation data for MLO 91-87 and 91-88 experimental fluids.

5°C, from 315°C to 310°C, as shown in Figure 43. An increase in the number of adjacent CF_2 groups from 4 to 5 has no effect on the degradation onset as is evident from Figure 43. It is of interest that the $-(CF_2CF_2CF_2O)_n-$ and $-(CF_2CF_2CF_2CF_2O)_n-$ arrangements exhibit essentially identical degradation profiles (Figure 43). Apparently, it requires at least three adjacent CF_2 groups to inhibit the "activity" effect of oxygen. Studies performed on aromatic/perfluoroalkylether compounds support these observations [Ref. 22].

It is unexpected that the introduction of difluoroformyl groups into the hexafluoropropene oxide system decreases the degradation onset by 25°C (see Figure 40) versus 5°C for the octafluorobutene oxide structure. Furthermore, the actual onset temperature (300°C) is lower for the copolymer $-[CF_2CF(CF_3)OCF_2CF(CF_3)OCF_2O]_n-$ than the 310°C determined for $-(CF_2CF_2CF_2CF_2OCF_2O)_n-$ (Figure 43). It is possible that the presence of the $-OCF_2-$ unit disrupts the protective shielding of trifluoromethyl groups and the arrangement approximates more closely a two carbon environment as represented by e.g. poly(tetrafluoroethylene oxide).

The presence of difluoroformyl groups in the tetrafluoroethylene oxide systems results in a drastic drop of the degradation onset from 310°C to 280-285°C. The degradation onsets for the two materials investigated $-(CF_2CF_2OCF_2O)_n-$ and $-[(CF_2CF_2O)_4CF_2O]_n-$ are virtually identical. However, the subsequent rate of degradation above this threshold is

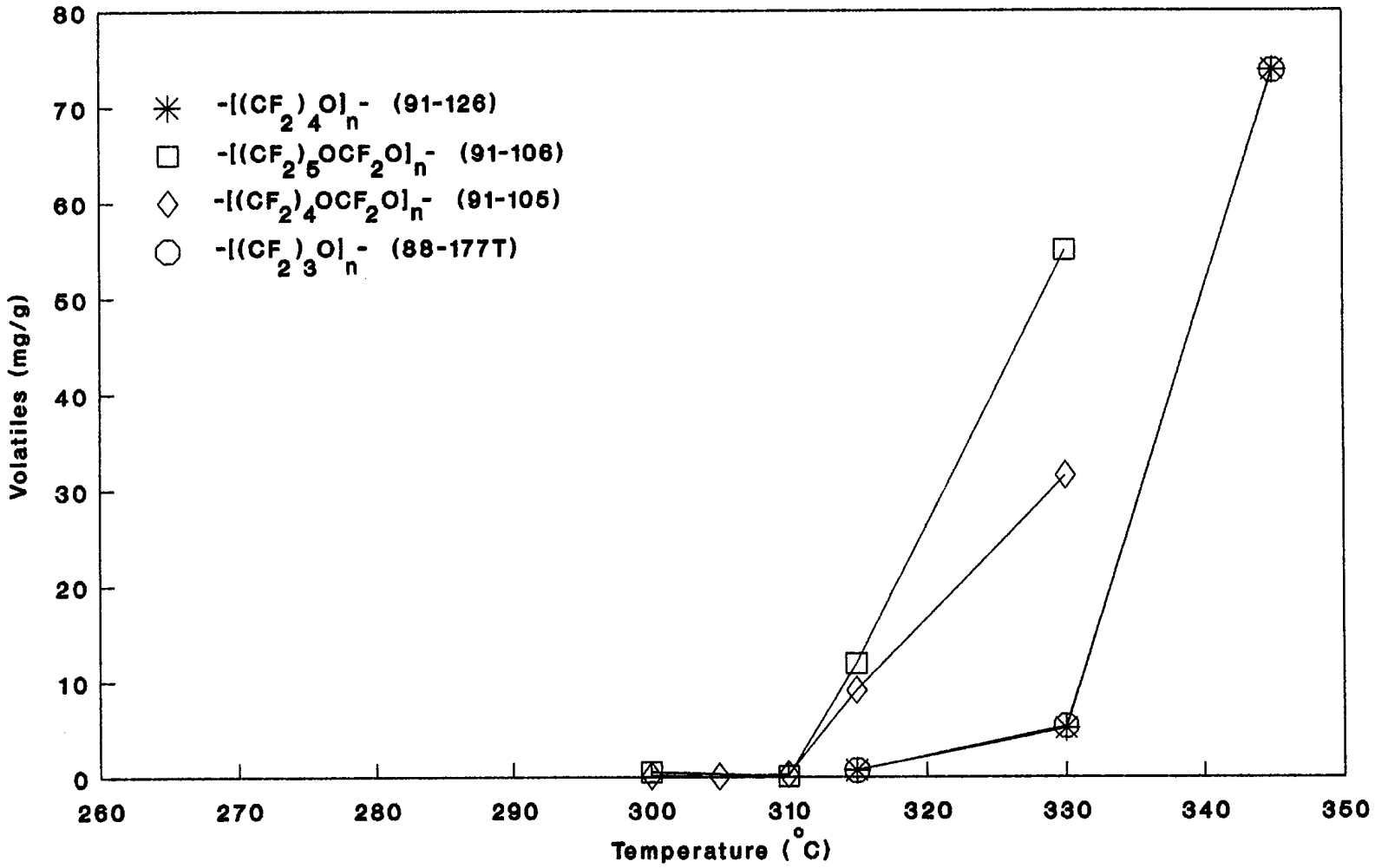

Figure 43. Effect of difluoroformyl groups on thermal oxidative behavior of perfluoropolyalkylethers containing 4 and 5 adjacent difluoromethylene groups.

significantly higher for the composition having the higher difluoroformyl proportion as is evident from Figure 41.

3.7 DEVELOPMENT OF QUANTITATIVE STRUCTURE/ACTIVITY (THERMAL OXIDATIVE STABILITY IN THE PRESENCE OF M-50) RELATIONSHIPS

Based on earlier data [Ref. 8] and the current investigations, it is obvious that there is a definite interdependence between structure and the thermal oxidative stability of perfluoroalkylethers. Establishment of QSARs to be utilized in conjunction with the quantitative structure/viscosity relationships discussed in Section 3.5 should allow to identify the best perfluoropolyalkylether arrangement for a given application without having to synthesize and evaluate a series of potential candidates. A structure/stability correlation based on energy parameters provides a meaningful approach. Although, as mentioned earlier, the perfluoropolyalkylethers studied are mixtures of telomers, the use of unimolecular compositions in the computational treatments seemed reasonable in view of the results obtained in the structure/viscosity studies. The compositions listed in Table 14 were utilized in this study.

A catalytic process, which is the case for the M-50 promoted degradations, must be dependent on juxtaposition of units or segments in a given material. This is of a particular importance in high molecular weight systems where in a single molecule a number of different configurations can exist. To permit the various molecular orientations, freedom of motion is necessary. In a computational treatment this can be achieved by

imparting energy (velocity) to molecular conformations (obtained using molecular mechanics). Arbitrarily, we have selected 313°K as the equilibrium temperature to determine the various energy components, given in Table 15, which were computed after geometry optimizations. These are average values of four different conformations. Representative conformations of the perfluoropolyalkylethers, listed in Table 15, are presented in Figures 44-48. The lack of uniformity in the structural arrangements illustrates the points discussed above.

To develop QSAR expressions the energy components given in Table 15 were employed in multivariate linear regression analyses. The equations, derived using different energy parameters, together with the corresponding Pearson correlation coefficients (r) are presented in Table 16. Employing just three descriptors gives r of 0.977 and s (standard error of estimate) of 3.61. The graphical presentation is depicted in Figure 49. To determine the validity of this approach, equations using the three energy components, namely bending, Van der Waals and stretch-bend energies, were derived employing 9 out of the 10 fluids. The degradation temperature of the excluded fluid was then calculated. This operation was performed for each of the 10 fluids. The relevant data are compiled in Table 17. The agreement between calculated and actual degradation temperature is illustrated in Figure 50.

Based on these results and the developed viscosity/structure correlations, apparently it is feasible to

TABLE 15

PERFLUOROPOLYALKYLETHER ENERGY COMPONENTS LISTING

Structure	Energy Components[a], (kcal/mol)					
	BOND	BEND	DIHED	VDW	SB	ES
$CF_3O[(CF_2CF_2O)_4CF_2O]_4CF_3$	12.65	13.75	-114.6	-10.17	1.73	226.9
$CF_3O(CF_2CF_2OCF_2O)_{13}CF_3$	10.20	14.66	-106.9	-5.87	1.61	189.7
$CF_3O[CF_2CF(CF_3)OCF_2CF(CF_3)OCF_2O]_6CF_3$	18.09	21.41	-104.0	-23.13	2.57	270.1
$CF_3O(CF_2CF_2O)_{20}CF_3$	15.66	15.16	-135.7	0.02	2.04	284.9
$CF_3O[CF_2CF(CF_2OCF_2CF_2OCF_2CF_2OCF_3)O]_5CF_3$	14.77	23.08	-101.2	-14.01	2.16	244.3
$CF_3O(CF_2CF_2CF_2CF_2OCF_2O)_8CF_3$	21.99	17.03	-125.1	-9.29	2.48	324.9
$CF_3O(CF_2CF_2CF_2CF_2CF_2OCF_2O)_7CF_3$	25.93	18.04	-133.4	-12.64	2.90	373.2
$CF_3O(CF_2CF_2CF_2O)_{14}CF_3$	24.58	17.04	-145.3	-0.97	2.34	382.0
$CF_3O(CF_2CF_2CF_2CF_2O)_{11}CF_3$	29.80	18.35	-156.4	-6.68	2.88	442.8
$CF_3O[CF_2CF(CF_3)O]_{14}CF_3$	20.41	21.12	-116.9	-5.24	2.54	316.8

a) BOND, bonding energy; BEND, bending energy; DIHED, torsion energy; VDW, Van der Waals energy; SB, stretch-bend energy; ES, electrostatic energy.

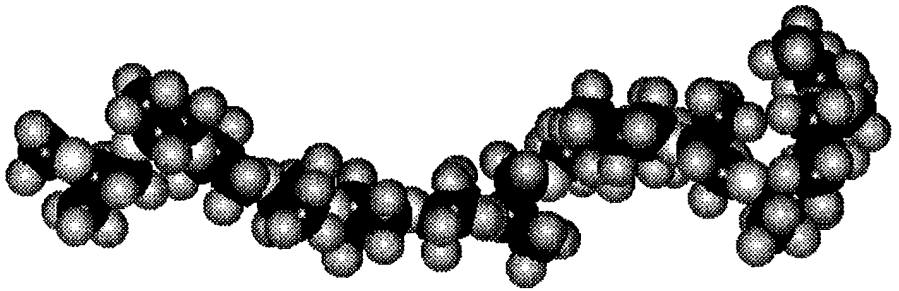

(a)

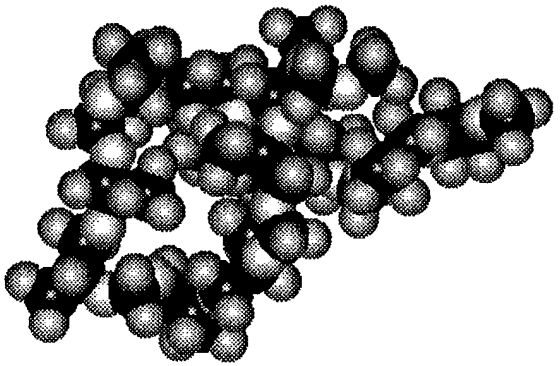

(b)

Figure 44. Geometry optimized conformations after molecular dynamics at 40°C:
(a) $CF_3O[CF_2CF(CF_3)O]_{14}CF_3$,
(b) $CF_3O[CF_2CF(CF_3)OCF_2CF(CF_3)OCF_2O]_6CF_3$.

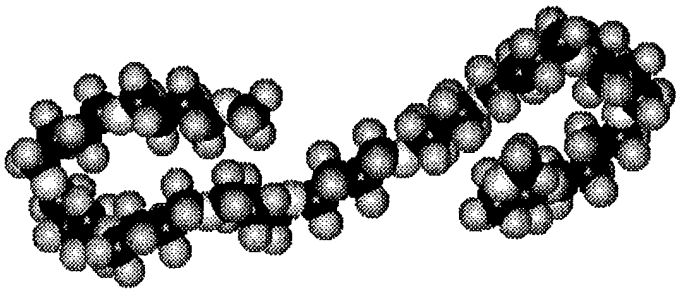

(a)

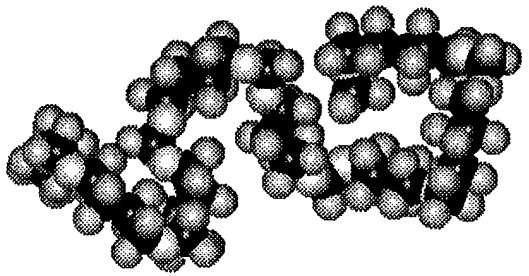

(b)

Figure 45. Geometry optimized conformations after molecular dynamics at 40°C: (a) $CF_3O(CF_2CF_2CF_2CF_2O)_{11}CF_3$, (b) $CF_3O(CF_2CF_2CF_2CF_2OCF_2O)_8CF_3$.

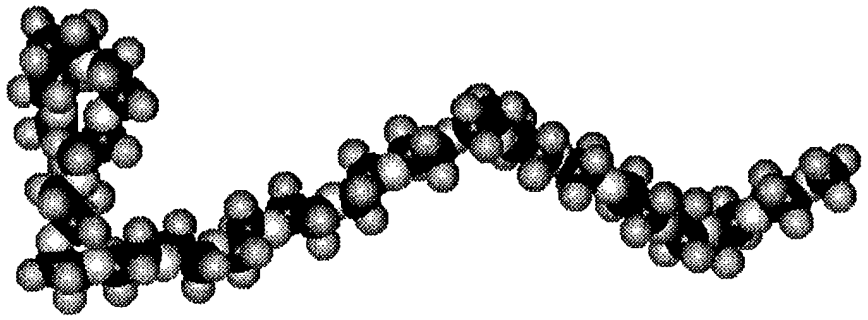

(a)

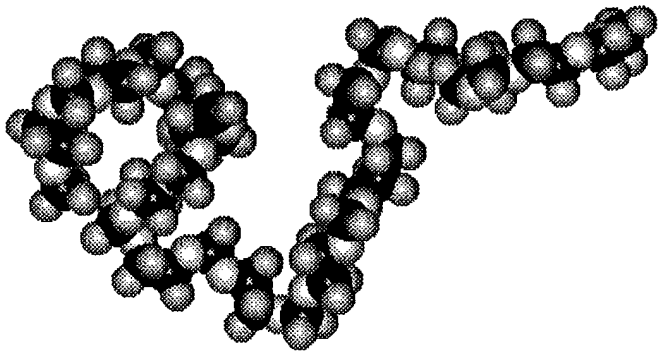

(b)

Figure 46. Geometry optimized conformations after molecular dynamics at 40°C: (a) $CF_3O(CF_2CF_2O)_{20}CF_3$, (b) $CF_3O(CF_2CF_2OCF_2O)_{13}CF_3$.

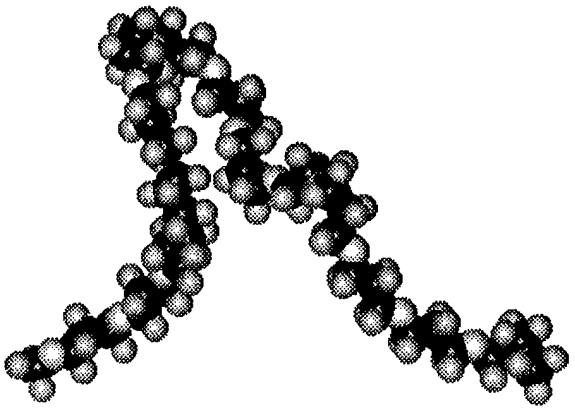

(a)

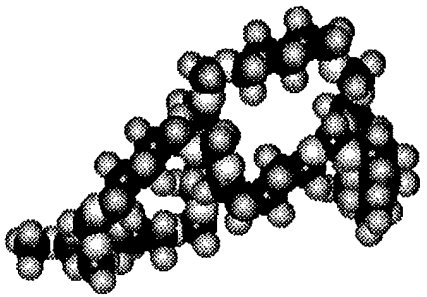

(b)

Figure 47. Geometry optimized conformations after molecular dynamics at 40°C: (a) $CF_3O(CF_2CF_2CF_2O)_{14}CF_3$, (b) $CF_3O(CF_2CF_2CF_2CF_2CF_2OCF_2O)_7CF_3$.

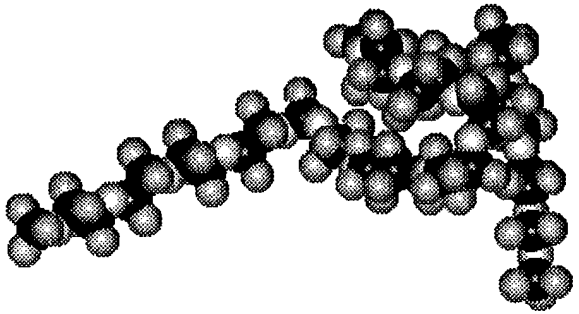

(a)

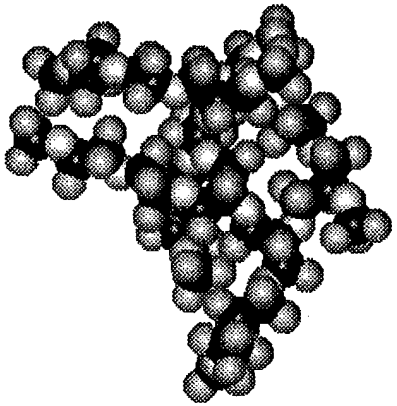

(b)

Figure 48. Geometry optimized conformations after molecular dynamics at 40°C: (a) $CF_3O[(CF_2CF_2O)_4CF_2O]_4CF_3$, (b) $CF_3O[CF_2CF(CF_2OCF_2CF_2OCF_2CF_2OCF_3)O]_5CF_3$.

TABLE 16

QSAR EXPRESSIONS BASED ON ENERGY DESCRIPTORS

No. of Variables	R[b]	S[c]	Variable Coefficients[a]						Constant
			BOND	BEND	DIHED	VDW	SB	ES	
6	0.982	4.48	-1.37	2.38	0.16	1.72	29.98	0.08	231.7
5	0.982	3.89	-0.70	2.59	0.05	1.75	29.74		225.4
4	0.982	3.50	-0.84	2.68		1.71	30.09		219.3
3	0.977	3.61		3.00		1.52	17.32		225.2
2	0.860	8.05		4.34		1.56			241.8
2	0.841	8.54					26.24		253.2
2	0.749	10.44		1.18			18.30		242.9

a) BOND, bonding energy; BEND, bending energy; DIHED, torsion energy; VDW, Van der Waals energy; SB, stretch-bend energy; ES, Electrostatic energy.
b) R is the Pearson correlation coefficient.
c) S is the standard error.

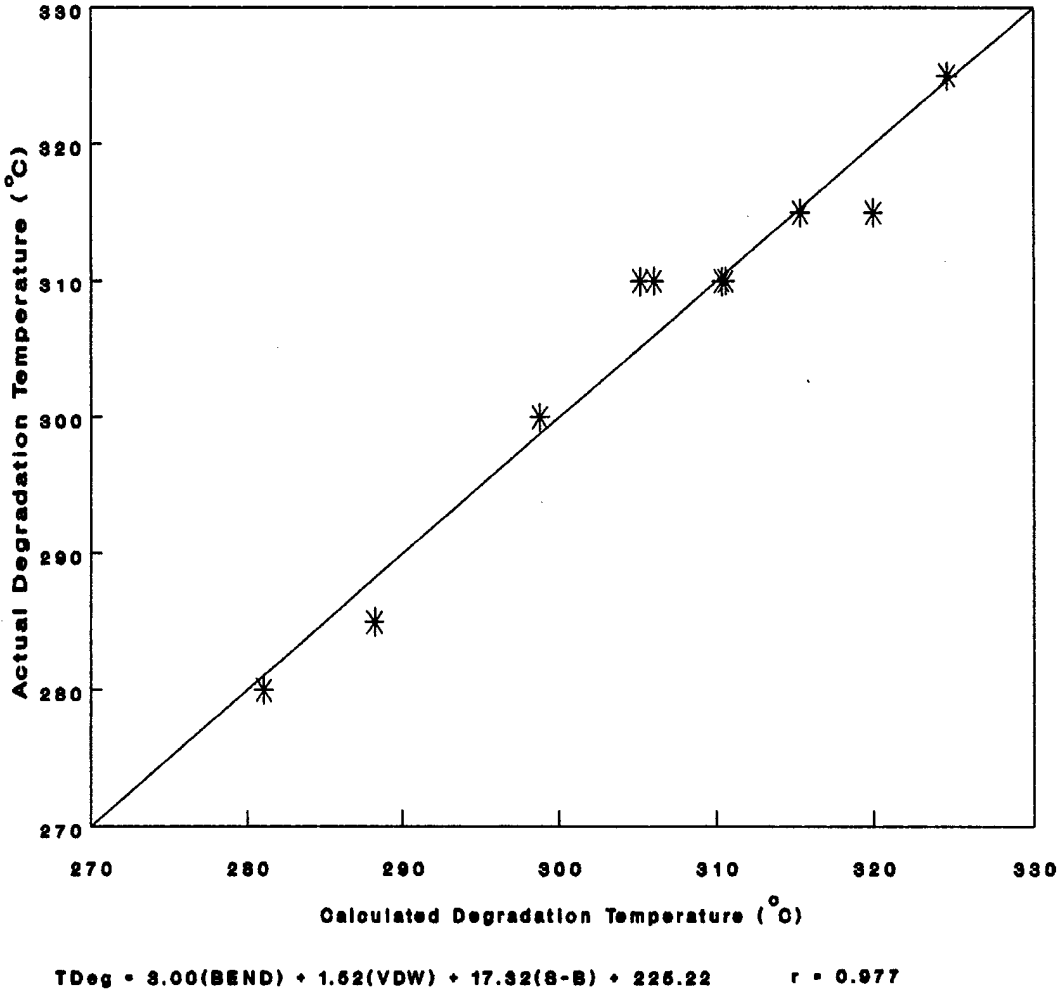

Figure 49. Plot of calculated versus actual degradation temperature as a function of bending, Van der Waals and stretch-bend energies.

TABLE 17

DEGRADATION TEMPERATURES CALCULATED FROM EQUATIONS DERIVED FROM DATA EXCLUDING THE FLUID OF INTEREST

Fluid excluded	R[b]	Variable[a] Coefficients			Constant	Degradation Temp °C	
		Bend	VDW	SB		Calc	Actual
$CF_3O[(CF_2CF_2O)_4CF_2O]_4CF_3$	0.961	2.88	1.47	16.89	228.2	280	282
$CF_3O(CF_2CF_2OCF_2O)_{13}CF_3$	0.975	2.93	1.50	15.34	231.5	285	290
$CF_3O[CF_2CF(CF_3)OCF_2CF(CF_3)OCF_2O]_6CF_3$	0.978	3.00	1.62	17.29	225.9	300	297
$CF_3O(CF_2CF_2O)_{20}CF_3$	0.984	3.02	1.41	17.76	222.2	310	304
$CF_3O[CF_2CF(CF_2OCF_2CF_2OCF_2CF_2OCF_3)O]_5CF_3$	0.977	3.15	1.52	16.62	224.3	310	312
$CF_3O(CF_2CF_2CF_2CF_2OCF_2O)_8CF_3$	0.985	3.18	1.55	16.27	224.2	310	304
$CF_3O(CF_2CF_2CF_2CF_2CF_2OCF_2O)_7CF_3$	0.977	2.97	1.51	17.58	225.1	310	311
$CF_3O(CF_2CF_2CF_2O)_{14}CF_3$	0.976	3.00	1.52	17.35	225.2	315	315
$CF_3O(CF_2CF_2CF_2CF_2O)_{11}CF_3$	0.988	2.86	1.57	20.45	221.6	315	322
$CF_3O[CF_2CF(CF_3)O]_{14}CF_3$	0.970	2.96	1.50	17.34	225.7	325	324

a) BEND, bending energy; VDW, Van der Waals energy; SB, stretch-bend energy.
b) R is the Pearson correlation coefficient.

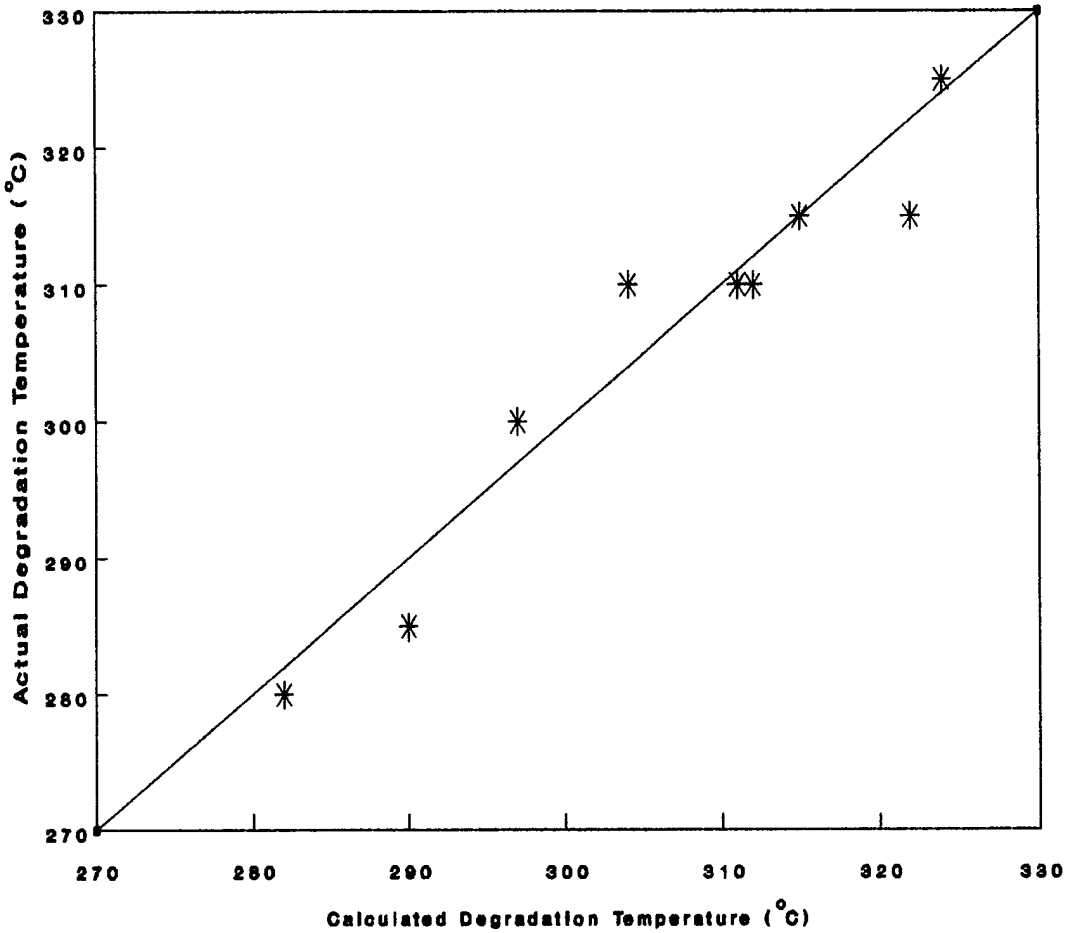

Figure 50. Plot of calculated versus actual degradation temperatures obtained from equations derived excluding the fluid of interest.

design a perfluoropolyalkylether system having specific stability and viscosity characteristics. It must be stressed that, unfortunately, [Ref. 8] perfluoropolyalkylethers exhibiting the highest thermal oxidative stabilities possess also the poorest viscosity/temperature profiles. Thus an optimum composition for a given application will have to be a compromise system.

4. EXPERIMENTAL

General

All solvents used were reagent grade and were dried and distilled prior to use. Operations involving moisture or air sensitive materials were carried out either in an inert atmosphere enclosure (Vacuum Atmospheres Model HE-93BO) under nitrogen bypass or *in vacuo*. The commercially available starting materials were usually purified by distillation, crystallization, or other appropriate means.

Infrared spectra were recorded as gas spectra, neat (on liquids) and as double mulls (Kel-F oil No. 10 and Nujol) on solids using a Perkin-Elmer Corporation infrared spectrophotometer Model 1330. The mass spectrometric (MS) analyses were obtained employing a Du Pont 21-491B double focusing mass spectrometer attached to a Varian Aerograph Model 2700 gas chromatograph (GC), equipped with a flame ionization detector and a Du Pont 21-094 data acquisition and processing system. The majority of product mixture identifications were performed using combined gas chromatography/mass spectrometry (GC/MS). Gas chromatography was conducted employing a 10 ft x 1/8 in stainless steel column packed with 4% OV-101 on 80/100 mesh Chromosorb G or a 3 ft x 1/8 in stainless steel column packed with 3% Dexsil 300 on 100/120 mesh Chromosorb WAW, using a programming rate of 8°C/minute from 50-300°C. Molecular weights were determined using a Mechrolab Model

302 vapor pressure osmometer. Viscosities were measured with Cannon-Manning semi-micro viscometers.

Materials

Poly(hexafluoropropene oxide), $F(CF(CF_3)CF_2O)_nC_2F_5$, oils of different molecular weights were obtained from Du Pont (Krytox 143 series); the linear isomer, $-[CF_2CF_2CF_2O]_n-$, was received from Daikin Co. (Demnum S-20 and S-100); Aflunox was procured from PCR Inc. The other perfluoropolyalkylethers were prepared by Exfluor Research Corp. and were provided by the U. S. Air Force.

Degradation

All the tests were carried out in pure oxygen (~400 mm Hg pressure at 25°C) in the presence of an M-50 alloy coupon over 24 h period at the denoted temperatures. At the end of exposure the volatile condensibles were removed in vacuo and weighed. Detailed description of the procedure and apparatus was reported previously [Ref. 23]. The temperature at which the total of volatile condensibles amounted to 0.50 ± 0.25 mg/g (mg of products formed per g of fluid employed) was defined as the degradation onset. To arrive at this point tests were carried out, if necessary, 5°C apart. Thus the onset temperature is given within ±5°C.

Computation

The molecular mechanics calculations of energies are based on MM2 developed by Allinger [Ref. 24] modified by Hypercube Inc. (MM^+; Hyperchem 3.0 software). The MM^+ parameters were

using the U.S. Air Force provided PM3 data set developed by J. J. P. Stewart specifically for perfluoroalkylethers. The bond lengths and angles used are listed below. Bond lengths: C–C = 1.554 Å, C–O = 1.354 Å,
C–F = 1.312 Å. Angles: C–C–C = 112.2°, C–C–O = 108.2°, C–O–C = 124.7°, O–C–O = 109.4°. To obtain valid derivations, based partially on the average molecular weights of the fluids studied (the exception being Krytox 143AC and its fluorinated product), all the stability computations were carried out on representative telomers having molecular weights as close as feasible to 2500. Each of the structures listed in Table 15 was geometry optimized at 0°K. Using the molecular dynamics program the temperature was increased to 313°K over 3 picoseconds. After equilibrium was reached over 5 picoseconds, data were collected over next 2 picoseconds for a total of 2000 data points. The conformations obtained at 0, 1, 1.5 and 2 picoseconds were geometry optimized and the energy parameters, subsequently calculated at the four time periods, were averaged. These are the energy parameters listed in Table 15. The regression analyses to develop the QSARs were performed with SPSS 4.01 computer program.

Preparation of $Cl_2C{=}CClCCl{=}CCl(OC_2H_5)$

Under nitrogen bypass to stirred hexachlorobutadiene (400 g, 1.53 mol), at 78°C was added (via an addition funnel) 576 mL of $NaOC_2H_5$ solution in ethanol (21% by weight) over a period of 6

hours. After the addition was completed, the solution was cooled to room temperature, followed by addition of water (800 mL) and ether extraction. Following separation the organic layers were dried over $MgSO_4$. Removal of the solvent gave a dark yellow solution (355 g). Based on the GC/MS, it contained 45% of the product which consisted of at least three isomers. Purification using a 3 ft spinning band column gave 95 g (23% yield) of 96% pure product, bp 60-61°C at 0.40-0.42 mm Hg. The two impurities present were the starting material, hexachlorobutadiene, and the di-substituted by-product. A representative MS of $Cl_2C{=}CClCCl{=}CCl(OC_2H_5)$ is given in Table 18.

Preparation of $Cl_3CCCl{=}CClCOCl$

At room temperature, into $Cl_2C{=}CClCCl{=}CCl(OC_2H_5)$ (25.9 g, 95.8 mmol) was bubbled chlorine over 7 3/4 hours; subsequently, the mixture was heated under nitrogen bypass at 125°C for 2 hours. The crude product (15.6 g) contained 66% of the desired product, as determined by GC. Purification by distillation, through a short column in vacuo, gave 18.9 g (71.5% yield) of 86% pure $Cl_3CCCl{=}CClCOCl$, bp 42-43°C at 0.001 mm Hg. The two impurities were $Cl_2C{=}CClCOCl$ and $Cl_2C{=}CClCCl{=}CCl(OC_2H_5)$. The mass spectrum of $Cl_3CCCl{=}CClCOCl$ is given in Table 19.

Preparation of Hexachlorofuran

To $Cl_3CCCl{=}CClCOCl$ (58.3 g, 165 mmol) was added $FeCl_3$ (0.6 g), and the mixture was stirred under nitrogen for 3 hours at 170°C. The product was then distilled out, bp 44-48°C at 0.001 mm

TABLE 18

ION FRAGMENTS AND INTENSITIES RELATIVE TO BASE PEAK OF $Cl_2C=CCl-CCl=CClOC_2H_5$

m/e	%	m/e	%	m/e	%	m/e	%
35	17.8	117	25.0	170	17.4	214	6.0
36	51.5	118	17.5	171	27.4	215	23.9
37	14.7	119	24.9	172	15.0	216	5.0
38	21.5	120	13.9	173	13.9	217	15.8
43	9.9	121	12.8	174	9.0	219	6.4
47	19.6	123	90.9	176	76.2	223	7.0
49	12.1	124	8.8	177	59.2	225	9.4
59	5.2	125	74.3	178	85.3	227	6.6
63	25.3	126	7.0	179	71.1	233	16.0
64	6.3	127	22.8	180	58.7	234	5.8
65	12.9	133	9.7	181	40.7	235	21.6
70	6.2	134	19.5	182	24.6	237	11.9
71	34.4	135	11.6	183	18.0	239	5.0
72	16.0	136	14.8	184	5.0	240	42.8
73	23.9	137	5.5	188	14.9	241	9.5
74	7.0	141	93.3	189	5.1	242	69.6
82	9.8	142	14.4	190	17.7	243	9.8
83	16.6	143	87.8	191	6.0	244	47.1
84	11.3	144	12.6	192	10.5	245	7.7
85	11.2	145	39.0	197	6.5	246	22.9
87	14.3	146	6.0	199	6.0	248	7.2
89	8.6	147	11.6	204	50.4	268	88.4
94	11.2	153	12.9	205	84.1	269	17.1
96	7.8	154	7.7	206	69.9	270	100.0
99	12.0	155	14.2	207	84.2	271	24.0
106	59.0	156	5.2	208	42.5	272	82.4
107	22.9	157	26.7	209	63.1	273	15.5
108	35.4	159	25.6	210	17.4	274	37.7
109	17.9	161	13.6	211	30.9	275	7.1
110	12.3	163	5.8	212	7.2	276	11.6
111	5.8	169	29.1	213	25.9		

Peaks having intensities lower than 5% of the base peak and lower than m/e 31 are not reported.

Significant Ions in Support of Structure and Composition

m/e	ion	m/e	ion
268	M	204	M - HCl - C_2H_4
240	M - C_2H_4	169	M - HCl - C_2H_4 - Cl
233	M - Cl	106	M - HCl - C_2H_4 - Cl - COCl

TABLE 19

ION FRAGMENTS AND INTENSITIES RELATIVE TO BASE PEAK OF Cl_3C-CCl=CClCOCl

m/e	%	m/e	%	m/e	%	m/e	%
35	31.6	89	18.3	131	6.8	212	18.4
36	54.7	90	8.2	134	5.0	213	100.0
37	19.0	94	18.9	141	62.6	214	29.3
38	17.0	96	13.9	142	7.4	215	88.6
47	25.2	103	5.9	143	59.8	216	26.3
49	18.4	105	11.3	144	6.4	217	67.7
53	14.3	106	78.2	145	24.1	218	11.9
54	9.8	107	17.7	147	8.1	219	19.8
59	11.7	108	52.0	176	21.7	239	44.8
61	5.2	109	6.2	178	21.9	240	5.5
63	50.0	110	18.3	179	8.5	241	61.1
65	22.6	112	6.6	180	17.3	242	8.5
70	19.9	117	68.4	181	6.3	243	44.9
71	59.6	118	6.6	182	7.0	244	5.1
72	19.3	119	61.2	186	9.8	245	20.6
73	22.7	120	6.1	188	9.9	247	5.8
74	5.7	121	25.0	204	15.3	274	19.0
82	18.3	122	5.0	206	15.4	276	24.0
83	5.1	123	13.3	208	11.6	278	21.5
84	15.9	125	6.6	210	5.4	280	13.6
87	13.2	129	6.2	211	95.6	282	5.1
88	13.0						

Peaks having intensities lower than 5% of the base peak and lower than m/e 31 are not reported.

Significant Ions in Support of Structure and Composition

m/e	ion	m/e	ion
274	M	176	M - COCl - Cl
239	M - Cl	141	M - COCl - 2Cl
211	M - COCl	117	Cl_3C
204	M - 2Cl		

Hg, giving 43.3 g (94.8% yield) of perchloro-2,5-dihydrofuran, which solidified after cooling below 0°C. Mass spectrum is given in Table 20.

Preparation of 2,2,5,5,-Tetrafluoro-3,4-dichlorofuran from hexachlorofuran

To hexachlorofuran (42.8 g, 0.155 mol) were added SbF_3 (56 g, 0.31 mol) and $SbCl_5$ (24 g, 80 mmol). The mixture was then stirred at 100°C for 2 hours under nitrogen atmosphere. Distillation, bp 72-74°C, gave 17.5 g (52% yield) of the desired product (purity >97%); the mass spectrum is presented in Table 21.

Attempted Preparation of 2,2,5,5,-Tetrafluoro-3,4-dichlorofuran from Dichloromaleic Anhydride

In a typical reaction, to a 600 mL stainless steel bomb (Parr Instrument Co.) was added dichloromaleic anhydride (50.0 g, 0.30 mol) followed by anhydrous HF (4 mL). Next SF_4 (259 g, 2.4 mol) was condensed in at -78°C using a high pressure hose. Subsequently, the reactor was warmed to room temperature, placed in a sand bath on a shaker, and heated at 345°C for 160 hours with constant shaking. The bomb was then cooled to 0°C (in an ice bath) and vented slowly. This was followed by warming to room temperature, and after 1 hour the contents were poured into a plastic bottle containing 4 g NaF to remove any remaining HF. After transfer to a round bottom flask, the products were separated from $NaF/NaHF_2$ mixture by bulb-to-bulb distillation *in vacuo*, initially at room temperature, then at 40°C. A 50.5 g

TABLE 20

ION FRAGMENTS AND INTENSITIES RELATIVE TO BASE PEAK OF

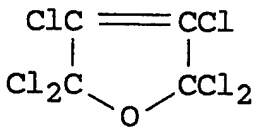

m/e	%	m/e	%	m/e	%	m/e	%
35	50.9	98	8.5	157	13.1	218	8.1
36	95.7	102	13.7	159	5.0	219	21.6
37	28.8	103	16.5	166	5.9	223	38.2
38	29.1	104	10.5	176	38.8	224	7.2
47	56.3	106	98.5	177	7.3	225	54.7
48	12.1	107	36.6	178	49.1	226	9.4
49	25.8	108	90.2	179	9.0	227	42.0
53	19.5	109	19.6	180	29.4	228	6.9
54	16.1	110	27.9	181	5.4	229	20.0
59	20.2	117	57.3	182	13.1	231	7.2
61	10.1	118	37.4	188	33.3	239	88.0
63	48.8	119	61.5	189	8.1	240	22.2
65	23.5	120	29.9	190	38.2	241	96.7
70	15.2	121	30.4	191	10.8	242	21.9
71	79.0	122	12.5	192	24.5	243	89.8
72	25.3	123	8.7	193	6.2	244	21.0
73	47.5	129	9.0	194	10.9	245	56.7
74	7.9	130	5.3	204	31.9	246	9.1
82	25.5	131	9.0	205	6.2	247	20.1
83	23.8	133	5.0	206	41.4	258	21.3
84	22.2	134	8.2	207	8.9	260	29.8
85	13.6	136	5.3	208	24.5	261	5.4
86	8.0	141	85.7	209	5.9	262	26.4
87	20.1	142	17.7	210	12.5	263	5.0
88	18.1	143	87.0	211	87.3	264	18.2
89	24.8	144	17.8	212	19.8	266	7.7
90	18.3	145	59.4	213	100.0	274	6.8
91	6.9	146	8.1	214	22.0	276	10.8
94	8.5	147	16.5	215	91.3	278	8.7
95	31.7	153	22.5	216	17.1	280	5.4
96	24.1	155	21.9	217	59.3		

Peaks having intensities lower than 5% of the base peak and lower than m/e 31 are not reported.

Significant Ions in Support of Structure and Composition

m/e	ion	m/e	ion	m/e	ion
274	M	204	M - 2Cl	63	$COCl$
239	M - Cl	176	M - $COCl_2$	47	CCl
211	M - $COCl$	141	M - $COCl_2$ - Cl		

TABLE 21

ION FRAGMENTS AND INTENSITIES RELATIVE TO BASE PEAK OF

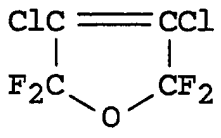

m/e	%	m/e	%	m/e	%	m/e	%
31	37.7	71	4.6	94	10.4	163	54.3
32	11.3	72	5.4	96	6.8	165	37.4
35	7.1	73	4.6	97	5.3	167	6.7
36	7.8	74	41.2	109	100.0	175	25.3
47	26.9	78	6.3	110	7.7	177	9.0
49	5.6	85	10.2	111	47.3	182	4.1
50	6.1	87	7.1	144	11.1	191	5.5
55	21.4	90	14.2	146	7.3	193	3.3
59	8.9	92	4.4	147	12.5	210	21.1
61	3.3	93	12.1	149	3.7	212	14.3
69	46.6						

Peaks having intensities lower than 3% of the base peak and lower than m/e 31 are not reported.

Significant Ions in Support of Structure and Composition

m/e	ion
210	M
175	M - Cl
163	M - CCl
147	M - COCl
109	M - COF_2-Cl

mixture consisting of 15% of the desired furan, and 84% lactone was collected.

Treatment of the Lactone/Furan Mixture with SF_4

The 50.5 g mixture obtained from the reaction of dichloromaleic anhydride with SF_4 was retreated with SF_4 (98 g, 0.91 mol) at 345°C over 160 hours using the procedure described above. After workup 47 g of the crude product was obtained which consisted of 74% 2,2,5,5-tetrafluoro-3,4-dichlorofuran, 23% lactone and 1.5% $CF_3CCl=CClCF_3$ and $CF_3CCl=CClCOF$. The furan, bp 72-74°C (purity 97%, GC), was isolated by distillation.

Preparation of Perfluorooxydiacetic acid

In a typical reaction, a 250 mL round bottom flask equipped with a magnetic stir bar, a Claisen adapter attached to a condenser and additional funnel, was charged with KOH (10.7 g, 190 mmol), $KMnO_4$ (15.0 g, 94.8 mmol), and 85 mL distilled water. After stirring for 10 minutes (until all KOH dissolved) 2,2,5,5-tetrafluoro-3,4-dichlorofuran (10.0 g, 47.4 mmol) was added dropwise over a period of 15 minutes. The reaction mixture was then stirred for 1 hour at room temperature. Subsequently, the temperature was slowly raised to 44°C and held there for 18 hours. After cooling to room temperature, H_2SO_4 (50 mL, 75%) was added slowly over a 30 minute period. The entire reaction mixture was continuously extracted with diethyl ether over a 7 hour period. The ether extracts were dried over $MgSO_4$; ether was removed by distillation under nitrogen bypass to give 7.5 g of crude product.

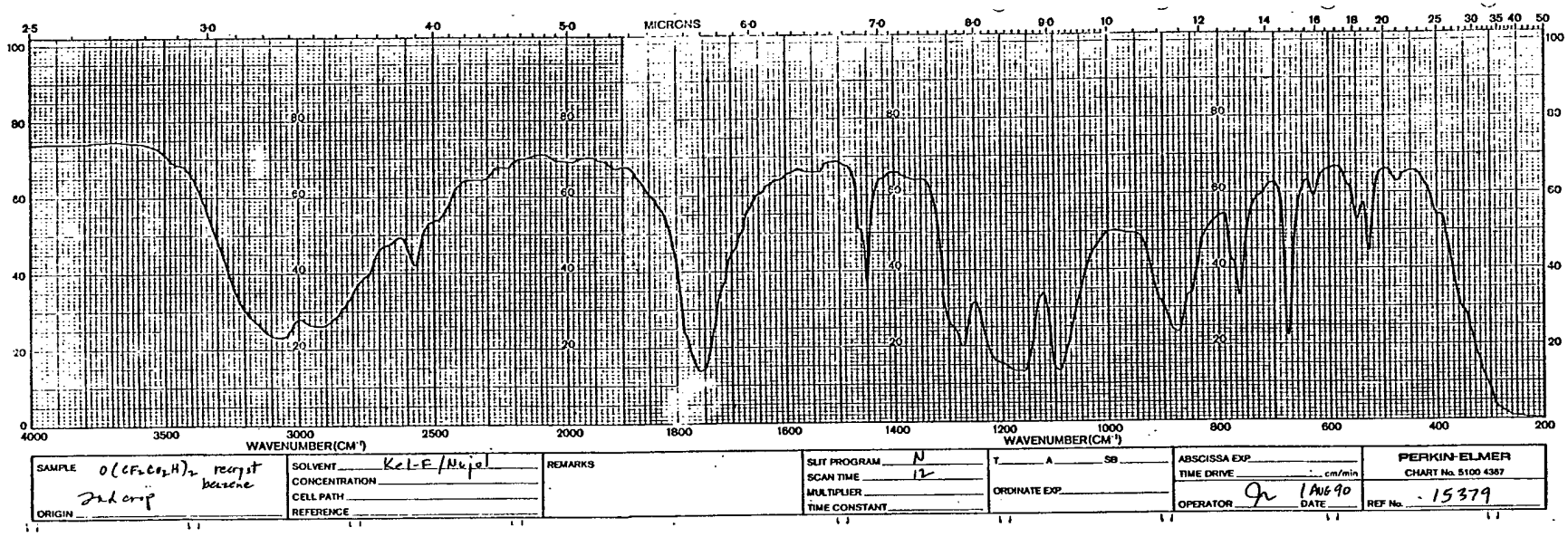

Figure 51. Infrared spectrum (Kel-F/Nujol double mull) of perfluoro-oxydiacetic acid (IR# 15379 ID# 2-90-140).

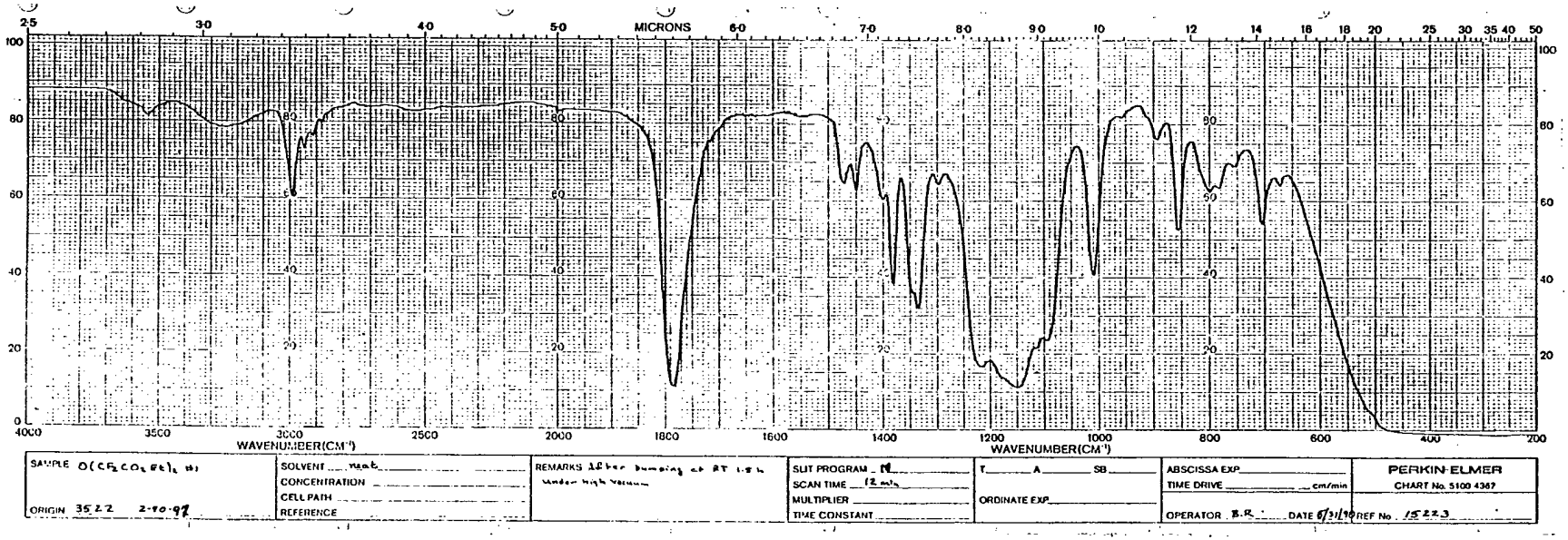

Figure 52. Infrared spectrum of $C_2H_5O_2CCF_2OCF_2CO_2C_2H_5$ (ID# 2-90-97, IR# 15223), thin film.

TABLE 22

ION FRAGMENTS AND INTENSITIES RELATIVE TO BASE PEAK OF $C_2H_5OC(O)CF_2OCF_2C(O)OC_2H_5$

m/e	%	m/e	%	m/e	%	m/e	%
27	52.7	55	6.8	94	9.5	162	10.9
28	68.3	56	5.7	95	30.2	187	14.9
29	100.0	57	7.2	96	53.9	189	26.7
30	44.9	59	40.2	97	12.1	190	17.8
31	45.2	60	8.5	98	5.1	191	5.6
32	8.1	65	10.5	115	11.8	207	21.6
33	6.4	66	10.1	116	9.5	210	5.6
41	11.8	67	10.2	121	10.1	215	30.7
42	11.0	73	22.1	123	35.8	216	7.1
43	34.0	74	17.8	124	49.8	217	9.3
44	34.8	75	7.0	125	31.5	225	21.5
45	51.3	76	6.4	126	6.1	235	31.5
46	9.5	77	10.1	139	6.0	236	7.6
47	33.2	78	28.6	142	10.5	243	17.1
48	5.1	79	11.8	152	23.8	263	44.6
50	30.7	80	11.4	153	5.0	264	20.4
51	38.3	93	14.3	161	10.7	291	5.0

Peaks having intensities less than 5% of the base peak and lower than m/e 27 are not reported.

Recrystallization from hot benzene in an inert atmosphere enclosure (the material is extremely hygroscopic) gave pure perfluorooxydiacetic acid, 5.9 g (61% yield) mp 77-78°C. Its infrared spectrum is given in Figure 51.

Preparation of Diethyl Ester of Perfluorooxydiacetic Acid

A 100 mL round bottom flask equipped with a magnetic stir bar was charged with ethanol (10 mL), benzene (50 mL), concentrated H_2SO_4 (1 mL), and perfluorooxydiacetic acid (2.3 g, 11.2 mmol). The flask was fitted with a reflux condenser and the mixture was refluxed overnight under nitrogen bypass. After cooling to room temperature it was poured into 50 mL of distilled water. The bottom layer was removed and extracted with 3 x 25 mL portions of diethyl ether. The organic portions were combined, washed with water, and dried over $MgSO_4$, and the volatile solvents were removed by distillation to give the ethyl ester, 2.2 g (75% yield; 83% purity, GC). The infrared spectrum is given in Figure 52, the mass spectrum in Table 22.

Preparation of $HOCH_2CF_2OCF_2CH_2OH$

In the inert atmosphere enclosure, a 100 mL round bottom three necked flask was charged with $LiAlH_4$ (1.2 g, 32 mmol) and fitted with a reflux condenser, nitrogen bypass valve, and a 25 mL addition funnel. Under nitrogen bypass, diethyl ether was added slowly via the addition funnel. The mixture was cooled to 0°C (ice/water bath) and a solution of $EtO_2CCF_2OCF_2CO_2Et$ (2.0 g, 7.63 mmol) in diethyl ether (20 mL) was added dropwise over a 40 minute

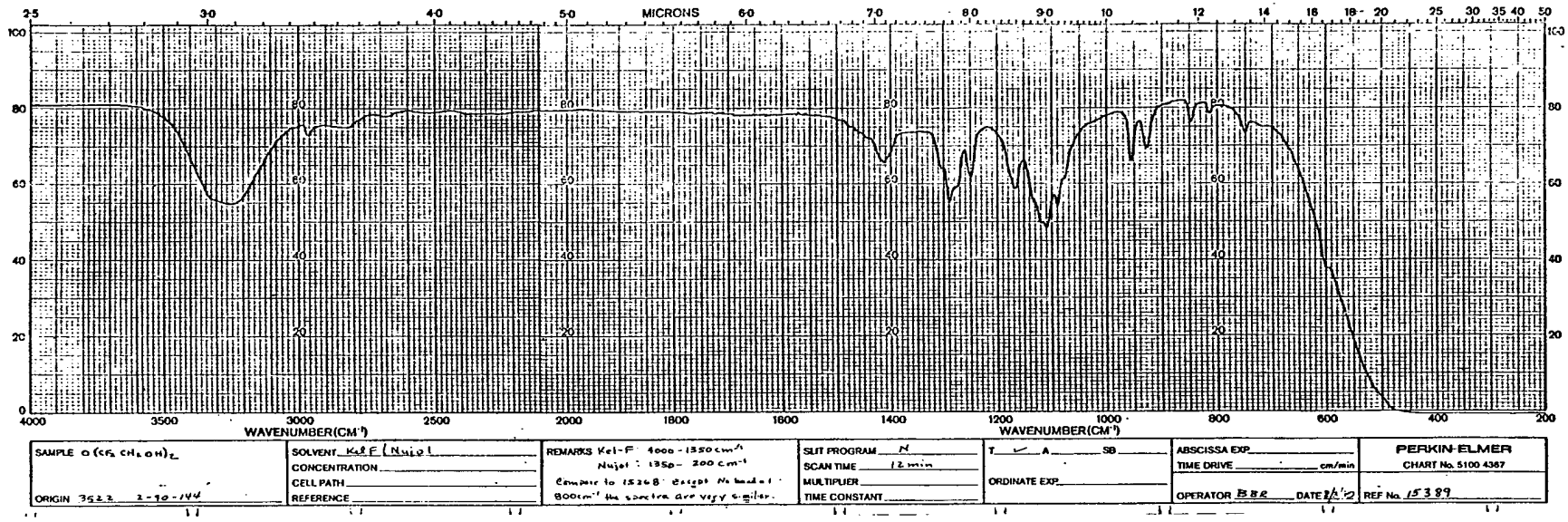

Figure 53. Infrared spectrum (Kel-F/Nujol double mull) of $HOCH_2CF_2OCF_2CH_2OH$ (IR# 15389, ID# 2-90-144).

period. The reaction was instantaneous, giving off gases after each drop. The mixture was allowed to warm slowly to room temperature, followed by 1 hour reflux. The excess of $LiAlH_4$ was destroyed with ethyl acetate at 0°C. After 15 minutes of stirring, water (5 mL) was added followed by aqueous H_2SO_4 (100 mL, 20%). The bottom layer was removed and continuously extracted with diethyl ether for 6 hours. The original ether layer was combined with the ether extract, dried over $MgSO_4$, and following solvent removal 1.3 g (96% yield) of crude diol was obtained. Crystallization from benzene gave white needles of $HOCH_2CF_2OCF_2CH_2OH$, 1.1 g (80.8% yield) mp 68-69°C (literature 68°C, Ref. 13); the infrared spectrum is given in Figure 53; the mass spectra of the free alcohol and of its trimethylsilyl derivative are given in Tables 23 and 24 respectively.

Attempted Preparation of $O(CF_2COCl)_2$

In an inert atmosphere enclosure, a 100 mL flask containing a magnetic stir bar was charged with 2.5 g (12.1 mmol) of $O(CF_2CO_2H)_2$ and 6.2 g (30.3 mmol) of phthalolyl chloride. The flask was then fitted with a reflux condenser and heated at 160°C for 2 hours under nitrogen bypass. After cooling to room temperature the volatiles were removed in vacuo initially at room temperature then at 50-55°C and were collected in a -196°C cooled trap.

The volatiles (2.4 g, 81% yield) exhibited 39 mm Hg vapor pressure at 24.1°C. Analysis by GC and GC/MS found the material

TABLE 23

ION FRAGMENTS AND INTENSITIES RELATIVE TO BASE PEAK OF $HOCH_2CF_2OCF_2CH_2OH$

m/e	%	m/e	%	m/e	%	m/e	%
14	15.4	48	5.4	77	7.5	119	5.6
15	6.6	49	17.2	78	24.2	122	5.0
18	9.6	50	15.4	79	18.6	123	7.0
19	12.6	51	67.6	80	64.1	125	3.2
20	13.4	52	7.7	81	81.4	127	63.9
26	5.4	53	9.6	82	31.5	128	28.1
27	4.7	54	5.0	83	11.8	129	5.1
28	38.0	58	15.1	91	13.9	130	5.3
29	65.6	59	19.7	92	47.7	131	3.2
30	39.7	60	18.3	93	14.6	138	7.6
31	100.0	61	74.1	94	9.3	139	55.1
32	45.2	62	53.9	95	3.0	140	10.5
33	97.1	63	30.3	97	7.0	141	18.5
34	9.9	64	69.0	98	3.9	142	3.5
36	3.8	65	46.6	99	4.1	143	7.1
41	5.7	66	19.0	101	13.8	145	3.5
42	59.0	67	40.1	108	14.9	147	15.2
43	25.1	69	3.0	109	6.8	148	8.0
44	17.2	71	14.0	110	10.0	158	5.7
45	27.6	72	5.1	111	36.4	161	3.9
46	16.2	73	4.0	112	7.4	178	1.1
47	34.1	74	5.5	113	16.0	179	6.7

Peaks having intensities lower than 3% of the base peak and lower than m/e 14 are not reported.

Significant Ions in Support of Structure and Composition

m/e	Intensity	Assignment	m/e	Intensity	Assignment
178	1.1	M^+	94	9.3	$(COF)_2^+$
161	3.9	$(M-OH)^+$	81	81.4	$(CF_2CH_2OH)^+$
147	15.2	$(M-CH_2OH)^+$	64	69.0	$(CF_2CH_2)^+$
141	18.5	$(M-OH-HF)^+$	61	74.1	$(CF{=}CHOH)^+$
127	63.9	$(CFOCH_2CF_2)^+$	31	100.0	$(CH_2OH)^+$
			20	13.4	$(HF)^+$

TABLE 24

ION FRAGMENTS AND INTENSITIES RELATIVE TO BASE PEAK OF

$Me_3SiOCH_2CF_2OCF_2CH_2OSiMe_3$

m/e	%	m/e	%	m/e	%	m/e	%
15	12.3	51	7.1	80	6.1	139	4.9
27	9.2	55	7.2	81	25.7	151	11.6
28	18.7	57	9.9	82	3.8	152	5.6
29	36.5	58	15.3	83	3.6	153	35.8
30	6.2	59	19.0	88	7.1	154	11.1
31	16.7	60	3.6	91	27.2	155	6.7
32	3.0	61	33.9	92	5.1	157	17.8
33	20.1	62	7.2	93	4.7	158	3.4
34	3.1	63	33.9	103	32.4	169	4.3
35	6.2	64	13.5	104	10.2	187	14.8
42	17.3	71	4.2	105	4.9	211	7.3
43	28.8	72	15.2	107	54.4	215	27.8
44	17.9	73	100.0	108	11.9	216	8.4
45	37.3	74	34.9	109	7.9	217	4.1
46	5.4	75	28.9	111	8.4	227	14.4
47	26.8	76	11.6	119	6.1	228	4.6
48	3.3	77	85.1	135	50.8	307	9.5
49	23.6	78	19.6	136	11.8		
50	3.0	79	16.1	137	8.5		

Peaks having intensities lower than 3% of the base peak and lower than m/e 15 are not reported.

Significant Ions in Support of Structure and Composition

m/e		m/e	
307	$[M - CH_3]^+$	103	$Me_3SiOCH_2^+$
153	$Me_3SiOCH_2CF_2^+$	73	Me_3Si^+

to consist of 16% perfluorooxydiacetic anhydride, 61% diacid chloride, and some unidentified higher boiling fractions.

Preparation of Methyl Ester of Perfluorooxydiacetic Acid

A 50 mL round bottom flask containing a magnetic stirring bar was charged with 3.3 g of a mixture containing 79% of perfluorooxydiacetic anhydride and 7.1% diacyl chloride (based on GC area %). After cooling to 0°C, 15 mL of methanol were added dropwise via addition funnel. A vigorous reaction occurred with the evolution of white fumes. The addition was completed in 0.5 hour. At this stage, 0.5 mL of concentrated H_2SO_4 was added and the mixture heated at 78°C for 19 hours. Following cooling to room temperature the mixture was treated with diethyl ether (75 mL) and then washed with 3 x 25 mL portions of water. The organic layer was dried over anhydrous $MgSO_4$ to give after solvent removal 3.07 g (94.2% yield) of the desired methyl diester. Its mass spectrum is presented in Table 25 and the infrared spectrum in Figure 54.

Preparation of Oxalyl Fluoride

In an inert atmosphere enclosure a 300 mL three-neck round bottom flask equipped with a magnetic stirring bar, reflux condenser, addition funnel, and nitrogen bypass inlet was charged with sodium fluoride (45 g, 1.07 mol, dried at 250°C in vacuo) followed by acetonitrile (90 mL, distilled from P_2O_5). Oxalyl chloride (45.4 g, 0.358 mol) was weighed into the addition funnel. After attachment to nitrogen bypass and connection to a receiver

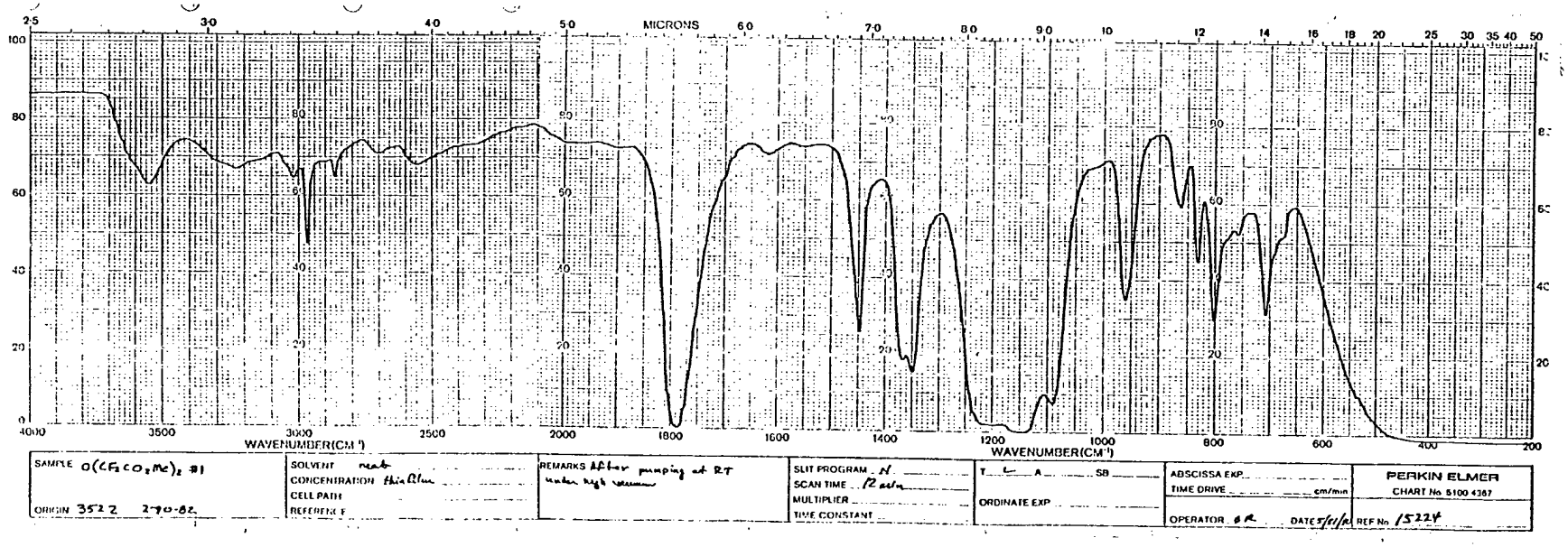

Figure 54. Infrared spectrum of $CH_3O_2CCF_2OCF_2CO_2CH_3$ (ID# 2-90-82, IR# 15224), thin film.

TABLE 25

ION FRAGMENTS AND INTENSITIES RELATIVE TO BASE PEAK OF $CH_3OC(O)CF_2OCF_2C(O)OCH_3$

m/e	%	m/e	%	m/e	%	m/e	%
31	35.1	62	5.9	90	9.2	126	4.7
32	12.4	64	5.2	93	15.2	143	8.3
33	8.0	65	61.5	94	33.0	156	8.5
43	26.8	66	20.0	95	8.0	175	41.7
44	23.5	67	8.0	96	2.6	176	7.2
45	80.3	69	5.3	108	4.2	207	5.3
46	11.3	73	4.2	109	72.2	215	8.6
47	36.5	74	4.1	110	19.7	235	3.3
49	3.0	75	14.4	111	4.4	249	25.8
50	39.2	78	26.8	113	3.0	250	5.7
51	24.8	79	20.8	116	7.1	343	3.1
59	100.0	80	13.2	121	17.0		
60	22.5	81	61.2	124	83.9		
61	9.7	82	8.4	125	16.4		

Peaks having intensities less than 3% of the base peak and lower than m/e 31 are not reported.

at -78°C, oxalyl chloride was added to the NaF/CH_3CN mixture over a period of 30 minutes at room temperature, followed by stirring for an additional hour. Subsequently, the reaction flask was heated at 75-85°C for 13 hours. After heating, the receiver flask was closed off and attached to the vacuum system and the products fractionated through traps held at -63°, -111°, and -196°C. Several fractionations were necessary to collect pure oxalyl fluoride in the -111°C trap (17.54 g, 52% yield). The infrared spectrum is given in Figure 55.

Direct Fluorination of Tetraglyme and Preliminary Analyses by Allied-Signal

An 8 hour reaction of tetraglyme was run in a continuous flow aerosol reactor producing 10.7 g of crude product. The reaction conditions were as follows: reactor temperature -20°C, fluorine:hydrogen ratio 1.4:1, tetraglyme pump flow rate 0.5 cc/minute, photochemical stage was on. Under the conditions of the test, only a small portion of the sample is actually introduced into the reactor through a small orifice. The rest is returned to the reservoir. The material is injected into the reactor as a fine spray. Any aerosol reactor is characterized by a long reaction time and a very low through-put.

After completion of the reaction, the product was fractionated on a vacuum line using a three-stage process of -45°C, - 78°C, and -196°C. The bulk of the sample stayed in the -45°C trap, indicating very little fragmentation of the tetraglyme

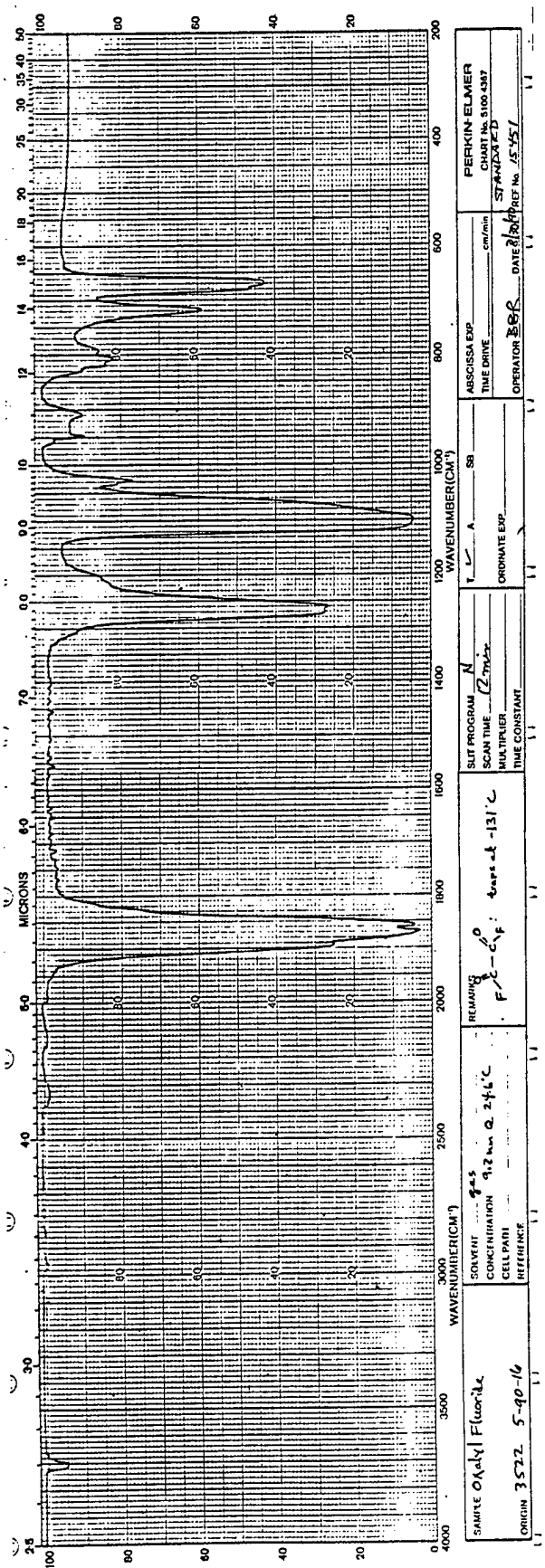

Figure 55. Infrared spectrum of oxalyl fluoride, FC(O)C(O)F (IR# 15451, ID# 5-90-16; gas phase: 9.2 mm at 24.6°C).

during the reaction. The contents of the -45°C trap were then fractionated again through two traps at -5°C and -45°C to remove any underfluorinated tetraglyme. The -45°C fraction which amounted 40-45% of the product, showed no residual hydrogen left using infrared analysis. The -5°C fraction exhibited a weak absorbance at 3000 cm^{-1}, indicating residual C-H bonds. GC analysis of the -45°C trap showed the sample to contain three peaks:

Retention Time	Peak Area	Area %
2.60 minutes	884	2.269
2.96 minutes	653	1.676
4.11 minutes	37423	96.05

The column used was a 12 ft x 1/8 in 5% SP-2401 on 100/120 Supelcoport. The temperature profile was 34°C for 2 minutes and ramped at 10°C/minute until all peaks eluted.

^{19}F NMR of the sample gave three peaks at -56.548 ppm (t), 89.813 ppm (s), and 91.802 ppm (q) referenced to $CFCl_3$. The NMR spectrum correlates very well with literature values. Very little contamination of the sample was seen in the spectrum, indicating that most of the impurities in the GC were from other perfluorinated tetraglyme fragments. Proton NMR was run to determine hydrogen content; however, it showed no evidence of residual hydrogen in the sample.

GC/MS and Infrared Spectral Analyses Performed by Ultrasystems on Perfluorotetraglyme Samples Received from Allied-Signal and NASA Lewis

In Figure 57 are given the gas chromatograms run on two different columns (OV-101 and Porapak Q) by Ultrasystems on the sample of perfluorotetraglyme received from Allied-Signal; in Figure 56 are given the corresponding GC traces of a perfluorotetraglyme sample obtained from NASA Lewis on 3 July 1985. For the samples run on the OV-101 column (Figures 56a and 57a), the purity of the material obtained from NASA (prepared by Exfluor Research Corp.) is definitely higher, 95 vs. 89%.

For GC/MS analysis the two samples were run on the Porapak Q column (see Figures 56b and 57b) in order to better separate the major impurity peaks which elute before the perfluorotetraglyme. For NASA Lewis material, the major impurity (6.3 minutes reaction time (RT)) appears to be $CF_3CF_2O(CF_2CF_2O)_3CF_3$; the Allied-Signal sample also contains this impurity (6.0 minutes RT) in addition to $CF_3O(CF_2CF_2O)_3CF_3$ (4.3 minutes RT). The mass spectrum of the 6 minute peak in the Allied-Signal material also exhibited a high output at m/e 59 which does not appear in the NASA Lewis sample. In fact, none of the perfluorinated ethers, including the perfluorotetraglyme (MS, Table 26), show any significant output at m/e 59. The m/e 59 ion is generally associated with $[CO_2CH_3]^+$; $[C_2FO]^+$ and $[C_3H_4F]^+$ can also account for this ion. The presence of m/e 15 $[CH_3]^+$ in the mass spectrum, however, seems to support $[CO_2CH_3]^+$ for the m/e 59

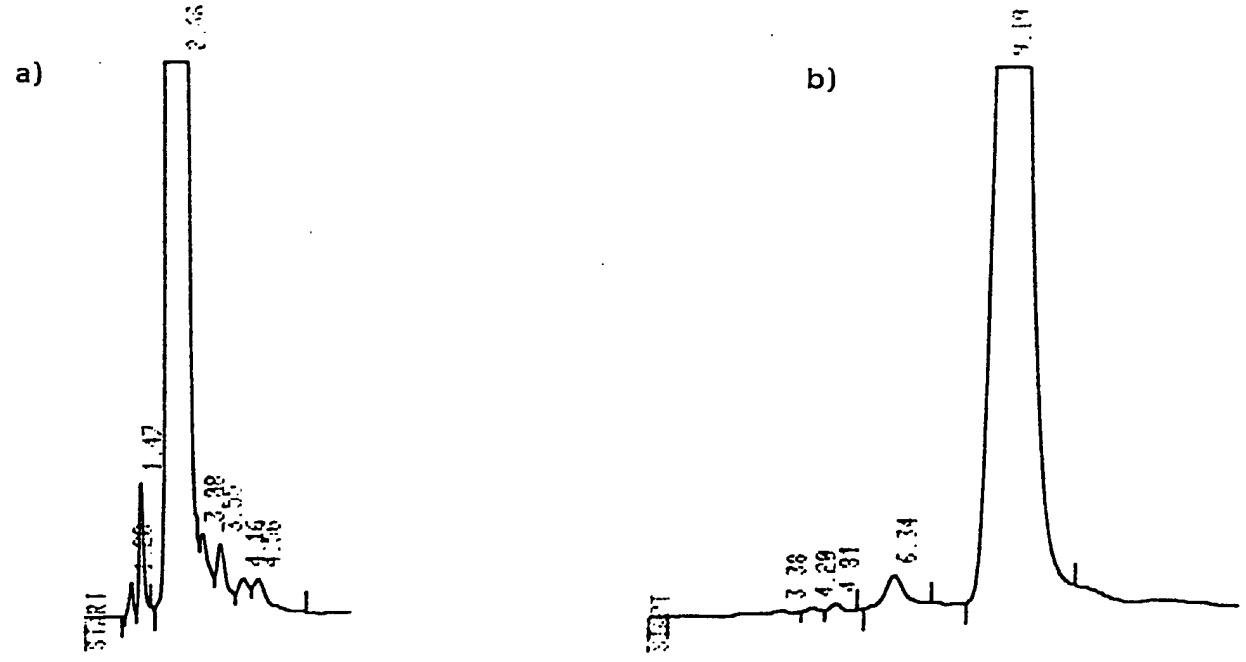

Figure 56. Gas chromatograms of $CF_3O(CF_2CF_2O)_4CF_3$ received from NASA Lewis: (a) 10' x 1/8" SS column, 4% OV-101 on Chromosorb G, isothermal 35°C; (b) 8' x 1/8" SS column, Porapak Q, programmed from 200-220°C at 8°/min.

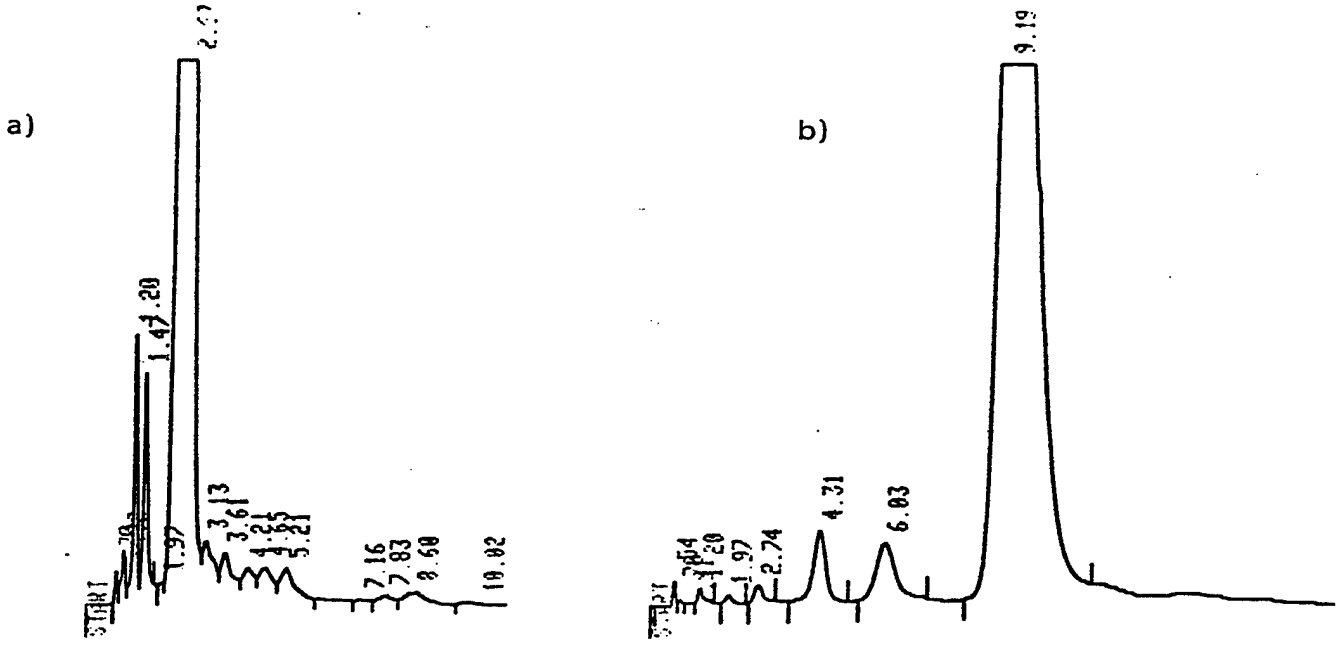

Figure 57. Gas chromatograms of $CF_3O(CF_2CF_2O)_4CF_3$ prepared by Allied-Signal: (a) 10' x 1/8" SS column, 4% OV-101 on Chromosorb G, isothermal 35°C; (b) 8' x 1/8" SS column, Porapak Q, programmed from 200-220°C at 8°/min.

TABLE 26

ION FRAGMENTS AND INTENSITIES RELATIVE TO BASE PEAK OF

$CF_3O(CF_2CF_2O)_4CF_3$ (MW 618)

m/e	%	m/e	%	m/e	%	m/e	%
28	14.2	78	16.2	136	10.6	252	3.3
31	22.1	81	6.9	163	30.7	279	12.5
47	26.4	97	35.7	164	3.8	301	24.2
50	23.0	98	3.9	185	60.1	302	3.7
51	3.5	100	44.2	186	12.7	329	12.9
66	17.6	101	6.5	191	7.5	367	7.8
69	82.1	116	4.6	213	39.2	395	7.6
70	15.4	119	100.0	214	7.0	417	8.1
75	29.7	120	26.9	235	9.8	511	5.0
76	4.1	135	62.3	251	25.7	599	4.4

Peaks having intensities lower than 3% of the base peak and lower than m/e 28 are not reported.

Significant Ions in Support of Structure and Composition

m/e		m/e	
599	$[M - F]^+$	185	$[CF_3OCF_2CF_2]^+$
417	$[CF_3O(CF_2CF_2O)_2CF_2CF_2]^+$	163	$[FOCCF_2CF_2O]^+$
301	$[CF_3OCF_2CF_2OCF_2CF_2]^+$	135	$[CF_3OCF_2]^+$
251	$[CF_3OCF_2CF_2OCF_2]^+$	119	$[C_2F_5]^+$
213	$[FOCCF_2CF_2OCF_2]^+$	69	$[CF_3]^+$

peak. In agreement with the above, the infrared spectrum of the Allied-Signal sample (Figure 58) shows a carbonyl absorption at 1760 cm^{-1}; the NASA Lewis material does not have this band (see Figure 59).

Analysis of the Products Obtained by Allied-Signal from Direct Fluorination of Diglycolic Acid

A 0.95 g sample received from Allied-Signal was subjected to fractionation on the vacuum line through traps kept at 0°C, -78°C, and -196°C. No material was present in the 0°C trap. In the -196°C cooled trap was collected 1.03 mmol of a mixture which consisted of SiF_4 (identified by infrared spectroscopy) and a fluorocarbon material which exhibited infrared absorptions at 1918 cm^{-1} and 1870 cm^{-1}. This is consistent with data reported for perfluoro-β-oxa-δ-valerolactone (bp 30°C, 1866 cm^{-1} for C=O stretch [Ref. 25]). The infrared spectrum is shown in Figure 60.

The bulk of the sample (0.78 g) condensed in the -78°C trap. This material exhibited a vapor pressure of 104 mm Hg at 23°C and 43 mm Hg at 0°C. In the infrared spectrum, given in Figure 61, there are several bands in the carbonyl region. None were near 1894 cm^{-1} reported for $O(CF_2COF)_2$ [Ref. 25]. The measured vapor pressure does not correspond to the value expected for a material of bp 37-38°C. Although the infrared absorptions in the carbonyl region would indicate the lactone, its bp 29-30°C is even lower than that of the diacetyl fluoride and thus higher vapor pressures should be measured if this was the product.

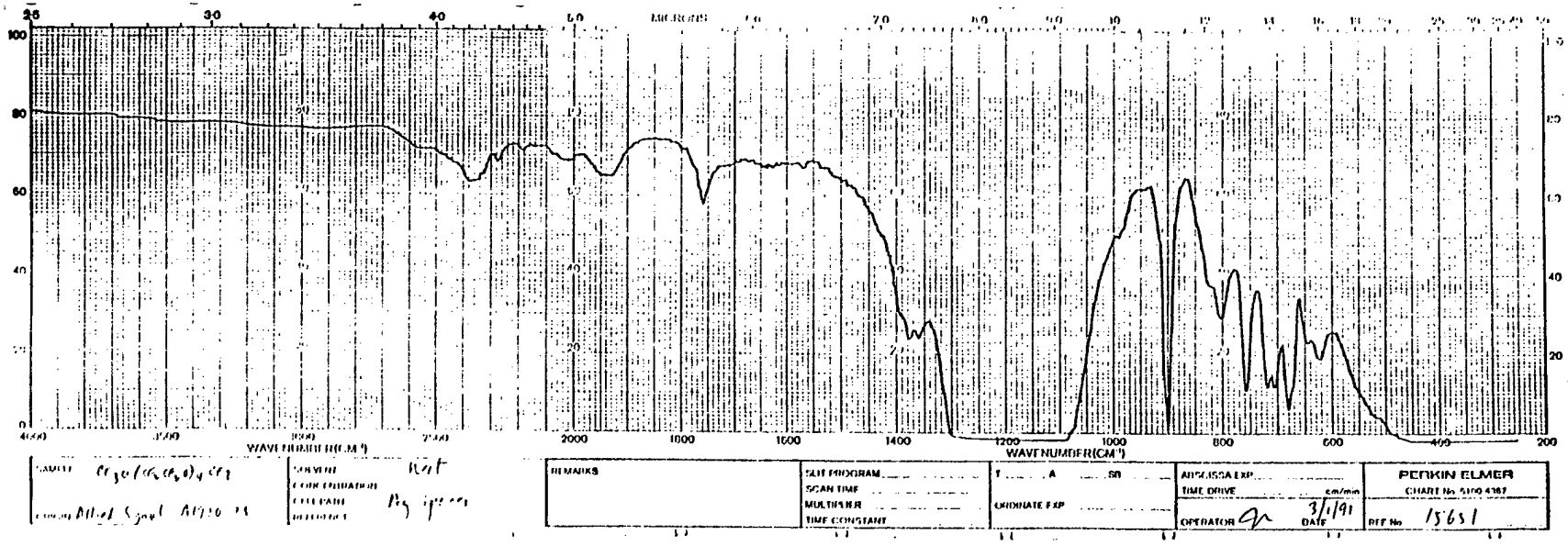

Figure 58. Infrared spectrum of $CF_3O(CF_2CF_2O)_4CF_3$ prepared by Allied-Signal (0.03 mm Ag spacer).

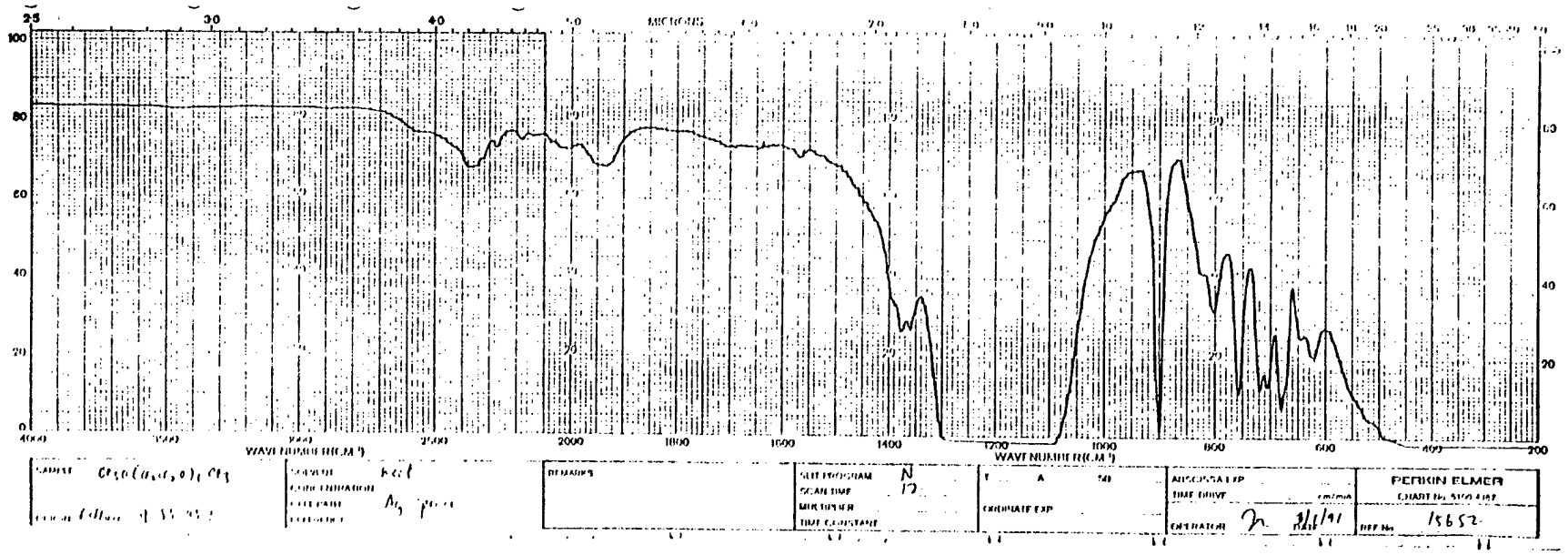

Figure 59. Infrared spectrum of $CF_3O(CF_2CF_2O)_4CF_3$ received from NASA Lewis (0.03 mm Ag spacer).

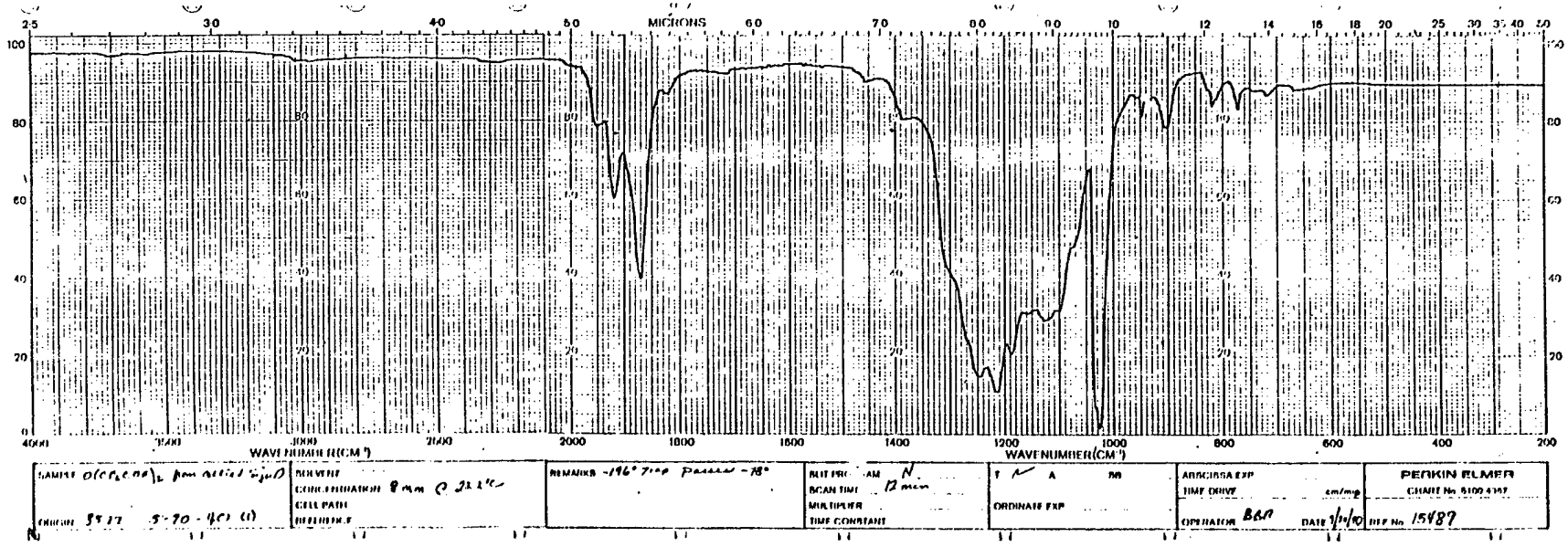

Figure 60. Infrared spectrum of the material isolated at -196°C from $O(CF_2COF)_2$ supplied by Allied-Signal (IR# 15489, ID# 5-89-40 (1); gas phase: 8.0 mm at 23.2°C).

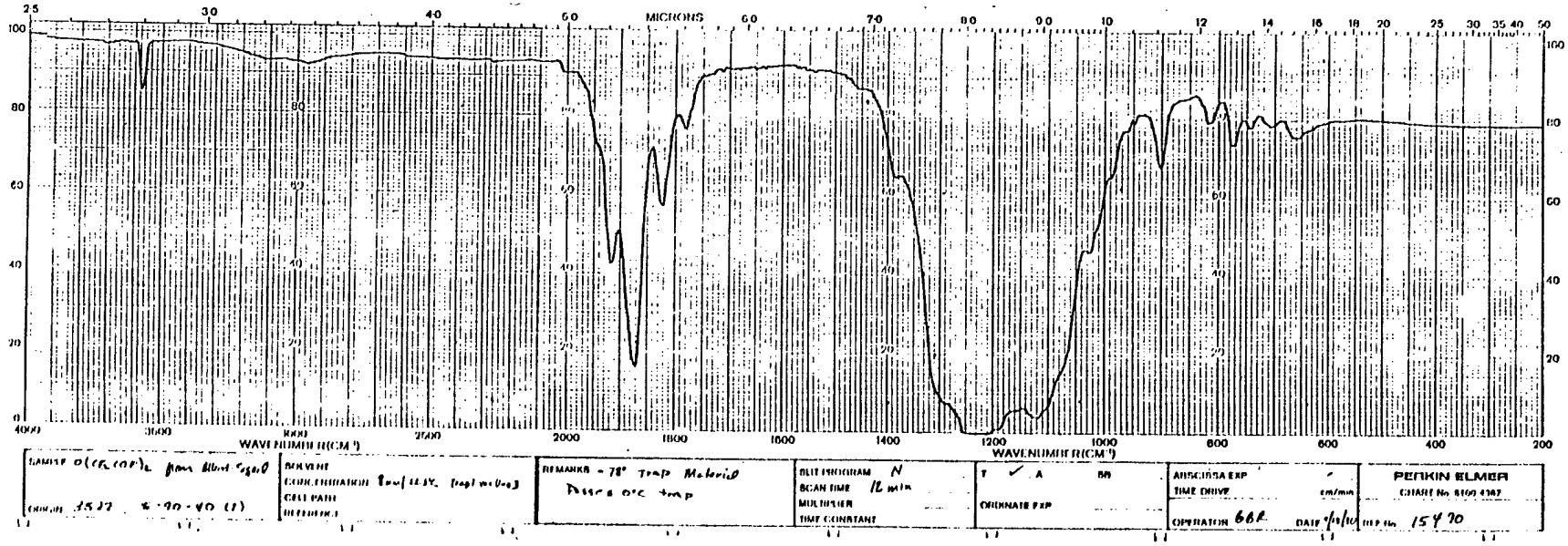

Figure 61. Infrared spectrum of the material isolated at -78°C from $O(CF_2COF)_2$ supplied by Allied-Signal (IR# 15490, ID# 5-90-40 (2); gas phase: 8.0 mm at 22.3°C).

GC analyses, both on the -78°C fraction itself and after the treatment with methanol, are shown in Figures 62 and 63, respectively. The better GC resolution of the methanol-treated material is not surprising in view of the reactivity of the -C(O)F linkages. The presence of -C(O)F groups was shown by infrared spectroscopy and was confirmed by the formation of methyl esters as determined by GC/MS: m/e 59 $[CO_2Me]^+$ and 109 $[CF_2CO_2Me]^+$. The first peak (Figure 63, 7.77 minutes) was methanol. All the other peaks exhibited the $[CO_2Me]^+$ ion indicating the presence of different types of carbonyl fluorides in the original material. Compounds having the arrangements $CF_2CF_2CF_2CF_2CO_2Me$ (m/e 259; peak at 16.74 minutes) were also present; the GC/MS showed clearly the absence of $O(CF_2CO_2Me)_2$. This means that none of the three precursors discussed above -the acid fluoride, lactone or anhydride- were present in the product mixture received from Allied-Signal. Among the products hydrogenated species were also observed, e.g., in the 15.93 minute GC peak (Figure 63). The m/e 51, $[CF_2H]^+$, ion comprised the base (100%) MS peak. Additional evidence of the presence of hydrogenated species were m/e 29 $[CHO]^+$, and/or $[C_2H_5]^+$ and 99 m/e $[C_2H_2F_3O]^+$.

Characterization Data: Experimental fluids MLO 88-48, MLO 88-51, MLO 88-129 and MLO 88-132

^{19}F NMR results for of the fluids listed above are presented in Tables 27-30.

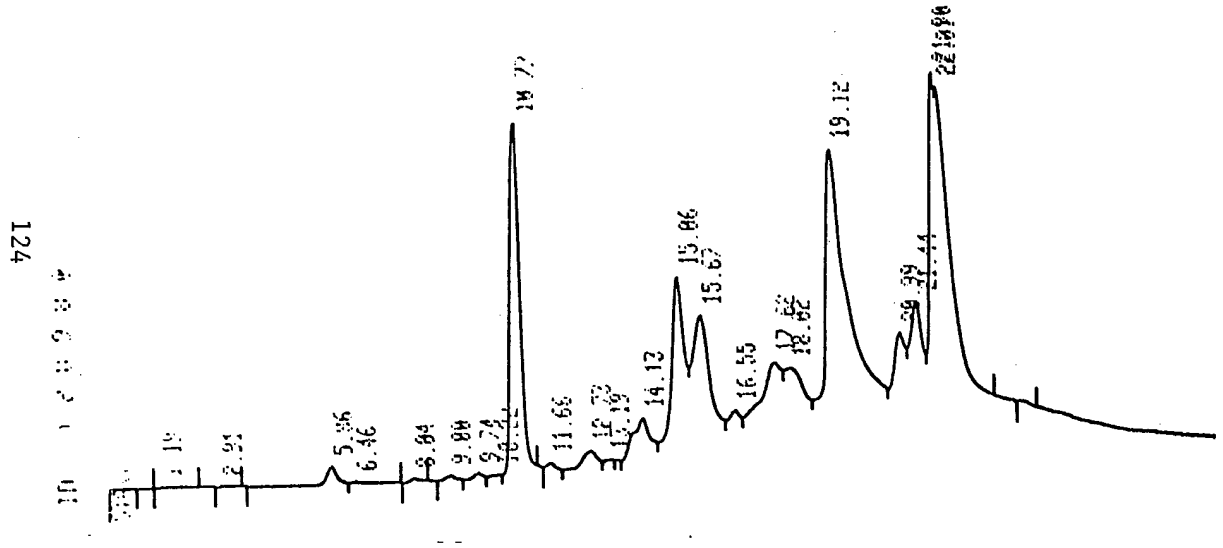

RUN # 13 OCT/12/90 10:38:20
ID 12898

AREA%

RT	AREA	TYPE	AR/HT	AREA%
1.19	3163	PB	0.305	0.013
2.91	2708	PB	0.178	0.011
5.86	149770	PV	0.292	0.625
6.46	19746	VB	0.424	0.082
8.04	17363	PB	0.189	0.073
9.00	33606	PP	0.264	0.140
9.74	27515	PP	0.224	0.115
10.22	5739	PP	0.247	0.024
10.77	2732100	PB	0.278	11.401
11.66	30203	BP	0.222	0.126
12.73	161760	PV	0.398	0.675
13.19	19848	VV	0.250	0.083
14.13	577200	PV	0.525	2.409
15.06	1956300	VV	0.397	8.163
15.67	2031200	VV	0.548	8.476
16.55	334090	VV	0.383	1.394
17.62	1459300	VV	0.713	6.090
18.02	1095400	VV	0.606	4.571
19.12	5547900	VV	0.717	23.151
20.99	835070	VV	0.374	3.485
21.44	1207100	VV	0.399	5.037
21.90	1603800	VV	0.171	6.693
22.01	4113200	D VB	0.457	17.164

TOTAL AREA= 2.3964E+07
MUL FACTOR= 1.0000E+00

Figure 62. GC trace of the product mixture (material collected at -78°C, ID# 5-90-40-1) prepared by direct fluorination of diglycolic acid by Allied-Signal.

(Column: 8' x 1/8" stainless steel packed with Porapak Q, 80/100 mesh.
Conditions: 35-220°C at 8°C/min.; 1.0 μL injected at 200°C, FID at 250°C.)

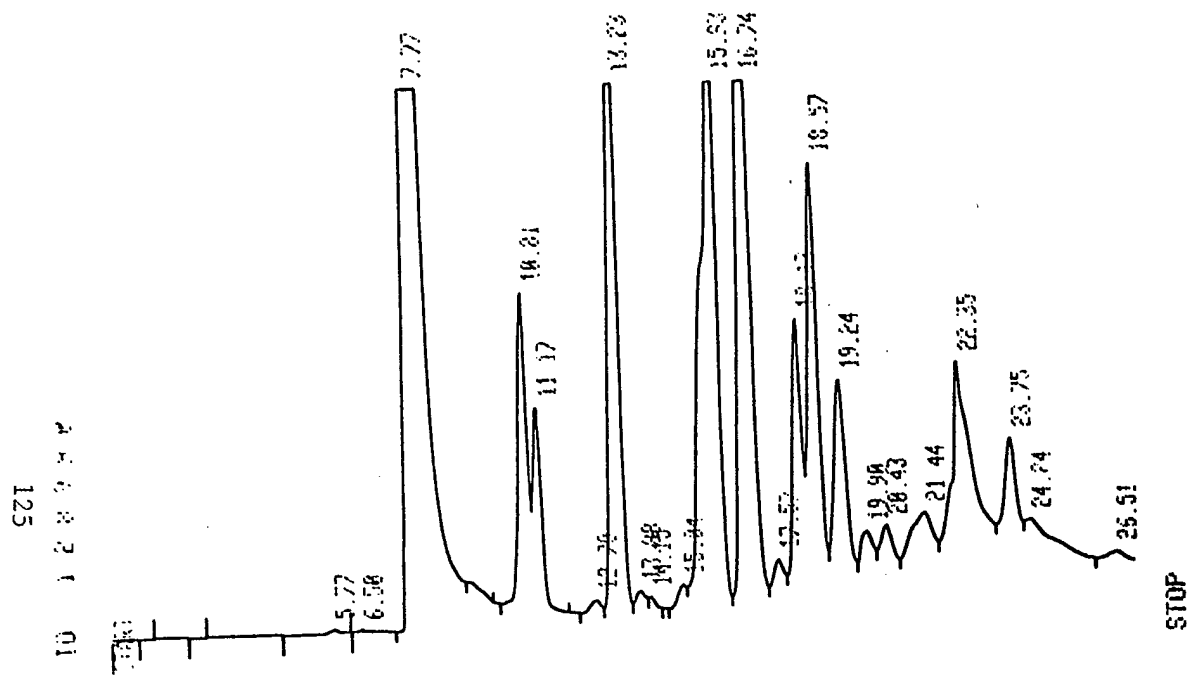

RUN # 14 OCT/12/90 11:31:15
ID 12899

AREA%

RT	AREA	TYPE	AR/HT	AREA%
5.77	522	PB	0.007	5.8893E-04
6.50	14226	BP	0.409	0.016
7.77	4.1949E+07	ISPH	0.543	47.327
10.81	2372500	TBV	0.265	2.677
11.17	1462200	TVP	0.255	1.650
12.70	110690	TPV	0.325	0.125
13.23	5870700	TVV	0.281	6.623
13.88	163500	TVV	0.297	0.185
14.15	73719	DTVV	0.214	0.083
15.04	165540	TPV	0.265	0.187
15.93	8589700	TVV	0.446	9.691
16.74	8245500	TVV	0.341	9.303
17.57	369870	TVV	0.350	0.417
18.13	2337400	TVV	0.297	2.637
18.57	3759800	TVV	0.307	4.242
19.24	2367800	TVV	0.393	2.671
19.90	677970	TVV	0.422	0.765
20.43	770420	TVV	0.450	0.869
21.44	1545800	TVV	0.784	1.744
22.35	4425000	TVV	0.715	4.992
23.75	1728600	TVV	0.450	1.950
24.24	1440800	TVV	0.974	1.626
26.51	194570	ITVB	0.632	0.220

TOTAL AREA= 8.8636E+07
MUL FACTOR= 1.0000E+00

Figure 63. GC trace of the methanol treated sample (ID# 5-90-40-2) of the material prepared by direct fluorination of diglycolic acid by Allied-Signal (precursor collected at -78°C, ID# 5-90-40-1).

(Column: 8′ x 1/8" stainless steel packed with Porapak Q, 80/100 mesh. Conditions: 35-220°C at 8°C/min.; 1.0 μL injected at 200°C, FID at 250°C.)

TABLE 27

^{19}F NMR RESULTS FOR MLO 88-48

Sample Identification: MLO 88-48

Structure Originally Proposed:

$CF_3O(CF_2CF_2CF_2CF_2O)_nCF_3$

Structure Postulated:

$CF_3CF_2CF_2O(CF_2CF_2CF_2CF_2O)_nCF_2CF_2CF_3$

^{19}F NMR Results:

δ ppm	Rel. Int.	Assignment
-80.5	1.0	$C\underline{F}_3CF_2CF_2O-$
-128.7	0.7	$CF_3C\underline{F}_2CF_2O-$
-82.7	0.7	$CF_3CF_2C\underline{F}_2O-$
-81.6	11.8	$-OC\underline{F}_2CF_2CF_2C\underline{F}_2O-$
-124.1	11.7	$-OCF_2C\underline{F}_2C\underline{F}_2CF_2O-$

Conclusions:

The lack of significant peaks in the region -50~-60 ppm indicates the absence of CF_3O- end group, whereas there is definite evidence for $CF_3CF_2CF_2O-$ arrangement.

TABLE 28

^{19}F NMR RESULTS FOR MLO 88-51

Sample Identification: MLO 88-51

Structure Originally Proposed:

$CF_3O(CF_2CF_2O)_nCF_3$

Structure Postulated:

Same as above.

^{19}F NMR Results:

δ ppm	Rel. Int.	Assignment
-54.7	0.9	$C\underline{F}_3OCF_2CF_2O-$
-89.4	0.6	$CF_3OC\underline{F}_2CF_2O-$
-87.2	14.8	$-OC\underline{F}_2C\underline{F}_2O-$

Conclusions:

The general arrangement is as originally proposed. However, the structure at the base of -89.4 ppm peak would indicate the possibility of a small quantity of material having CF_3CF_2O end groups.

TABLE 29

^{19}F NMR RESULTS FOR MLO 88-129

Sample Identification: MLO 88-129

Structure Originally Proposed:

$CF_3O(CF_2OCF_2CF_2O)_nCF_3$

Structure Postulated:

Same as above.

^{19}F NMR Results:

δ ppm	Rel. Int.	Assignment
-56.4	0.8	$C\underline{F}_3OCF_2O-$
-52.7	0.5	$CF_3OC\underline{F}_2O-$
-54.8	0.4	$C\underline{F}_3OCF_2CF_2O-$
-89.4	0.3	$CF_3OC\underline{F}_2CF_2O-$
-86.2	0.5	$C\underline{F}_3CF_2OCF_2O-$
-87.3	0.3	$CF_3C\underline{F}_2OCF_2O-$
-50.5	6.7	$CF_3CF_2OC\underline{F}_2O-$ $-OC\underline{F}_2OCF_2CF_2-$
-89.0	14.7	$-OCF_2OC\underline{F}_2C\underline{F}_2-$

Conclusions:

The ^{19}F NMR results are consistent with the proposed structure. In addition to the end groups CF_3OCF_2O- and $CF_3OCF_2CF_2O-$ originally proposed, CF_3CF_2O- is also present in a significant amount.

TABLE 30

^{19}F NMR RESULTS FOR MLO 88-132

Sample Identification: MLO 88-132

Structure Originally Proposed:

$CF_3O[(CF_2CF_2O)_4CF_2O]_nCF_3$

Structure Postulated:

$CF_3O[(CF_2CF_2O)_3CF_2O]_nCF_3$

^{19}F NMR Results:

δ ppm	Rel. Int.	Assignment
-50.4	1.5	$-OC\underline{F}_2OCF_2CF_2OCF_2CF_2OCF_2CF_2-$
-89.0	3.5	$-OCF_2OC\underline{F}_2CF_2OCF_2CF_2OCF_2C\underline{F}_2-$
-87.3	7.2	$-OCF_2OCF_2C\underline{F}_2OC\underline{F}_2C\underline{F}_2OC\underline{F}_2CF_2-$ $CF_3C\underline{F}_2O-$
-54.8	0.7	$C\underline{F}_3OCF_2CF_2O-$
-89.4	0.5	$CF_3OC\underline{F}_2CF_2O-$
-56.5	0.1	$C\underline{F}_3OCF_2O-$
-52.7	0.05	$CF_3OC\underline{F}_2O-$
-86.2	0.1	$C\underline{F}_3CF_2O-$

Conclusions:

If $(CF_2CF_2O)_4$ was present, the ratio of peaks at -89.0 ppm and -87.3 ppm should be 1:3 instead of 1:2; consequently, the arrangement proposed for the major component is $CF_3O[(CF_2CF_2O)_3CF_2O]_nCF_3$. Based on the presence of other low intensity peaks, arrangement CF_3CF_2O- must be also present but in lower concentrations.

For the fluid MLO 88-48 the GC/MS spectra for the three peak pattern (see Figure 1) are given in the order of elution in Tables 31-33.

For the fluid MLO 88-51 the GC/MS spectrum of the two peak pattern (see Figure 2) are given in the order of elution in Tables 34 and 35.

For the fluid MLO 88-129 the representative GC/MS is given in Table 36 and the listing of the prominent ions is compiled in Table 37.

For the fluid MLO 88-132 the representative GC/MS is given in Table 38 and the listing of the prominent ions is compiled in Table 39.

Characterization Data: Chlorofluoropolyalkylether Fluids MLO 90-9 and MLO 88-134

The ^{19}F NMR data for the fluid MLO 90-9 are listed in Table 40 and the mass spectra of the two peak pattern (see Figure 6a) are given in the order of elution in Tables 41 and 42. The mass spectra of the extra components in the volatiles collected following thermal oxidative degradation of MLO 90-9 (see Figure 8a) are depicted in Table 43.

The ^{19}F data for the fluid MLO 88-134 are listed in Table 44 and the representative mass spectrum of the two peak pattern (large and small, Figure 7), are compiled in Tables 45 and 46, respectively.

TABLE 31

ION FRAGMENTS AND INTENSITIES RELATIVE TO BASE PEAK OF $C_3F_7O[CF_2CF_2CF_2CF_2O]_nC_3F_7$

m/e	%	m/e	%	m/e	%	m/e	%
31	48.5	101	20.0	162	7.8	219	30.2
43	3.5	109	10.2	169	88.6	220	4.8
47	39.9	112	9.2	170	46.1	231	7.7
50	28.6	113	4.5	171	3.4	235	41.5
51	8.4	119	59.7	178	6.7	236	9.0
62	8.8	120	7.0	181	15.9	243	5.1
66	21.2	128	7.6	182	3.0	281	5.3
69	74.9	131	79.6	185	3.8	316	9.7
70	11.0	132	11.3	193	4.8	331	3.6
74	5.9	135	3.3	197	91.3	335	4.0
78	20.1	143	5.2	198	27.3	347	4.9
81	19.9	145	11.5	199	6.3	385	44.4
85	4.9	147	9.5	200	7.5	386	13.7
93	16.6	150	94.9	201	4.5	397	3.5
97	15.9	151	21.8	208	11.5		
100	100.0	159	7.4	216	4.0		

Peaks having intensities lower than 3% of the base peak and lower than m/e 31 are not reported.

TABLE 32

ION FRAGMENTS AND INTENSITIES RELATIVE TO BASE PEAK OF $C_4F_9O[CF_2CF_2CF_2CF_2O]_nC_3F_7$

m/e	%	m/e	%	m/e	%	m/e	%
31	20.4	100	52.6	159	3.5	219	100.0
47	14.4	101	6.2	169	42.6	220	22.6
50	16.0	109	4.6	170	13.8	235	14.0
51	4.0	112	5.1	181	10.8	247	6.3
62	4.5	119	37.7	185	5.3	269	4.2
66	11.7	120	3.5	197	54.6	285	8.4
69	49.7	131	52.8	198	15.3	316	4.1
70	6.4	132	5.9	199	3.1	335	4.9
78	9.4	145	3.5	200	3.7	347	4.9
81	10.1	150	46.1	201	3.3	385	15.0
93	6.2	151	7.4	208	5.4	435	11.1
97	4.3						

Peaks having intensities lower than 3% of the base peak and lower than m/e 31 are not reported.

TABLE 33

ION FRAGMENTS AND INTENSITIES RELATIVE TO BASE PEAK OF $C_2F_5O[CF_2CF_2CF_2CF_2O]_nC_3F_7$

m/e	%	m/e	%	m/e	%	m/e	%
31	27.5	100	63.4	159	4.5	220	6.4
47	22.0	101	9.5	162	3.3	231	5.5
50	21.6	109	6.9	169	41.3	235	16.7
51	6.2	112	5.0	170	25.3	269	12.9
62	5.3	119	100.0	181	18.1	285	6.6
66	21.6	120	11.8	185	22.4	316	6.7
69	64.7	131	53.9	186	3.3	319	9.7
70	7.7	132	5.6	197	81.2	335	22.0
78	11.2	135	4.4	198	18.9	336	5.3
81	11.1	145	4.1	200	3.5	385	13.4
93	9.6	150	77.0	208	8.2	397	3.3
97	5.4	151	12.6	219	44.9		

Peaks having intensities lower than 3% of the base peak and lower than m/e 31 are not reported.

TABLE 34

ION FRAGMENTS AND INTENSITIES RELATIVE TO BASE PEAK OF $CF_3O[CF_2CF_2O]_nCF_3$

m/e	%	m/e	%	m/e	%	m/e	%
31	22.4	98	11.0	186	15.7	302	8.0
32	5.3	100	67.9	191	25.5	307	3.0
44	3.5	101	9.1	192	3.9	329	32.0
47	37.4	116	7.2	213	95.3	330	7.9
50	25.0	119	100.0	214	20.8	351	19.2
51	5.1	120	26.8	215	4.0	367	5.2
66	28.9	131	5.9	216	13.0	395	7.1
69	82.8	135	70.8	235	23.9	417	21.2
70	7.5	136	7.7	236	3.1	418	3.0
75	57.2	150	4.5	251	24.7	445	20.4
76	6.5	163	47.8	252	3.3	446	4.3
78	21.0	164	6.6	279	12.1	467	12.7
81	8.7	169	5.8	281	3.3	533	7.9
85	4.0	185	92.9	301	41.4	561	8.7
97	86.6						

Peaks having intensities lower than 3% of the base peak and lower than m/e 31 are not reported.

TABLE 35

ION FRAGMENTS AND INTENSITIES RELATIVE TO BASE PEAK OF $C_2F_5O[CF_2CF_2O]_nCF_3$

m/e	%	m/e	%	m/e	%	m/e	%
31	19.2	97	95.3	169	5.9	301	28.8
32	5.9	98	9.2	185	75.5	302	4.8
44	4.0	100	57.5	186	11.1	313	4.1
47	27.3	101	5.6	191	25.8	329	29.3
50	23.1	116	4.9	213	90.7	330	7.0
66	22.5	119	100.0	214	14.2	351	28.7
69	69.1	120	23.2	215	3.6	352	5.2
70	3.9	131	5.2	216	8.6	395	3.3
73	6.0	135	35.7	235	25.6	417	13.1
75	44.2	136	3.2	236	3.5	445	18.3
76	3.9	147	3.2	251	16.2	467	16.0
78	17.2	150	4.0	263	3.0	533	3.3
81	8.2	163	33.9	279	6.2	561	7.7
85	4.5	164	3.7	281	4.6	583	3.9

Peaks having intensities lower than 3% of the base peak and lower than m/e 31 are not reported.

TABLE 36

ION FRAGMENTS AND INTENSITIES RELATIVE TO BASE PEAK OF $CF_3O[CF_2OCF_2CF_2O]_nCF_3$ AND $CF_3O[CF_2OCF_2CF_2O]_nCF_2OC_2F_5$

m/e	%	m/e	%	m/e	%	m/e	%
31	10.4	100	26.0	191	5.5	302	10.2
32	3.4	101	6.7	197	3.0	329	6.4
44	7.2	113	11.4	201	4.3	341	6.4
47	30.9	116	16.4	213	29.0	342	3.2
50	19.1	119	75.7	214	6.8	351	14.1
51	4.3	120	16.7	235	36.3	355	3.2
66	23.6	135	72.4	236	4.2	367	23.6
69	66.2	136	8.6	251	52.3	395	7.0
75	13.7	147	7.4	252	11.4	417	14.9
78	3.8	163	40.8	263	7.8	429	6.7
81	4.7	164	7.2	279	17.9	430	3.3
85	6.2	169	5.3	281	10.3	433	3.4
97	54.1	185	100.0	282	3.7	483	8.1
98	6.7	186	16.2	301	45.9	511	3.3

Peaks having intensities lower than 3% of the base peak and lower than m/e 31 are not reported.

TABLE 37

LISTING OF PROMINENT IONS SUPPORTING THE STRUCTURE ASSIGNMENT FOR MLO 88-129

Major Components: $CF_3O[CF_2OCF_2CF_2O]_nCF_3$
$CF_3O(CF_2OCF_2CF_2O)CF_2OC_2F_5$

m/e	ion
113	OCF_2COF
135	CF_3OCF_2
163	CF_2OCF_2COF
185	$CF_3OCF_2CF_2$, $C_2F_5OCF_2$
213	$CF_2CF_2OCF_2COF$
251	$CF_3OCF_2OCF_2CF_2$, $CF_3OCF_2CF_2OCF_2$
279	$CF_2OCF_2CF_2OCF_2COF$
301	$C_2F_5OCF_2OCF_2CF_2$
317	$CF_3OCF_2OCF_2CF_2OCF_2$
351	$C_2F_5OCF_2CF_2OCF_2CF_2$
367	$C_2F_5OCF_2OCF_2CF_2OCF_2$, $CF_3OCF_2CF_2OCF_2OCF_2CF_2$
417	$CF_3O[CF_2CF_2OCF_2O]_2$
433	$CF_3(OCF_2OCF_2CF_2)_2$, $CF_3(OCF_2CF_2OCF_2)_2$
483	$C_2F_5(OCF_2OCF_2CF_2)_2$
549	$CF_3(OCF_2CF_2OCF_2)_2OCF_2CF_2$, $C_2F_5(OCF_2OCF_2CF_2)_2OCF_2$

TABLE 38

ION FRAGMENTS AND INTENSITIES RELATIVE TO BASE PEAK OF $CF_3O[(CF_2CF_2O)_3CF_2O]_nCF_3$

m/e	%	m/e	%	m/e	%	m/e	%
31	51.7	109	3.9	186	26.3	330	12.2
32	4.8	112	3.8	187	4.3	351	20.0
40	4.7	113	23.8	191	33.3	352	4.7
44	7.9	114	3.4	192	6.4	367	8.1
47	84.0	116	23.2	194	5.7	395	11.2
48	7.3	117	4.9	197	3.4	417	33.1
50	59.0	119	82.3	213	91.6	418	10.5
51	10.0	120	29.3	214	21.6	445	21.1
66	73.9	128	7.2	215	6.6	446	4.6
67	7.7	131	8.6	216	20.2	467	14.6
69	71.2	135	84.5	217	3.1	468	3.9
70	11.3	136	11.1	235	34.8	483	19.9
75	73.1	137	4.4	236	8.7	484	3.0
76	6.9	144	3.9	251	45.8	511	17.4
78	32.4	147	7.4	252	9.4	512	3.1
79	5.1	150	9.8	259	3.3	533	14.8
81	19.2	159	3.0	260	3.7	561	5.0
85	8.6	163	80.1	263	5.0	582	3.5
87	3.8	164	13.2	279	23.2	599	11.9
93	4.6	166	6.9	280	3.8	627	8.6
94	6.3	167	3.4	282	3.7	649	3.4
97	86.2	169	6.7	301	46.0	715	10.9
98	14.8	181	7.3	302	10.4	765	4.0
100	100.0	185	85.9	329	58.7	809	13.1
101	15.6						

Peaks having intensities lower than 3% of the base peak and lower than m/e 31 are not reported.

TABLE 39

LISTING OF PROMINENT IONS SUPPORTING THE STRUCTURE ASSIGNMENT FOR MLO 88-132

Major Components: $CF_3O[(CF_2CF_2O)_3CF_2O]_nCF_3$
$C_2F_5O[(CF_2CF_2O)_3CF_2O]_nCF_3$

m/e	ion
113	OCF_2COF
119	C_2F_5
135	C_2F_5O, CF_3OCF_2
163	CF_2OCF_2COF
185	$CF_3OCF_2CF_2$
213	$CF_2CF_2OCF_2COF$
235	$C_2F_5OCF_2CF_2$
251	$CF_3OCF_2OCF_2CF_2$
301	$CF_3OCF_2CF_2OCF_2CF_2$
329	$CF_2CF_2OCF_2CF_2OCF_2COF$
351	$C_2F_5(OCF_2CF_2)_2$
367	$CF_3OCF_2(OCF_2CF_2)_2$
417	$CF_3(OCF_2CF_2)_3$
445	$(CF_2CF_2O)_3CF_2COF$
483	$CF_3OCF_2(OCF_2CF_2)_3$, $CF_3O(CF_2CF_2O)_3CF_2$
533	$C_2F_5(OCF_2CF_2)_3OCF_2$
599	$CF_3O(CF_2CF_2O)_3CF_2OCF_2CF_2$
715	$CF_3O(CF_2CF_2O)_3CF_2(OCF_2CF_2)_2$
809	$CF_2O(CF_2CF_2O)_3CF_2OCF_2CF_2OCF_2CF_2OCF_2COF$
831	$CF_3O(CF_2CF_2O)_3CF_2(OCF_2CF_2)_3$

TABLE 40

^{19}F NMR RESULTS FOR MLO 90-9

Structure Postulated:

$ClCF_2CF_2O[CF_2CF(CF_2Cl)O]_nX$

$X = CF_3$, $CF_2CF_2CF_2Cl$

^{19}F NMR Data:

ppm	Rel. Int.	Assignment
-52.2	1.1	$C\underline{F}_3O-$
-73.1	1.5	$ClC\underline{F}_2CF_2O-$, $ClC\underline{F}_2CF_2CF_2O-$
-85.8	1.5	$ClCF_2C\underline{F}_2O-$, $ClCF_2CF_2C\underline{F}_2O-$
-122.5	0.5	$ClCF_2C\underline{F}_2CF_2O-$
-66.0	3.8	$-CF_2CF(C\underline{F}_2Cl)O-$
-67.3	0.5	$-CF_2CF(C\underline{F}_2Cl)O-$ (end unit)
-75.2	2.4	$-C\underline{F}_2CF(CF_2Cl)O-$
-79.9	1.5	
-77.5	0.5	$-C\underline{F}_2CF(CF_2Cl)O-$ (end unit)
-138~-140	2.5	$-CF_2C\underline{F}(CF_2Cl)O-$ $-CF_2C\underline{F}(CFHCl)O-$ (?) $-CFHC\underline{F}(CF_2Cl)O-$ (?)
-64.8	0.5	?

There is no evidence for the existence of the end group $ClCF_2CF(CF_2Cl)O-$. The end groups such as $ClCF_2CF_2O-$, $ClCF_2CF_2CF_2O-$, and CF_3O- are present in an approximate ratio of 2:1:1.5.

TABLE 41

ION FRAGMENTS AND INTENSITIES RELATIVE TO BASE PEAK OF

$ClCF_2CF_2O[CF(CF_2Cl)CF_2O]_nCF_3$

m/e	%	m/e	%	m/e	%	m/e	%
31	20.4	96	1.7	150	12.8	251	7.7
35	6.2	97	20.7	151	4.2	253	2.7
36	9.8	99	1.3	153	2.0	263	1.7
37	1.9	100	22.5	163	18.1	279	4.5
38	5.2	101	2.8	164	1.1	281	1.6
39	3.3	109	4.6	165	7.9	282	1.1
47	20.2	112	2.5	166	8.6	295	4.7
50	16.9	113	10.2	167	1.1	297	3.2
51	1.8	115	4.3	168	1.4	301	15.1
62	1.9	116	14.1	169	21.8	302	1.5
66	14.2	118	6.9	170	1.8	303	7.1
67	1.0	119	39.0	184	1.0	313	3.4
68	3.5	120	2.6	185	100.0	317	15.3
69	84.2	128	3.6	186	17.4	318	1.5
70	7.6	131	33.0	187	71.5	319	7.6
75	3.1	132	3.8	188	7.6	329	2.4
78	20.0	134	1.1	197	5.4	345	1.7
81	9.8	135	97.8	201	25.8	347	1.1
85	81.4	136	14.6	202	2.5	395	1.5
86	5.4	137	71.2	203	15.0	411	4.5
87	57.7	138	6.2	213	3.6	413	3.1
88	1.8	144	1.2	229	9.1	499	1.9
93	4.8	147	9.4	231	4.1	501	1.1
94	4.5	149	1.9	235	4.7		

Peaks having intensities lower than 1% of the base peak and lower than m/e 31 are not reported.

Significant Ions in Support of Structure and Composition

m/e		m/e	
499 -	$[ClCF_2CF_2[OCF(CF_2Cl)CF_2]_2]^+$ $[CF_3O[CF_2CF(CF_2Cl)O]_2CF_2]^+$	185 -	$[ClCF_2CF_2CF_2]^+$
		135 -	$[ClCF_2CF_2]^+$
317 -	$[ClCF_2CF_2OCF(CF_2Cl)CF_2]^+$ $[CF_3OCF_2CF(CF_2Cl)OCF_2]^+$	85 -	$[ClCF_2]^+$
201 -	$[ClCF_2CF_2CF_2O]^+$	78 -	$[CF_2CO]^+$

TABLE 42

ION FRAGMENTS AND INTENSITIES RELATIVE TO BASE PEAK OF

$ClCF_2CF_2O[CF(CF_2Cl)CF_2O]_nCF_2CF_2CF_2Cl$

m/e	%	m/e	%	m/e	%	m/e	%
31	20.1	86	5.6	135	100.0	203	12.6
32	1.9	87	48.8	136	10.5	213	1.2
35	3.4	88	1.5	137	60.3	229	6.8
36	8.5	93	2.7	138	4.0	231	2.0
37	1.1	94	1.8	147	5.5	251	1.4
38	3.4	97	11.4	149	1.0	282	2.2
39	2.3	99	1.2	150	9.4	301	8.2
47	12.6	100	34.2	151	1.4	303	2.8
50	13.9	101	2.9	163	12.2	313	2.8
51	1.3	109	1.5	165	5.2	317	3.8
62	1.3	112	1.3	166	2.1	319	2.7
66	9.7	113	6.3	169	22.3	329	6.3
68	2.4	115	2.1	170	1.3	331	2.2
69	60.8	116	13.7	185	95.7	351	1.8
70	2.2	118	6.4	186	12.0	433	2.9
75	1.9	119	28.8	187	54.6	435	1.8
78	4.8	120	1.8	188	5.6		
81	8.5	131	24.7	201	25.6		
85	92.8	132	1.7	202	1.8		

Peaks having intensities lower than 1% of the base peak and lower than m/e 31 are not reported.

Significant Ions in Support of Structure and Composition

m/e		m/e	
433	$[ClCF_2CF_2CF_2OCF_2CF(CF_2Cl)CF_2]^+$	185	$[ClCF_2CF_2CF_2]^+$
317	$[ClCF_2CF_2OCF(CF_2Cl)CF_2]^+$	135	$[ClCF_2CF_2]^+$
251	$[ClCF_2CF_2CF_2OCF_2]^+$	85	$[ClCF_2]^+$
201	$[ClCF_2CF_2CF_2O]^+$		

TABLE 43

ION FRAGMENTS AND INTENSITIES RELATIVE TO BASE PEAK OF

$ClCF_2CF_2OCF_2CF=CF_2$ (MW 282)

m/e	%	m/e	%	m/e	%	m/e	%
31	12.6	81	10.4	120	1.6	181	2.5
32	2.8	85	35.9	128	1.9	185	6.2
44	1.7	87	17.9	131	100.0	187	1.0
47	6.0	93	7.1	132	9.3	201	2.0
50	7.1	97	8.3	135	59.9	209	1.3
62	1.8	100	23.9	136	1.6	213	1.2
64	2.7	109	33.1	137	28.6	229	1.0
66	4.3	110	1.0	147	4.7	263	1.0
67	2.0	112	4.3	149	1.0	282	25.6
69	28.9	116	4.2	150	45.8	283	1.6
73	1.3	118	1.3	151	1.4	284	9.5
78	1.3	119	44.2	169	1.9		

Peaks having intensities lower than 1% of the base peak and lower than m/e 31 are not reported.

Significant Ions in Support of Structure and Composition

m/e		m/e	
282	$[M]^+$	119	$[C_2F_5]^+$
150	$[CF_2CF_2]^+$	109	$[C_3F_3O]^+$
135	$[ClCF_2CF_2]^+$	85	$[ClCF_2]^+$
131	$[CF_2CF=CF_2]^+$		

TABLE 44

^{19}F NMR RESULTS FOR MLO 88-134

Structure Postulated:

$ClCF_2CF_2O[CF_2CF(CF_2Cl)O]_nX$

$X = CF_3$, $CF_2CF_2CF_2Cl$

^{19}F NMR Data:

ppm	Rel. Int.	Assignment
-52.1	0.5	$C\underline{F}_3O-$
-73.0	1.1	$ClC\underline{F}_2CF_2O-$, $ClC\underline{F}_2CF_2CF_2O-$
-85.8	1.1	$ClCF_2C\underline{F}_2O-$, $ClCF_2CF_2C\underline{F}_2O-$
-122.4	0.6	$ClCF_2C\underline{F}_2CF_2O-$
-65.7	5.8	$-CF_2CF(C\underline{F}_2Cl)O-$
-67.2	0.6	$-CF_2CF(C\underline{F}_2Cl)O-$ (end unit)
-73.0	4.5	$-C\underline{F}_2CF(CF_2Cl)O-$
-79.3	1.2	
-77.3	?	$-C\underline{F}_2CF(CF_2Cl)O-$ (end unit)
-137.8~-138.7	3.2	$-CF_2C\underline{F}(CF_2Cl)O-$
-64.7	0.5	?
-78.7	1.3	
-143.0	0.4	
-139.5	0.2	

The end groups $ClCF_2CF_2O-$, $ClCF_2CF_2CF_2O-$, and CF_3O- are present in an approximate ratio of 1.5:1.8:1.0. The NMR results indicate that this sample should have a higher molecular weight than MLO 90-9.

TABLE 45

ION FRAGMENTS AND INTENSITIES RELATIVE TO BASE PEAK OF

$ClCF_2CF_2O[CF_2CF(CF_2Cl)O]_nCF_2CF_2CF_2Cl$ AND
$ClCF_2CF_2O[CF_2CF(CF_2Cl)O]_{n+1}CF_3$

m/e	%	m/e	%	m/e	%	m/e	%
31	15.7	93	3.5	149	2.6	279	1.6
32	2.6	94	2.9	150	13.9	285	1.3
35	4.6	96	1.1	151	4.3	301	12.8
36	15.1	97	14.9	153	1.9	302	1.0
37	1.5	100	22.2	163	22.6	303	4.9
38	6.2	101	2.2	164	2.1	313	2.2
39	3.2	109	3.9	165	12.1	317	11.1
40	1.0	112	2.2	166	7.5	319	8.8
47	15.5	113	8.8	167	1.6	321	1.3
50	11.8	115	3.7	168	3.2	329	5.8
51	2.0	116	12.5	169	17.3	331	2.1
62	1.3	118	4.8	170	1.8	345	2.8
66	11.0	119	20.6	185	100.0	347	1.8
68	1.7	120	1.4	186	22.3	351	3.2
69	60.4	128	3.0	187	78.8	367	3.6
70	2.8	131	41.6	188	8.9	369	2.4
78	3.7	132	4.1	201	17.1	433	1.0
81	8.3	135	92.4	202	1.0	499	1.3
85	82.7	136	11.4	203	9.6	549	0.8
86	4.3	137	71.6	213	1.9	681	0.1
87	38.1	138	5.2	229	4.3	731	0.1
88	1.6	147	12.4	231	1.8		

Peaks having intensities lower than 1% of the base peak and lower than m/e 31 are not reported. High mass peaks which are less than 1% but which are important to structure determination are also listed.

Significant Ions in Support of Structure and Composition

m/e

731 - $[ClCF_2CF_2CF_2[OCF(CF_2Cl)CF_2]_3]^+$
681 - $[ClCF_2CF_2[OCF_2CF(CF_2Cl)]_3]^+$
549 - $[ClCF_2CF_2CF_2[OCF(CF_2Cl)CF_2]_2]^+$
499 - $[ClCF_2CF_2[OCF_2CF(CF_2Cl)]_2]^+$
433 - $[CF_3[OCF(CF_2Cl)CF_2]_2]^+$
367 - $[ClCF_2CF_2CF_2OCF(CF_2Cl)CF_2]^+$
317 - $[ClCF_2CF_2OCF_2CF(CF_2Cl)]^+$
201 - $[ClCF_2CF_2CF_2O]^+$, $[ClCF_2CF_2OCF_2]^+$
185 - $[ClCF_2CF_2CF_2]^+$
135 - $[ClCF_2CF_2]^+$

TABLE 46

ION FRAGMENTS AND INTENSITIES RELATIVE TO BASE PEAK OF

$ClCF_2CF_2O[CF_2CF(CF_2Cl)O]_nCF_2CF(CF_3)OCF_2CF_2CF_2Cl$

m/e	%	m/e	%	m/e	%	m/e	%
31	12.7	101	1.4	165	7.0	301	19.0
32	4.8	109	1.7	166	5.5	302	1.7
35	2.3	112	1.3	168	2.1	303	8.2
36	9.6	113	11.0	169	43.4	313	3.4
38	4.2	115	3.9	170	3.4	317	6.0
39	1.3	116	8.8	185	100.0	319	4.4
47	11.2	118	2.8	186	13.5	329	9.7
50	8.0	119	32.2	187	48.0	331	3.0
66	5.7	120	1.4	188	5.1	335	1.5
68	1.0	128	1.5	197	1.0	345	1.2
69	35.4	131	31.9	201	13.7	351	27.8
70	1.6	132	2.6	203	8.2	352	3.2
78	2.4	135	96.7	207	1.7	353	12.9
81	4.0	136	7.6	213	5.3	367	1.7
85	55.9	137	41.6	229	2.3	483	1.1
86	2.3	138	2.8	235	1.8	499	0.4
87	34.3	147	10.3	251	1.0	533	1.2
93	1.8	149	1.9	263	1.1	715	0.2
94	1.5	150	19.1	279	1.4		
97	19.3	151	2.8	285	4.4		
100	23.0	163	19.3	297	1.2		

Peaks having intensities lower than 1% of the base peak and lower than m/e 31 are not reported. High mass peaks which are less than 1% but which are important to structure determination are also listed.

Significant Ions in Support of Structure and Composition

m/e

715 - $[ClCF_2CF_2CF_2OCF(CF3)CF_2[OCF(CF_2Cl)CF_2]_3]^+$
533 - $[ClCF_2CF_2CF_2OCF(CF3)CF_2[OCF(CF_2Cl)CF_2]_2]^+$
499 - $[ClCF_2CF_2[OCF_2CF(CF_2Cl)]_2]^+$
351 - $[ClCF_2CF_2CF_2OCF(CF_3)CF_2]+$
317 - $[ClCF_2CF_2OCF_2CF(CF_2Cl)]^+$
185 - $[ClCF_2CF_2CF_2]^+$
135 - $[ClCF_2CF_2]+$
85 - $[ClCF_2]^+$

NMR Data: Commercial Fluids Krytox 143AC, Demnum S-20, Demnum S-100 and Aflunox 2507

Proton and ^{19}F NMR spectra of Krytox 143AC (MLO 71-6) were reported [Ref. 26]. The multiscan ^{1}H and ^{19}F NMR spectra of the fluorinated Krytox 143AC (MLO 91-21) are presented in Figures 64 and 65, respectively. The corresponding NMR spectra of Aflunox 2507 (MLO 88-298) are given in Figures 66 and 67.

The ^{1}H and ^{19}F NMR spectra of Demnum S-20 (MLO 88-177) are depicted in Figures 68 and 69. The chemical shift assignments are listed in Table 47. The corresponding data for Demnum S-100 are presented in Figures 70 and 71 and Table 48.

^{19}F NMR Data: Second Series of Experimental Fluids

The ^{19}F NMR shifts together with intensities and assignments are presented for the fluids MLO 91-87, 88, 105, 106, 126, 127, 132, 157, 158, 160 and 161 in Tables 49-59, respectively.

Fractional Distillation Data of Perfluoropolyalkylether Fluids

The fractional distillation data for selected Experimental fluids are listed in Table 60.

Thermal Oxidative Stability Testing of Perfluoropolyalkylether Fluids Summary of Results

All the thermal oxidative testing details for the commercial and second series experimental fluids are compiled in Table 61.

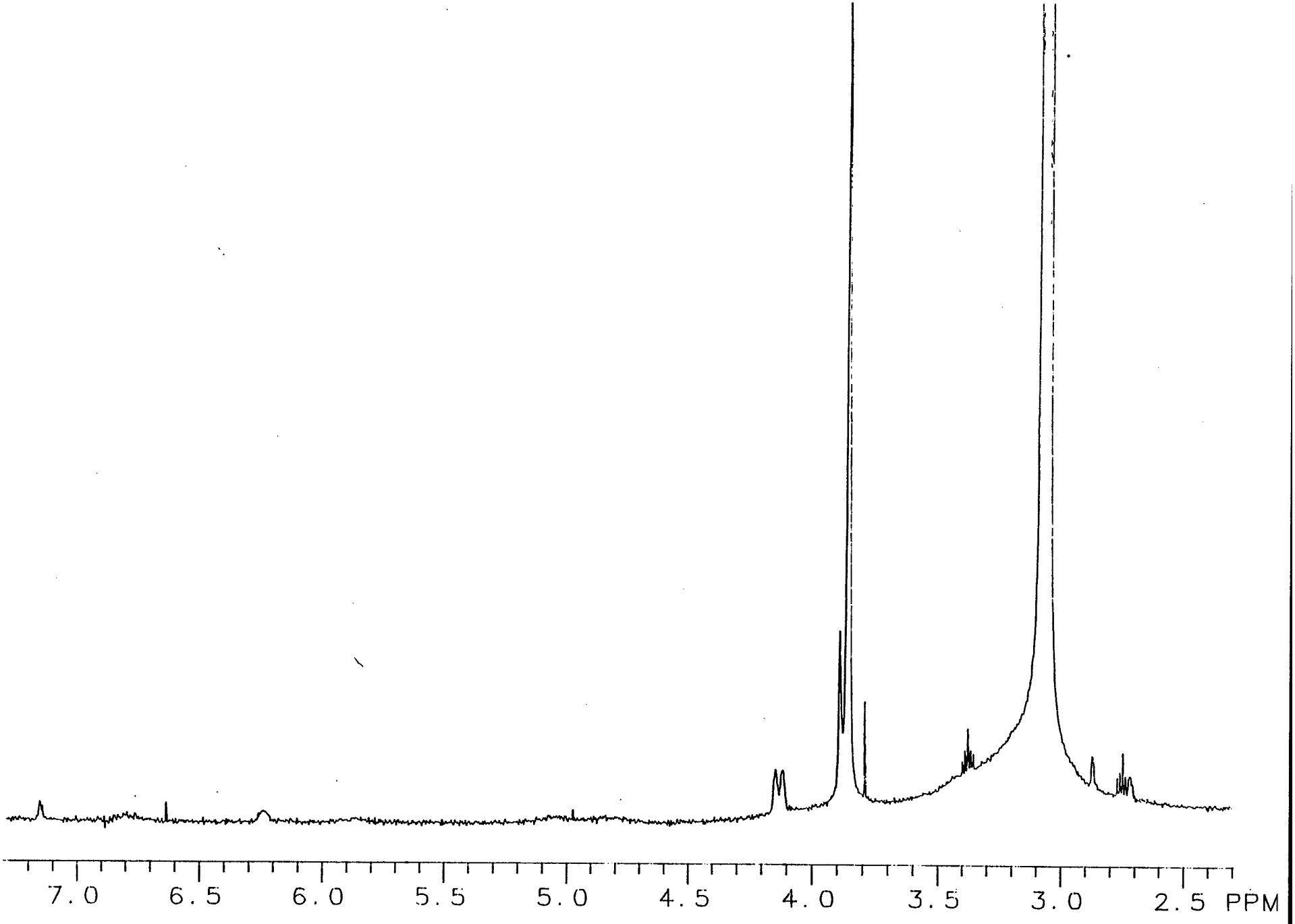

Figure 64. Multiscan ^{1}H NMR spectrum of fluorinated Krytox 143AC (MLO 91-21).

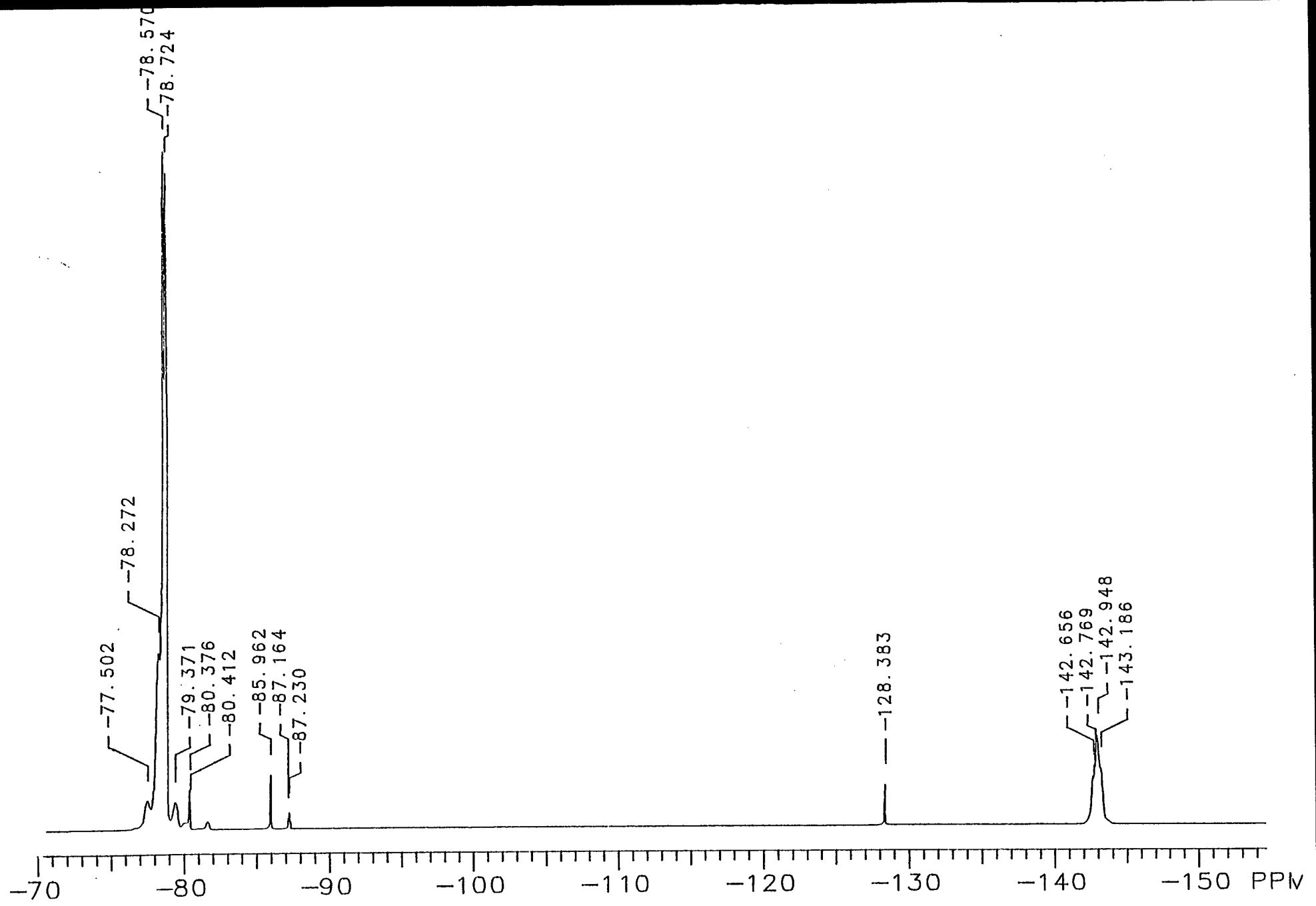

Figure 65. ^{19}F NMR spectrum of fluorinated Krytox 143AC (MLO 91-21).

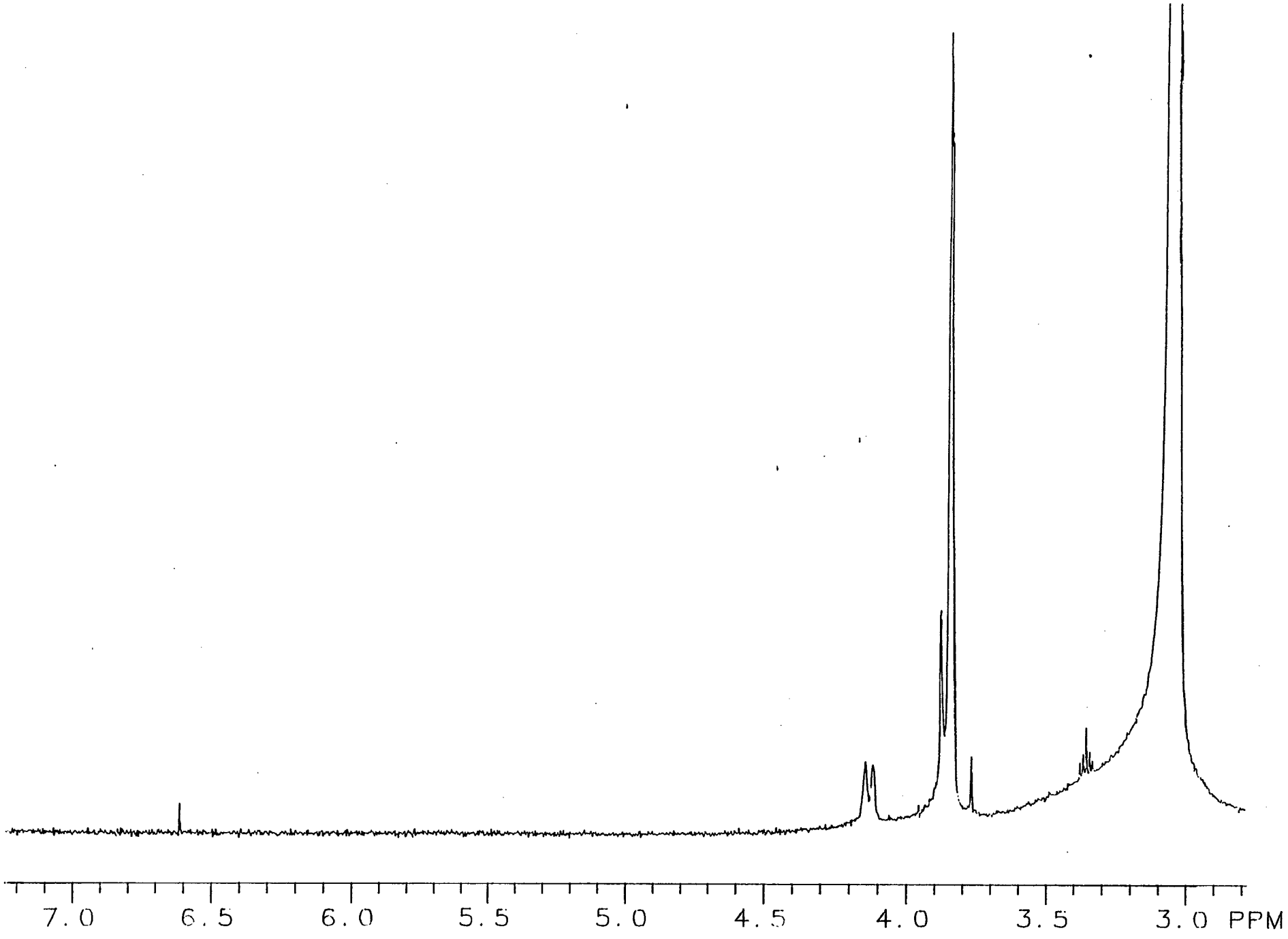

Figure 66. Multiscan ^{1}H NMR spectrum of Aflunox 2507 (MLO 88-298).

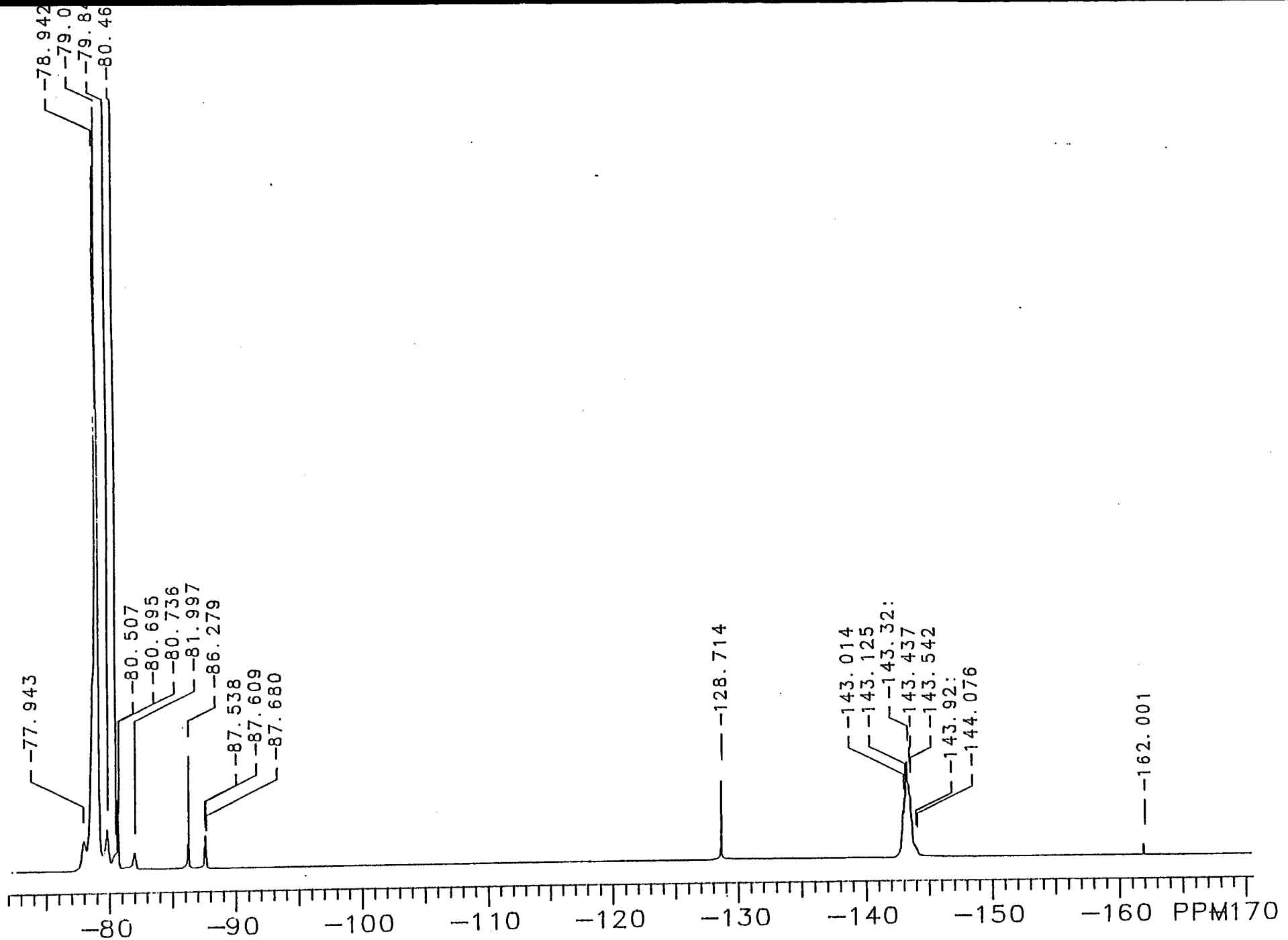

Figure 67. ^{19}F NMR spectrum of Aflunox 2507 (MLO 88-298).

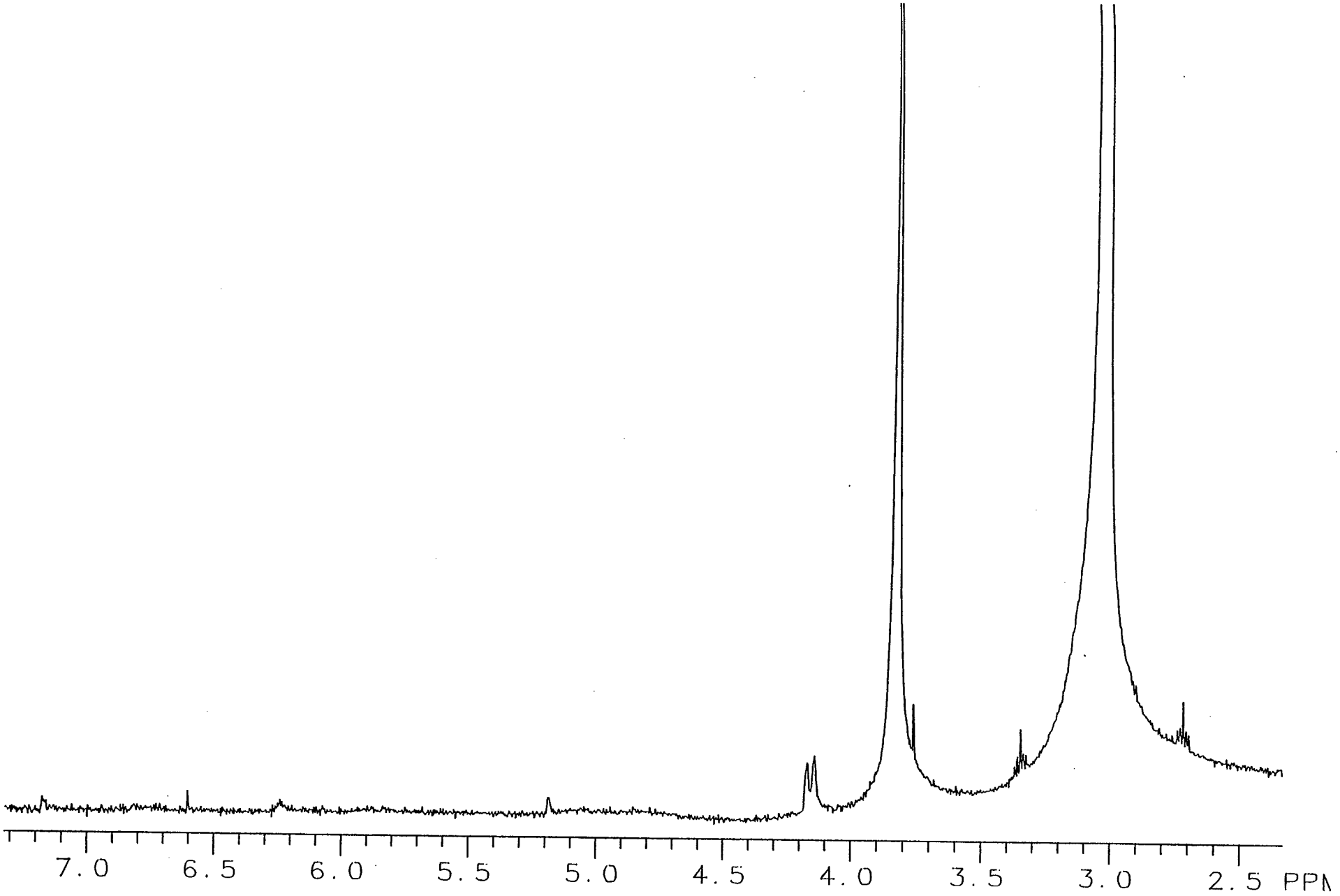

Figure 68. Multiscan ^{1}H NMR spectrum of Demnum S-20 (MLO 88-177).

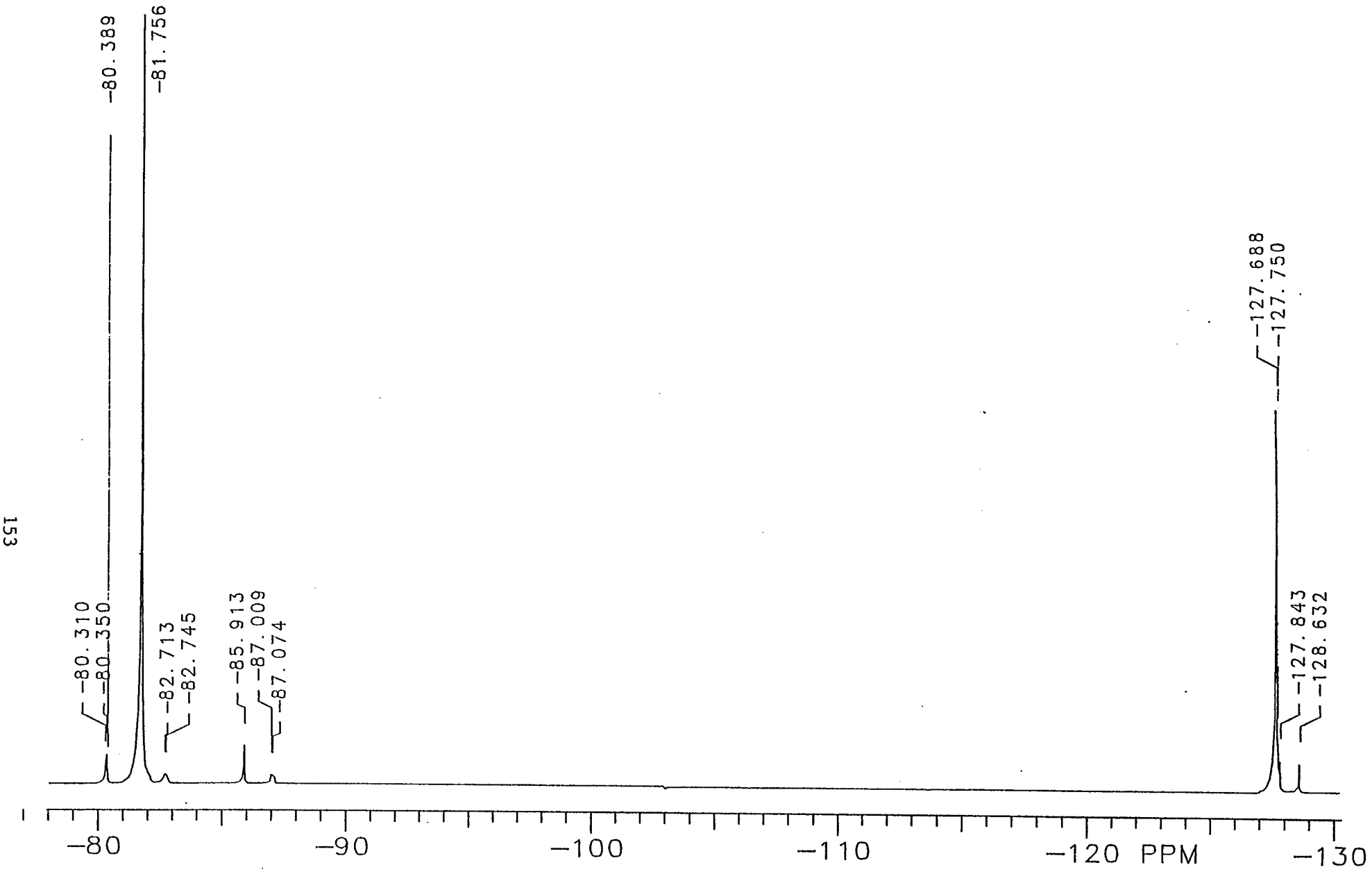

Figure 69. ^{19}F NMR spectrum of Demnum S-20 (MLO 88-177).

TABLE 47

^{19}F NMR CHEMICAL SHIFT ASSIGNMENT OF DEMNUM S-20 (MLO 88-177)

(ppm)	Rel. Int.	Assignment
-80.4	0.4	$C\underline{F}_3CF_2CF_2O-$
-81.8	7.9	$-OC\underline{F}_2CF_2C\underline{F}_2O-$
-82.7	0.3	$CF_3CF_2C\underline{F}_2O-$
-85.9	0.4	$C\underline{F}_3CF_2O-$
-87.0	0.25	$CF_3C\underline{F}_2O-$
-127.7	3.9	$-OCF_2C\underline{F}_2CF_2O-$
-128.6	0.25	$CF_3C\underline{F}_2CF_2O-$

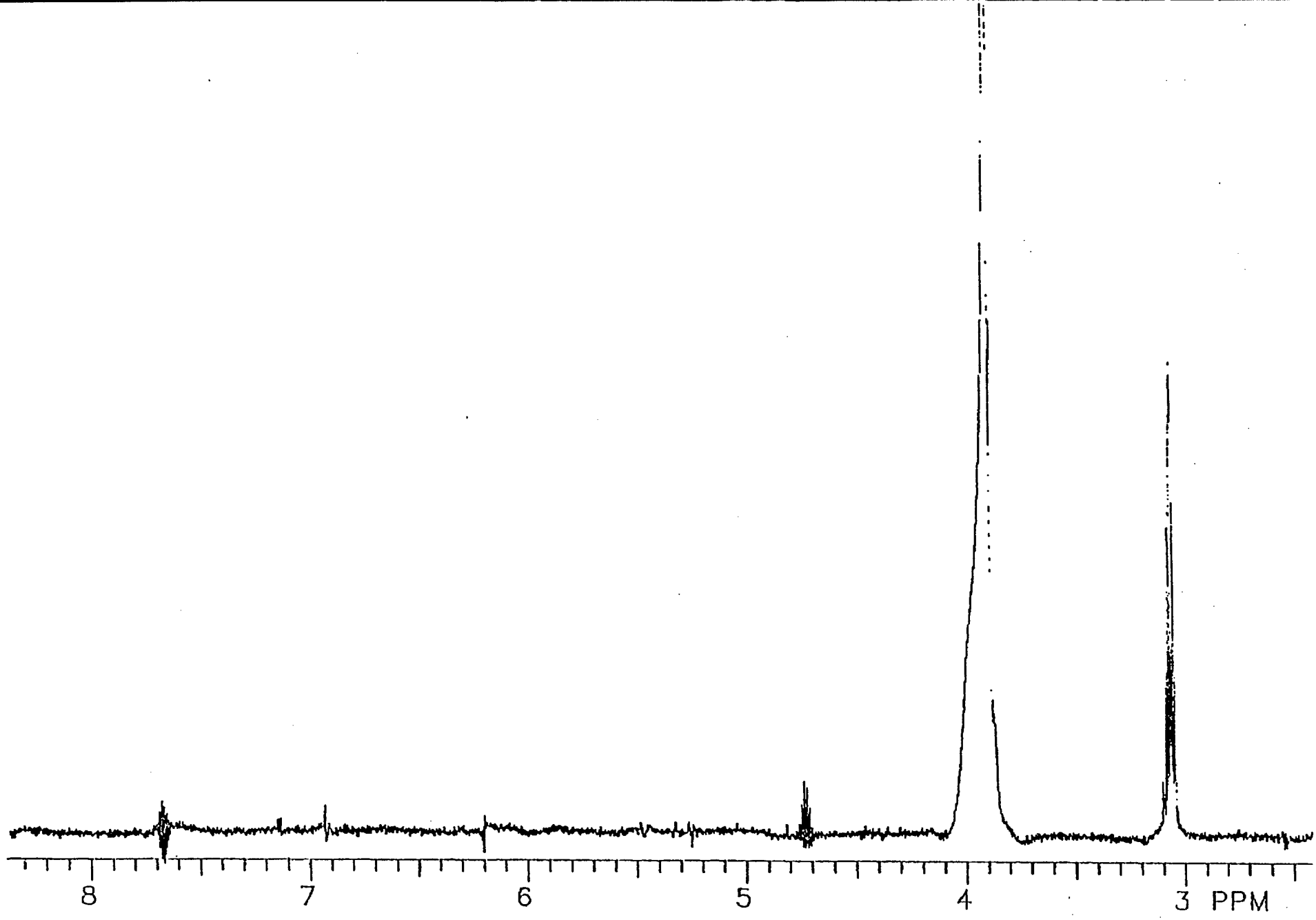

Figure 70. Multiscan ^{1}H NMR spectrum of Demnum S-100.

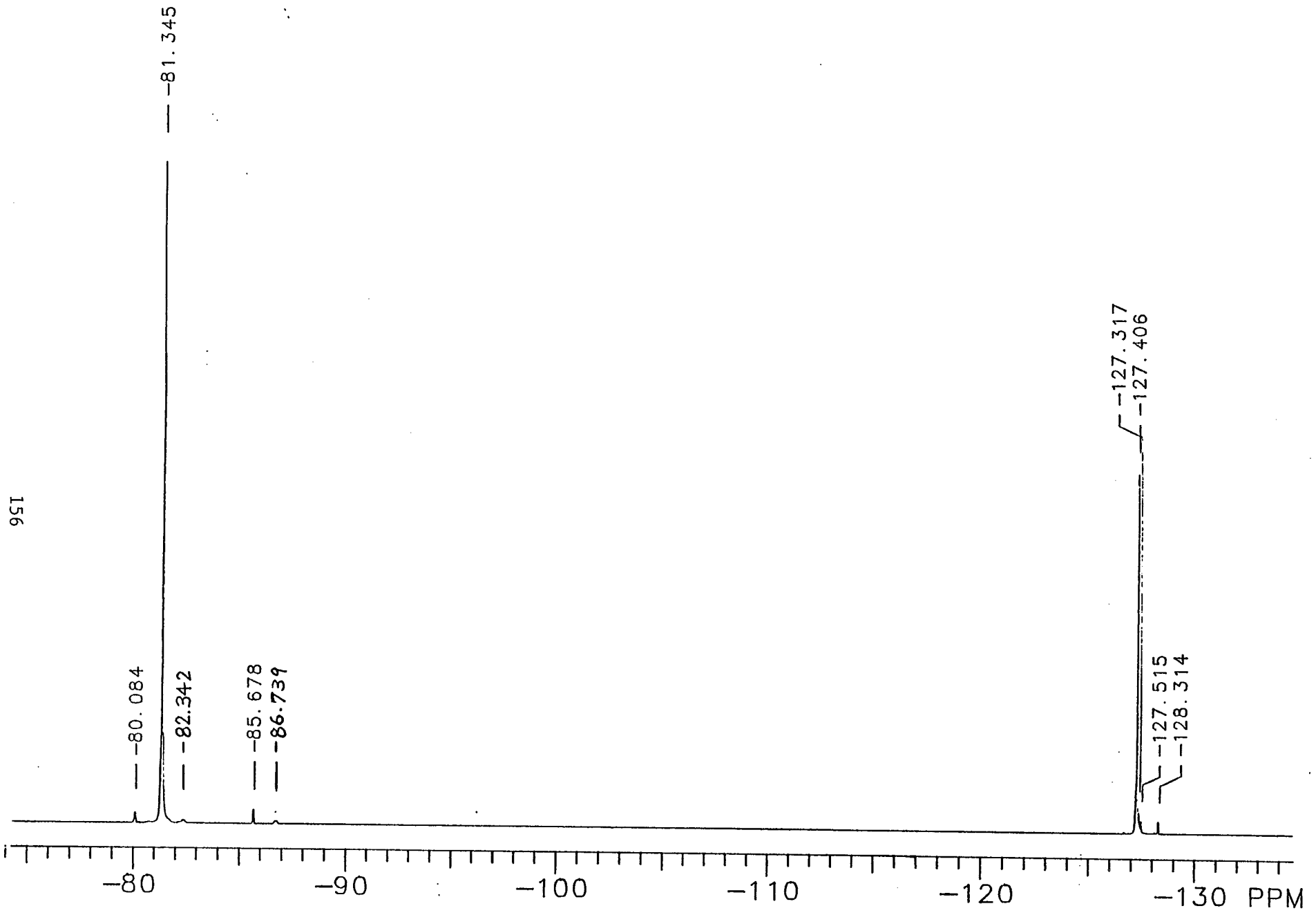

Figure 71. ^{19}F NMR spectrum of Demnum S-100.

TABLE 48

^{19}F NMR CHEMICAL SHIFT ASSIGNMENT OF DEMNUM S-100

(ppm)	Rel. Int.	Assignment
-80.1	0.27	$C\underline{F}_3CF_2CF_2O-$
-81.3	13.1	$-OC\underline{F}_2CF_2C\underline{F}_2O-$
-82.3	0.2 (?)	$CF_3CF_2C\underline{F}_2O-$
-85.7	0.27	$C\underline{F}_3CF_2O-$
-86.7	0.17	$CF_3C\underline{F}_2O-$
-127.4	6.5	$-OCF_2C\underline{F}_2CF_2O-$
-128.3	0.18	$CF_3C\underline{F}_2CF_2O-$

End group ratio of $CF_3CF_2CF_2O-$: CF_3CF_2O- = 1 : 1

Calculated MW = 6300

TABLE 49

^{19}F NMR of-$O(CF_2CF_2O)_m[CF_2CF(CF_3)O]_n(CF_2CF_2O)_p$- (MLO 91-87)[a]

ppm	Rel. Int.	Assignment
-52.7	0.1	$C\underline{F}_3O$-
-54.8	0.1	
-77.3(shoulder)		
-78.1(shoulder)	3.0	$-C\underline{F}_2CF(C\underline{F}_3)O$-
-78.6(main peak)		
-80.5	0.05	$C\underline{F}_3CF_2CF_2O$-
-81.0	0.25	$(C\underline{F}_3)_2CFO$-
-84.3	0.05	?
-86.1	b	$CF_3CF_2C\underline{F}_2O$-
-87.3	0.3	$-OC\underline{F}_2C\underline{F}_2O$-
-89.4	b	$CF_3OC\underline{F}_2CF_2O$-
-128.3	b	$CF_3C\underline{F}_2CF_2O$-
-138.5	b	$(CF_3)_2C\underline{F}O$-
-142.9	0.6	$-CF_2C\underline{F}(CF_3)O$-
-144.3	b	?

[a] Based on the data listed below the ratio of $CF_2CF(CF_3)O$ to CF_2CF_2O is approximately 8:1. The end groups CF_3, $(CF_3)_2CF$ and $CF_3CF_2CF_2O$ are present in an approximate ratio of 4:2.5:1.

[b] The relative intensity < 0.05.

TABLE 50

^{19}F NMR of $CF_2O[CF_2CF(CF_3)O]_m(CF_2CF_2O)_nX$
$CFO[CF_2CF(CF_3)O]_q(CF_2CF_2O)_pX$
$CF_2O[CF_2CF(CF_3)O]_r(CF_2CF_2O)_sX$ (MLO 91-88)

ppm	Rel. Int.	Assignment
-52.7	0.1	$C\underline{F}_3OCF(CF_3)CF_2O-$
-54.8	0.15	$C\underline{F}_3OCF_2CF_2O-$
-78.9	1.7	$-C\underline{F}_2CF(C\underline{F}_3)O-$
-80.5	0.1	$C\underline{F}_3CF_2CF_2O-$?
-81.5	0.5	$-OC\underline{F}_2CF(OR)C\underline{F}_2O$
-84.4	0.5	$-OCF_2CF(CF_3)OCF_2CF_2O-$
-87.2	2.4	$-OC\underline{F}_2C\underline{F}_2O-$
-89.2	0.1	$CF_3OC\underline{F}_2CF_2O-$
-143.4	0.4	$-CF_2C\underline{F}(CF_3)O-$, $-CF_2-C\underline{F}(O)-CF_2-$

The ratio of CF_2CF_2O to $CF_2CF(CF_3)O$ is approximately 1.8:1. The end groups are $CF_3OCF(CF_3)CF_2O$, $CF_3CF_2CF_2-$ and $CF_3OCF_2CF_2$ in the ratio of 1:1:1.5.

TABLE 51

^{19}F NMR of $XO(CF_2CF_2CF_2CF_2OCF_2O)_nX$, MLO 91-105

ppm	Rel. Int.	Assignment
-49.9	3.5	$-OC\underline{F}_2O-$
-52.0	0.15(?)	$-O\underline{F}_2OC\underline{F}_2O-$
-54.5	0.4	$C\underline{F}_3O(CF_2)_4O-$
-56.4	a	$C\underline{F}_3OCF_2O-$
-80.6	0.8	$C\underline{F}_3CF_2CF_2O-$ (major), $C\underline{F}_3CF_2CF_2CF_2O-$
-81.7	a	$-CF_2CF_2OC\underline{F}_2CF_2CF_2CF_2O-$
-83.5	6.8	$-OC\underline{F}_2CF_2CF_2C\underline{F}_2OCF_2O-$
-84.7	0.5	$CF_3CF_2C\underline{F}_2O-$
-86.1	a	$C\underline{F}_3CF_2O-$
-87.2	a	$CF_3C\underline{F}_2O-$, $-OC\underline{F}_2C\underline{F}_2O-$
-124.2	7.0	$-OCF_2C\underline{F}_2C\underline{F}_2CF_2O-$
-124.9	b	$CF_3C\underline{F}_2C\underline{F}_2CF_2O-$
-128.8	0.5	$CF_3C\underline{F}_2CF_2O-$
-130.0	a	?

a Peak is of extremely low intensity.

b Peak intensity cannot be determined due to poor resolution.

Table 52

^{19}F NMR of $XO(CF_2CF_2CF_2CF_2CF_2OCF_2O)_nX$ MLO (91-106)

ppm	Rel. Int.	Assignment
-49.8	3.5	$-OC\underline{F}_2O-$
-52.0	a	$-OC\underline{F}_2OC\underline{F}_2O-$
-54.5	0.4	$C\underline{F}_3O-$
-56.5	a	$C\underline{F}_3OCF_2O-$
-76.7	a	?
-80.4	0.9	$C\underline{F}_3CF_2CF_2CF_2O-$
-81.2	a	?
-81.5	a	?
-83.3(major)	6.3	$-C\underline{F}_2CF_2CF_2CF_2C\underline{F}_2OCF_2O-$
-83.8(shoulder)		$CF_3CF_2CF_2C\underline{F}_2O-$
-84.7	a	$CF_3CF_2C\underline{F}_2O$
-86.2	b	$C\underline{F}_3CF_2O-$
-89.0	b	$-OCF_2C\underline{F}_2OCF_2O-$
-119.1	a	?
-120.6	2.9	$-CF_2CF_2C\underline{F}_2CF_2CF_2OCF_2O-$
-121.4	b	?
-124.1	5.9	$-CF_2C\underline{F}_2CF_2C\underline{F}_2CF_2OCF_2O-$
-125.1	1.1	$CF_3C\underline{F}_2C\underline{F}_2CF_2O-$
-128.8	b	$CF_3C\underline{F}_2CF_2O-$

a Peak is of extremely low intensity.

b Peak intensity cannot be determined due to the poor resolution or low intensity.

TABLE 53

^{19}F NMR of $X(CF_2CF_2CF_2CF_2O)_nX$ (MLO 91-126)

ppm	Rel.Int.	Assignment
-54.6	a	$C\underline{F}_3OCF_2CF_2CF_2CF_2O-$
-80.5	0.9	$C\underline{F}_3CF_2CF_2O-$ (major), $C\underline{F}_3CF_2CF_2CF_2O-$
-81.6	7.6	$-C\underline{F}_2CF_2CF_2C\underline{F}_2O-$
-82.7	0.6	$CF_3CF_2C\underline{F}_2O-$ (major), $CF_3CF_2CF_2C\underline{F}_2O-$
-83.9	a	?
-84.2	a	?
-86.1	b	$C\underline{F}_3CF_2O-$
-87.2	a	$CF_3C\underline{F}_2O-$
-109	a	?
-121.3	a	?
-122.0	a	?
-124.0	7.6	$-CF_2C\underline{F}_2C\underline{F}_2CF_2O-$
-125.0	b	$CF_3C\underline{F}_2C\underline{F}_2CF_2O-$
-128.3	a	?
-128.7	0.6	$CF_3C\underline{F}_2CF_2O-$
-129.1	a	?
-130.7	a	?
-131.5	a	?

a Peak is of extremely low intensity.

b Peak intensity cannot be determined due to the poor resolution or low intensity.

TABLE 54

^{19}F NMR OF $XO[CF_2CF(CF_3)O]_nX$ (MLO 91-127)

ppm	Rel.Int.	Assignment
-52.7	0.18	$C\underline{F}_3OCF(CF_3)CF_2O-$
-54.5	0.01	$C\underline{F}_3OCF_2CF(CF_3)O-$
-56.0	0.01	$C\underline{F}_3OCF_2CF_2O-$
-59.9	a	?
-70.0	b(broad)	?
-72.2	b	$ClC\underline{F}_2CF_2CF_2O-$
-73.1	a	$ClC\underline{F}2CF_2O-$
-77.3	]	
-78.1	├ 6.7	
-78.6	major]	$-OC\underline{F}_2CF(C\underline{F}_3)O-$
-79.6	0.1	?
-80.5	0.15	$C\underline{F}_3CF_2CF_2O-$
-81.1	0.45	$(C\underline{F}_3)_2CFO-$
-82.8	b	$-OC\underline{F}_2CF_2C\underline{F}_2O-$
-83.4	b	$-OC\underline{F}_2CF_2CF_2C\underline{F}_2O$
-84.1	b	?
-86.1	0.09	$C\underline{F}_3CF_2O-$
-87.1	0.06	$CF_3C\underline{F}_2O-$, $-OC\underline{F}_2C\underline{F}_2O-$?
-89.0	a	$CF_3OC\underline{F}_2CF_2O-$?
-120.9	b	?
-121.2	b	?
-124.0	b	$-OCF_2C\underline{F}_2C\underline{F}_2CF_2O-$
-125.9	b	?
-127.2	b	$-OCF_2C\underline{F}_2CF_2O-$
-128.4	major] 0.1	$CF_3C\underline{F}_2CF_2O-$
-128.5	]	
-138.2	0.08(broad)	$(CF_3)_2C\underline{F}O-$
-142.6	1.3	$-OCF_2C\underline{F}(CF_3)O-$
-144.3	0.05	$CF_3OC\underline{F}(CF_3)CF_2O-$

a Peak is of extremely low intensity.
b Peak intensity cannot be determined due to poor resolution or low intensity.

TABLE 55

^{19}F NMR OF $XO[CF_2CF(CF_3)OCF_2CF(CF_3)OCF_2O]_nX$ (MLO 91-132)

ppm	Rel.Int.	Assignment
-44.5	a	$-OCF_2CF(CF_2CF_3)OC\underline{F}_2OCF(CF_2CF_3)CF_2O-$
-45.1	a	?
-45.6	0.4	$-OCF_2CF(CF_3)OC\underline{F}_2OCF(CF_3)CF_2O-$
-47.7	0.7	$-OCF_2CF(CF_3)OC\underline{F}_2OCF_2CF(CF_3)O-$
-49.9	major ┐	$-OCF(CF_3)CF_2OC\underline{F}_2OCF_2CF(CF_3)O-$
	├ 0.3	
-50.1	┘	$-OCF_2CF_2OC\underline{F}_2OCF_2CF(CF_3)O-$
-52.7	0.13	$C\underline{F}_3OCF(CF_3)CF_2O-$, $-OC\underline{F}_2OC\underline{F}_2O-$?
-54.7	0.2	$C\underline{F}_3OCF_2CF(CF_3)O-$
-56.5	b	$C\underline{F}_3OCF_2CF_2O-$
-77.5	shoulder? ┐	
-78.5	4.5 ┘	$-OC\underline{F}_2CF(C\underline{F}_3)O-$
-79.3	0.3	$-OC\underline{F}_2CF(CF_2C\underline{F}_3)O-$
-80.5	0.12	$C\underline{F}_3CF_2CF_2O-$
-81.3	0.9	$(C\underline{F}_3)_2CFO-$
-82.8	1.2	?
-84.6	b	$-OC\underline{F}_2CF_2CF_2C\underline{F}_2O-$?
-86.1	0.1	$C\underline{F}_3CF_2O-$
-87.3	0.5	$-OCF_2C\underline{F}_2OC\underline{F}_2C\underline{F}_2OC\underline{F}_2C\underline{F}_2OC\underline{F}_2CF_2OCF_2O-$ major; $CF_3C\underline{F}_2O-$
-89.0	0.15	$-OCF_2OC\underline{F}_2CF_2OCF_2CF_2OCF_2CF_2OCF_2C\underline{F}_2OCF_2O-$
-89.5	0.06	$CF_3OC\underline{F}_2CF_2O-$
-122.6 ┐		
├	b	$-OCF_2CF(C\underline{F}_2CF_3)O-$
-122.7 ┘		
-124.0	b	$-OCF_2C\underline{F}_2C\underline{F}_2CF_2O-$
-125.0	a	$CF_3C\underline{F}_2C\underline{F}_2CF_2O-$
-127.6	a	$CF_3C\underline{F}_2CF_2OCF_2OCF(CF_3)CF_2O-$?
-127.7	a	$CF_3C\underline{F}_2CF_2OCF_2OCF_2CF(CF_3)O-$?
-128.5 ┐		$CF_3C\underline{F}_2CF_2OCF(CF_3)CF_2O-$
├	0.09	
-128.7 ┘		$CF_3C\underline{F}_2CF_2OCF_2CF(CF_3)O-$
-138.7	0.15	$(CF_3)_2C\underline{F}O-$
-141.2	a	$-OCF_2CF_2OCF_2C\underline{F}(CF_2CF_3)OCF_2O-$
-142.0	a	$-OCF_2OCF_3C\underline{F}(CF_2CF_3)OCF_2CF_2O-$
-143.5	0.3	$-CF_2C\underline{F}(CF_3)OCF_2OC\underline{F}(CF_3)CF_2O-$
-144.6	0.8	$-OCF_2OCF_2C\underline{F}(CF_3)OCF_2CF(CF_3)O-$

a Peak is of extremely low intensity.
b Peak intensity cannot be determined due to poor resolution or low intensity.

TABLE 56

^{19}F NMR of $XO[(CF_2CF_2O)_4CF_2O]_nX$ (MLO 91-157)

ppm	Rel.Int.	Assignment
-47.4	a	$-CF_3CF_2OC\underline{F}_2O-$?
-49.5	a	$-OCF(CF_3)O\underline{CF}_2OCF_2CF_2-$?
-50.4	0.8	$-(CF_2CF_2O)_4C\underline{F}_2O(CF_2CF_2O)_4-$
-52.7	b	$CF_3OC\underline{F}_2O$
-54.6	0.6	$C\underline{F}_3(OCF_2CF_2)_xO-$
-54.8(major)		
-56.5	a	$C\underline{F}_3OCF_2O-$
-73.0	a	$ClC\underline{F}_2CF_2O$?
-78.4	a	$-OC\underline{F}_2CF(C\underline{F}_3)O-$?
-79.2	a	side chain $C\underline{F}_3$
-80.5	a	$-C\underline{F}_3CF_2CF_2O-$?
-81.6	a	$(C\underline{F}_3)_2CFO-$?
-83.1	a	?
-83.9	a	?
-85.1	a	$-OF(C\underline{F}_3)-$?
-86.2	6.2	$C\underline{F}_3CF_2O-$
-87.3	5.5	$-OCF_2OCF_2C\underline{F}_2O(C\underline{F}_2C\underline{F}_2O)_2C\underline{F}_2CF_2O-$
-89.0	1.7	$-OCF_2OC\underline{F}_2CF_2O(CF_2CF_2O)_2CF_2C\underline{F}_2OCF_2O-$
-109.6	a	?
-122.7	a	$-OCF_2CF(C\underline{F}_2CF_3)O-$?
-124.0	a	$-OCF_2C\underline{F}_2C\underline{F}_2CF_2O-$?

[a] Peak is of extremely low intensity

[b] Peak intensity cannot be determined due to the poor resolution or low intensity.

TABLE 57

^{19}F NMR OF XO[$CF_2CF(CF_2OCF_2CF_2OCF_2CF_2OCF_3)O$]X (MLO 91-158)

ppm	Rel.Int.	Assignment
-50.4	a	-OC<u>F</u>$_2$O-
-52.3	0.15	C<u>F</u>$_3$OCF(R)CF$_2$O-, -OC<u>F</u>$_2$OC<u>F</u>$_2$O- ?
-54.4	]	
	├ 1.8	
-54.7	major]	-CF$_2$CF(CF$_2$OCF$_2$CF$_2$OCF$_2$CF$_2$OC<u>F</u>$_3$)O-
-55.5	b	?
-76.6	0.9	-C<u>F</u>$_2$CF(CF$_2$OCF$_2$CF$_2$OCF$_2$CF$_2$OCF$_3$)O-
-78.5	b	-OC<u>F</u>$_2$CF(C<u>F</u>$_3$)O- ?
-80.2	1.1	-CF$_2$CF(C<u>F</u>$_2$OCF$_2$CF$_2$OCF$_2$CF$_2$OCF$_3$)O-
-81.9	b	-OC<u>F</u>$_2$CF$_2$CF$_2$C<u>F</u>$_2$O-, -OC<u>F</u>$_2$CF$_2$C<u>F</u>$_2$O-
-83.6	b(broad)	?
-85.1	b(broad)	-OCF(C<u>F</u>$_3$)O- ?
-86.1	b	C<u>F</u>$_3$CF$_2$O-
-87.3	3.5	-CF$_2$CF(CF$_2$OC<u>F</u>$_2$C<u>F</u>$_2$OC<u>F</u>$_2$CF$_2$OCF$_3$)O- (major), CF$_3$C<u>F</u>$_2$O-
-89.3	1.2	-CF$_2$CF(CF$_2$OCF$_2$CF$_2$OCF$_2$C<u>F</u>$_2$OCF$_3$)O-
-124.4	b	-OCF$_2$C<u>F</u>$_2$C<u>F</u>$_2$CF$_2$O-
-127.2	b	-OCF$_2$C<u>F</u>$_2$CF$_2$O-
-142.0	]]	
	├ 0.6 ├	-OCF$_2$C<u>F</u>(R)O-
-142.6	]	
-144.0		CF$_3$OC<u>F</u>(R)CF$_2$O-

a Peak is of extremely low intensity.
b Peak intensity cannot be determined due to poor resolution or low intensity.

TABLE 58

^{19}F NMR of $XO(CF_2CF_2OCF_2O)_nX$, MLO 91-160

ppm	Rel. Int.	Assignment
-47.3	b	$-OCF(CF_3)OC\underline{F}_2OCF_2CF_2O-$?
-50.5	2.3	$-OCF_2CF_2OC\underline{F}_2OCF_2CF_2O-$
-51.4	a	?
-52.0	a	$-OC\underline{F}_2OC\underline{F}_2O-$
-52.8	0.2	$CF_3OC\underline{F}_2O-$
-54.8	0.17	$C\underline{F}_3OCF_2CF_2O-$
-55.9	a	$C\underline{F}_3OCF(CF_3)O-$?
-56.5	0.3	$C\underline{F}_3OCF_2O-$
-73.1	0.04	$C\underline{F}_2ClCF_2O-$
-78.6	a	$-OC\underline{F}_2CF(CF_3)O-$?
-79.0	b	$-OC\underline{F}_2CF(C\underline{F}_3)O-$?
-80.3	b(broad)	?
-80.9	b	$C\underline{F}_3CF_2CF_2O-$?
-81.8	b	$-OC\underline{F}_2CF_2CF_2C\underline{F}_2O-$
-82.1	b	$CF_3CF_2C\underline{F}_2O-$?
-85.1	a	$-OCF(C\underline{F}_3)O-$
-86.2	0.1	$C\underline{F}_3CF_2O-$
-87.3	0.2	$CF_3C\underline{F}_2O-$, $-OCF_2OCF_2C\underline{F}_2OC\underline{F}_2CF_2CF_2OCF_2O-$
-89.0	4.8	$-OCF_2OC\underline{F}_2C\underline{F}_2OCF_2O$ (major), $-OCF_2OC\underline{F}_2CF_2OCF_2C\underline{F}_2OCF_2O-$
-89.5	0.1?	$CF_3OC\underline{F}_2CF_2O-$
-89.9	a	?
-124.0	a	$-OCF_2C\underline{F}_2C\underline{F}_2CF_2O-$

a Peak is of extremely low intensity.

b Peak intensity cannot be determined due to poor resolution or low intensity.

TABLE 59

^{19}F NMR of $XO[CF_2CF_2O]nX$ (MLO 91-161)

ppm	Rel.Int.	Assignment
-54.2	a	$C\underline{F}_3OCF_2CF(CF_3)$- ?
-54,8	0.9	$C\underline{F}_3OCF_2CF_2O$-
-77.9	a	$-OC\underline{F}_2CF(C\underline{F}_3)O$- ?
-78.9	a	$-OC\underline{F}_2CF(C\underline{F}_3)O$- ?
-80.6	b	$C\underline{F}_3CF_2CF_2O$-
-81.5	b	$CF_3CF_2C\underline{F}_2O$- ?
-83.0	b	?
-83.4	b	?
-85.1	a	$-OCF(C\underline{F}_3)O$- ?
-86.1	0.2	$C\underline{F}_3CF_2O$-
-87.3	12.0	$-OC\underline{F}_2C\underline{F}_2O$- (major), $CF_3C\underline{F}_2O$-
-88.1	a	?
-89.4	0.6	$CF_3OC\underline{F}_2CF_2O$-
-136.6	a	?

[a] Peak is of extremely low intensity

[b] Peak intensity cannot be determined due to the poor resolution or low intensity.

TABLE 60

SEPARATION AND CHARACTERIZATION DATA FOR SELECTED PERFLUOROALKYLETHER FLUIDS[a]

Material		BP, °C	Viscosity, cSt		VI	MW (Osm)
			40°C	100°C		
$-(CF_2CF_2CF_2O)_n-$	Demnum S-20	As Received	23.8	5.48	179	2500
	Fraction 1	86-142/0.001 mm Hg	9.24	2.44	77	1740
	Fraction 2	142-175/0.001 mm Hg	14.3	3.48	123	2190
	Fraction 3	175-225/0.001 mm Hg	24.7	5.48	168	2940
	Residue	>225/0.001 mm Hg	80.6	15.5	205	5410
$-(CF_2CF_2CF_2CF_2OCF_2O)_n-$	(MLO 91-105)	180-330/0.5 mm Hg	20.8	5.04	183	2500
	Fraction 1	114-150/0.001 mm Hg	10.8	2.89	119	1960
	Fraction 2	150-162/0.001 mm Hg	13.3	3.44	140	2190
	Fraction 3	162-201/0.001 mm Hg	19.0	4.64	172	2760
	Residue	>201/0.001 mm Hg	36.1	8.27	215	4030
$-(CF_2CF_2CF_2CF_2O)_n-$	(MLO 91-126)	180-330/0.5 mm Hg	52.0	7.73	114	2600
	Fraction 1	50-170/0.001 mm Hg	21.2	3.88	52	1800
	Fraction 2	170-206/0.001 mm Hg	42.4	6.50	103	2570
	Fraction 3	206-231/0.001 mm Hg	64.5	8.97	114	3180
	Residue	>231/0.001 mm Hg	116.6	14.5	126	4210
$-[CF_2CF_2OCF_2CF(CF_2CF_3)OCF_2O]_n-$	(MLO 91-131)	180-330/0.5 mm Hg	22.6	5.00	155	2900
	Fraction 1	52-164/0.001 mm Hg	11.3	2.82	90	2160
	Fraction 2	164-190/0.001 mm Hg	18.1	4.11	131	2800
	Fraction 3	190-212/0.001 mm Hg	25.3	5.39	155	3260
	Residue	>212/0.001 mm Hg	44.0	8.58	177	4630
$-[(CF_2CF(CF_3))_2OCF_2O]_n-$	(MLO 91-132)	180-330/0.5 mm Hg	28.4	6.00	165	3050
	Fraction 1	130-163/0.001 mm Hg	15.3	3.50	106	2300
	Fraction 2	163-189/0.001 mm Hg	24.8	5.22	148	3200
	Residue	>189/0.001 mm Hg	51.6	9.76	178	4070
$-[(CF_2CF_2O)_4CF_2O]_n-$	(MLO 91-157)	180-330/0.5 mm Hg	15.4	3.95	162	2870
	Fraction 1	50-157/0.001 mm Hg	7.38	2.17	93	1970
	Fraction 2	157-166/0.001 mm Hg	10.9	2.96	128	2570
	Fraction 3	166-194/0.001 mm Hg	14.6	3.74	152	2870
	Residue	>194/0.001 mm Hg	28.4	6.40	188	4350

TABLE 60 (CONCLUDED)

SEPARATION AND CHARACTERIZATION DATA FOR SELECTED PERFLUOROALKYLETHER FLUIDS[a]

Material	BP, °C	Viscosity, cSt 40°C	Viscosity, cSt 100°C	VI	MW (Osm)
$-[CF_2CF(CF_2OCF_2CF_2OCF_2CF_2OCF_3)O]_n-$ (MLO 91-158)	180-330/0.5 mm Hg	67.1	8.71	102	3950
Fraction 1	70-161/0.001 mm Hg	25.6	4.21	35	2770
Fraction 2	161-189/0.001 mm Hg	45.2	6.34	84	3350
Fraction 3	189-220/0.001 mm Hg	81.8	9.73	96	4310
Residue	>220/0.001 mm Hg	169.5	18.0	117	6300
$-(CF_2CF_2OCF_2O)_n-$ (MLO 91-160)	180-330/0.5 mm Hg	10.5	3.32	215	2640
Fraction 1	99-147/0.001 mm Hg	5.96	2.03	149	2030
Fraction 2	147-166/0.001 mm Hg	7.81	2.58	187	2470
Fraction 3	166-186/0.001 mm Hg	9.98	3.19	213	2700
Residue	>186/0.001 mm Hg	17.4	5.12	257	3850
$-(CF_2CF_2O)_n-$ (MLO 91-161)	180-330/0.5 mm Hg	16.7	4.04	141	3000
Fraction 1	120-160/0.001 mm Hg	10.0	2.68	104	2400
Fraction 2	160-173/0.001 mm Hg	12.7	3.24	124	2800
Residue	>173/0.001 mm Hg	26.9	5.78	166	4250

a) The original material as received from WL/MLBT was redistilled at 0.001 mm Hg and two or three fractions plus a residue was obtained

TABLE 61

COMPARISON OF THERMAL OXIDATIVE BEHAVIOR OF VARIOUS PERFLUOROALKYLETHER FLUIDS[a]

Test No.	Fluid Type	g	Temp. °C	Volatiles mg/g	Coupon Weight Change, mg/cm^2
1	Krytox (MLO 71-6)	3.02	260	0.13	+0.1
28[b]	ditto	9.99	300 (72h)	38.2	+0.4
32	ditto	3.41	315	44.0	+0.5
105	Aflunox (MLO 88-298)	3.09	315	0.19	+0.1
93	ditto	3.03	325	5.5	+0.4
106	ditto	3.07	330	12.7	+0.7
2	Fomblin Z (Z25-P28)	3.17	260	57.4	-0.2
94	Fomblin Z (Z25-P151)	3.05	315	3.4	no coupon
98	ditto	3.06	315	5.5	no coupon[r]
3	Demnum S-20 (MLO 86-51)	3.74	260	1.0	+0.2
27[c]	Demnum S-20 (MLO 88-177)	9.94	260 (68h)	0.7	n.d.
29[d]	Aged Demnum S-20	9.93	300	1.4	+3.1
83[l]	ditto	2.90	300	0.07	n.d.
41	Demnum S-20	3.05	315	16.8	+1.1
78	ditto	6.38	315	10.4	+1.2
79[i]	Aged Demnum S-20	3.24	315	5.4	+0.7
82[k]	ditto	2.99	315	0.70	0.0
77	Demnum S-20	3.05	330	37.8	+1.0
31[e]	Aged Demnum S-20	3.29	330	13.3	+0.8

TABLE 61 (continued)

COMPARISON OF THERMAL OXIDATIVE BEHAVIOR OF VARIOUS PERFLUOROALKYLETHER FLUIDS[a]

Test No.	Fluid Type	g	Temp. °C	Volatiles mg/g	Coupon Weight Change, mg/cm^2
80[j]	Aged Demnum S-20	3.10	330	5.3	+1.2
84[m]	ditto	2.90	345	73.7	+0.3
53	Demnum S-20	3.03	345	2.6	no coupon
99	Demnum S-100	3.22	315	8.0	+0.54
100[r]	ditto	3.20	315	4.7	(Si_3N_4) +0.48
102[t]	Aged Demnum S-100	3.09	315	0.65	+0.18
101[s]	ditto	3.16	330	6.1	+2.4
104	Demnum S-100	3.13	330	22.5	+1.8
4	Brayco 814Z (MLO 78-80)	3.32	260	4.8	+0.2
35	ditto	3.36	275	62.2	+0.4
38	Fluor. Krytox (MLO 91-21)	3.08	315	0.03	+0.1
89	ditto	3.05	325	0.3	+0.06
87[o]	ditto	3.03	325(40h)	3.8	-0.2
55	ditto	3.02	330	2.0	+0.2
46	ditto	3.08	345	27.4	-0.1
52	ditto	3.03	345	0.99	no coupon
57	ditto	3.01	360	4.8	no coupon
56[h]	ditto	3.05	360(N_2)	0.69	0.0
36	MLO 91-87[f]	3.20	300	0.06	+0.1
39	ditto	3.04	315	0.59	+0.1

TABLE 61 (continued)

COMPARISON OF THERMAL OXIDATIVE BEHAVIOR OF VARIOUS PERFLUOROALKYLETHER FLUIDS[a]

Test No.	Fluid Type	g	Temp. °C	Volatiles mg/g	Coupon Weight Change, mg/cm^2
48	MLO 91-87	3.05	330	55.6	0.0
37	MLO 91-88[g]	3.20	300	0.09	+0.1
40	ditto	3.14	315	2.2	+0.1
49	ditto	3.04	330	121.6	-0.2
59	$-[(CF_2)_5OCF_2O]_n-$ (MLO 91-106)	3.01	300	0.53	-0.06
96	ditto	3.05	310	0.10	0.0
50	ditto	3.15	315	11.9	+0.1
42	ditto	3.18	330	55.0	+0.1
60	$-[(CF_2)_4O]_n-$ (MLO 91-126)	3.03	315	0.99	-0.06
86[n]	Aged MLO 91-126	2.82	315	0.71	0.0
91[p]	ditto	2.87	315	1.6	+0.4
43	MLO 91-126	3.06	330	5.1	+0.06
47	ditto	3.04	345	73.8	+0.4
58	$-[(CF_2CF_2O)_4CF_2O]_n-$(MLO91-157)	3.02	280	0.53	0.0
54	ditto	3.02	290	3.7	-0.1
44	ditto	3.02	300	25.7	+0.4
45	$[CF_2CF_2O]_n$ (MLO 91-161)	3.04	300	0.26	0.0
92[q]	ditto	2.76	300(48h)	28.9	+0.8
61	ditto	3.04	310	0.62	0.0
51	ditto	3.01	315	18.06	0.0

TABLE 61 (continued)

COMPARISON OF THERMAL OXIDATIVE BEHAVIOR OF VARIOUS PERFLUOROALKYLETHER FLUIDS[a]

Test No.	Fluid Type	g	Temp. °C	Volatiles mg/g	Coupon Weight Change, mg/cm^2
62	-$[CF_2CF(CF_3)CF_2CF(CF_3)OCF_2O]_n$- (MLO 91-132)	3.03	300	0.56	+0.06
107[v]	Aged MLO 91-132	2.80	310	59.6	+0.06
64	MLO 91-132	3.07	315	5.0	+0.2
66	ditto	3.04	325	33.6	+0.2
63	-$[CF_2CF[(OCF_2CF_2)_2OCF_3]O]_n$- (MLO 91-158)	3.02	300	0.13	-0.06
85	ditto	3.01	305	0.30	0.0
95	ditto	3.01	310	0.03	0.0
65	ditto	3.02	315	9.0	+0.1
67	ditto	3.05	325	175.0	-1.4
68	-$[(CF_2)_4OCF_2O]_n$- (MLO 91-105)	3.06	300	0.13	0.0
81	ditto	3.05	305	0.07	-0.06
88	ditto	3.02	310	0.30	+0.06
70	ditto	3.06	315	9.1	-0.06
76	ditto	3.04	330	31.5	+0.06
72	-$(CF_2CF_2OCF_2O)_n$- (MLO 91-160)	3.04	275	0.06	0.0
90	ditto	3.01	285	0.03	0.0
75	ditto	3.06	290	2.2	-0.06
69	ditto	3.04	300	118.4	-0.5
71	-$[CF_2CF(CF_3)O]_n$- (MLO 91-127)	3.01	315	0.30	0.0

TABLE 61 (concluded)

COMPARISON OF THERMAL OXIDATIVE BEHAVIOR OF VARIOUS PERFLUOROALKYLETHER FLUIDS[a]

Test No.	Fluid Type	g	Temp. °C	Volatiles mg/g	Coupon Weight Change, mg/cm^2
74	$-[CF_2CF(CF_3)O]_n-$ (MLO 91-127)	3.05	325	1.6	+0.06
73	ditto	3.06	330	18.8	-0.06

(a) All the tests were performed in pure oxygen at the denoted temperature in the presence of an M-50 coupon over a 24 h period using the modified, scaled-down, sealed version of the AFML Micro-O-C-Test arrangement.
(b) Test conducted for 72 h.
(c) Test conducted for 68 h.
(d) Fluid and coupon from Test 27 used for this test.
(e) Fluid from Test 29 used for this test.
(f) MLO 91-87, $CF_3O[CF_2CF_2O]_m[CF_2CF(CF_3)O]_n[CF_2CF_2O]_pCF_3$
(g) MLO-91-88, $CF_2O[CF_2CF(CF_3)O]_n[CF_2CF_2O]_mCF_3$
$|$
$CFO[CF_2CF(CF_3)O]_q[CF_2CF_2O]_pCF_3$
$|$
$CF_2O[CF_2CF(CF_3)O]_r[CF_2CF_2O]_sCF_3$
(h) Test conducted in nitrogen.
(i) Fluid from Test 78 used for this test.
(j) Fluid from Test 79 used for this test.
(k) Fluid from Test 80 used for this test.
(l) Fluid from Test 82 used for this test.
(m) Fluid from Test 85 used for this test.
(n) Fluid from Test 60 used for this test.
(o) This test was conducted over a 40 h period.
(p) Fluid from Test 43 used for this test.
(q) This test was conducted over a 48 h period.
(r) Si_3N_4 ball used in this test.
(s) Fluid from Test 99 used for this test.
(t) Fluid from Test 100 used for this test.
(u) Fluid from Test 101 used for this test.
(v) Fluid from Test 64 used for this test.

5. REFERENCES

1. C.E. Snyder, Jr., L.J. Gschwender and, C. Tamborski, Lubr. Eng., 37, 344 (1981).
2. D. Sianesi, V. Zamboni, R. Fontanelli, and M. Binaghi, Wear, 18, 85 (1971).
3. D. Sianesi, A. Pasetti, R. Fontanelli, G.C. Bernardi, and G. Caporiccio, Chim. Ind. (Milan), 55, 208 (1973).
4. D. Sianesi, A. Pasetti, and G. Belardinelli, U.S. Patent 3,715,378 (1973).
5. Daikin Industries, European Patent Application 0148482, 20 December 1984
6. Daikin Industries,Demnum Fluid Bulletin.
7. EI Du Pont de Nemours and Co. Inc., Krytox Fluid Bulletin.
8. K.J.L. Paciorek and R.H. Kratzer, J. Fluorine Chem., 67, 169 (1994).
9. Hybrid Fluorosilicones for Aircraft Fuel Tank Sealants, AFML-TR-70-278, Part II, February 1972.
10. W.J. Feast, W.K.R. Musgrave, and N, Reeves, J. Chem. Soc., C., 2429 (1970).
11. E.S. Blake and J.K. Schaar, Ind. Eng. Chem. Prod. Res. Dev., 8, 212 (1969).
12. W. Dmowski, R.A. Kolinski, and R. Wozniacki, Pol. J. Chem., 52, 1297 (1978).
13. R.A. Kolinski, H. Plenkiewicz, H. Voellnagel-Neugebauer, and R. Wozniacki, Pol. J. Chem., 51, 1365 (1977).

14. C.W. Tullock and D.D. Coffman, J. Org. Chem., 25, 2016 (1960).

15. Synthesis and Structure-Property Correlations of Perfluoropolyalkylether Fluids. Ultrasystems Defense, Inc. Proposal P-89-C-128, September 1989.

16. K.J.L. Paciorek, R.H. Kratzer, J. Kaufman, T.I. Ito, and J.H. Nakahara, Crosslinking of Perfluorocarbon Polymers, AFML-TR-78-65, May 1978.

17. R. Anderson and T. Psarras, Development of High Temperature Functional Fluids, AFML-TR-71-208, November 1971.

18. K.J.L. Paciorek, S.R. Masuda, J.H. Nakahara, C.E. Snyder, Jr., and W.M. Warner, Ind. Eng. Chem. Res., 30, 2531 (1991).

19. K.J.L. Paciorek, and S.R. Masuda, Ind. Eng. Chem. Res., 34, 1390 (1995).

20. J. Pacansky, M. Miller, W. Hatton, B. Liu and A. Scheiner, J. Amer. Chem. Soc., 113, 329 (1991).

21. P. H. Kasai, Macromol., 25, 6791 (1992).

22. K.J.L. Paciorek, S.R. Masuda, W-H. Lin, and J.H. Nakahara, Perfluoroalkyl and Perfluoroalkylether-Substituted Quinoxalines, J. Fluorine Chem., in press.

23. K.J.L. Paciorek, R.H. Kratzer, J. Kaufman and J.H. Nakahara, J. Appl. Polym. Sci. 24, 1397 (1979).

24. N.L. Allinger, J. Amer. Chem. Soc., 99, 8127 (1977).

25. J.R. Throckmorton, J. Org. Chem., 34, 3438 (1969).

26. K.L. Paciorek, T.I. Ito, and R.H. Kratzer, Thermal Oxidative Degradation Reactions of Perfluoroalkylethers, NASA CR-165516, October 1981.